Stromal and epithelial interactions in three-dimensional cell biology models of ovarian cancer

Barbara Grun
University College London

July 2012

Declaration

I, Barbara Grun, confirm that the work presented in this thesis is my own. Where information has been derived from other sources, I confirm that this has been indicated in the thesis.

Abstract

Over the past years it has become increasingly apparent that the tumour microenvironment plays a crucial role in tumour initiation/development/metastasis. The interactions of the tumour microenvironment and the malignant epithelial cells in epithelial ovarian cancer (EOC) biology remain poorly understood. This is in part due to the lack of representative *in vitro* models of disease that closely resemble the *in vivo* situation.

A tumour exhibits a three-dimensional (3D) architecture comprising the malignant epithelial cells surrounded by the tumour stroma, which predominately contains the so-called cancer associated fibroblasts (CAFs). *In vitro* 3D models using primary epithelial cancer cell lines showed striking morphological similarities with the primary tumours. Immunohistochemistry and proteomic profiling further revealed that 3D models more closely resemble the primary tumour compared to traditional 2D culture methods.

To further develop these 3D models and to recreate the interactions of epithelial cells with the microenvironment *in vitro,* heterotypic 3D models were established. Mesenchymal stem cells (MSCs) and immortalized normal ovarian fibroblasts (INOFs) were used to represent the tumour stroma and co-cultured with malignant and non-malignant epithelial ovarian cells. These 3D models proved an improvement to the previously established homotypic 3D models and offered a very good representation of the *in vivo* tumour.

Finally, the recruitment of CAFs into the tumour stroma by EOC cell lines was investigated. Both MSCs and INOFs showed the ability to transdifferentiate into CAFs upon treatment with conditioned medium from an EOC cell line. Transdifferentiation was assessed by the expression of α-smooth muscle actin (αSMA), Vimentin and fibroblast specific protein (FSP). Both differentiated cell lines were also able to induce increased proliferation and invasion rates in a transformed ovarian surface epithelial cell line. These results provide *in vitro* evidence that both MSCs and INOFs can serve as precursor cell types of CAFs in EOC.

Acknowledgements

First and foremost I would like to thank my supervisor, Prof Simon Gayther, for his encouragement to pursue a PhD, his great ability to motivate and to spark enthusiasm and his help in guiding my research. I would also like to thank him for the valuable comments regarding the writing of this thesis. Many thanks to every member of the Gynaecological Cancer Research Laboratories: Thanks to Dr Dimitra Dafou for introducing me to the world of tissue culture and her support at the beginning of my PhD; thanks to Dr Susan Ramus, Dr Chris Jones, Tanya Sher, Mark Cox, Eva Wozniak and Jeremy Ford. This group has been a source of friendship and good advice.

Special thanks goes to Kate Thornton for helping me with all the hazardous lab work during my pregnancy. Thanks to my fellow PhD students: Lydia Quaye, James Morris, Ken Choi, Kate McAllister, Maria Notaridou, Sheetal Dyall, Jane Hayward and Will Stott.

A very special thanks goes to my colleague and friend Kate Lawrenson for many insightful discussions about research, sharing knowledge and numerous extracurricular activities. I am immensely grateful for her invaluable comments and suggestions during the writing of this thesis.

I would like to thank Prof Ian Jacobs, Director of the UCL Institute for Women's Health (during the time of my PhD thesis), Executive Dean of the Faculty of Biomedicine (during the time of my PhD thesis), and Medical Advisor to the Eve Appeal; Dr John Timms and his group at the Cancer Proteomics Laboratory for guidance and help during my journey into the world of proteomics; Dr Elisabeth Benjamin for help in analysing histopathological samples; Tomas Adejumo for FAC sorting services and introduction to FACS analysis; Daniel Ciantar and his colleagues at the UCL Imaging Facility for their help with confocal microscopy; The staff at the UCLH advanced diagnostics laboratory and histology service.

This PhD was supported by an MRC studentship and would not have been possible without the support of the Eve Appeal Gynaecological Cancer Research Fund.

A special note goes to my biology teacher Claudia Kogel. Without her stimulating and inspiring lessons I would not have chosen to pursue a career in science.

Finally I would like to thank my family and in particular my wonderful husband Alex for their support and encouragement. Alex, thank you for taking care of our live while I was stuck in the lab, your encouragement to keep going and for taking me out for dinner after long days at work. Special thanks to my little man Max. Thanks for being such a wonderful, happy and loving son. You certainly have not made my writing up any faster, but your constant source of energy made it more enjoyable indeed.

Contents

List of Figures

List of Tables

List of Abbreviations

2D	two-dimensional
2D-DIGE	2D-difference in gel electrophoresis
3D	three-dimensional
BRCA1/2	breast-cancer gene ½
Ca125	cancer antigen 125
CAF	cancer associated fibroblast
CK7	cytokeratin 7
CM	conditioned medium
DNA	deoxyribonucleic acid
ECM	extracellular matrix
EGF	epidermal growth factor
EOC	epithelial ovarian cancer
FBS	foetal bovine serum
FSP	fibroblast specific protein
FACS	fluorescence activated cell sorting
GFP	green fluorescent protein
H&E	haematoxylin and eosin
hTERT	human telomerase reverse transcriptase
INOF	immortalised normal ovarian fibroblast
IOSE	immortalised ovarian surface epithelium
LOH	loss of heterozygosity
MALDI-TOF MS	Matrix assisted laser desorption ionization time-of-flight mass spectrometry
MCS	multicellular spheroid
MMLV	murine molony leukaemia virus
MSC	mesenchymal stem cells

MTT	thiazolyl blue tetrazolium bromide
NOSE	normal ovarian surface epithelium
OCP	oral contraceptive pill
PBS	phosphate-buffered saline
polyHEMA	poly-2-hydroxyethyl methacrylate
RNA	ribonucleic acid
RCCS	rotary cell culture system
SDS-PAGE	sodium dodecyl sulfate polyacrylamide gel electrophoresis
SFM	serum-free medium
SMA	smooth muscle actin
SV40	simian virus 40
TGF-β	transforming growth factor beta
VEGF	vascular endothelial growth factor

I Introduction

I.1 Epithelial ovarian cancer

Epithelial ovarian cancer (EOC) is the leading cause of death due to gynaecological malignancies in the western world (Jemal, Siegel et al. 2007). Prompt diagnosis is hindered as a result of vague symptoms and most cases are discovered at advanced stages (Wikborn, Pettersson et al. 1996). First line treatment of advanced ovarian cancer includes cytoreductive surgery and chemotherapy. Although the initial response rates to platinum based chemotherapeutics are high (McGuire, Hoskins et al. 1996), overall disease free survival is poor and most cancers will recur and develop chemoresistance. However, if the disease is diagnosed at the earliest stages when the tumour is still confined to the ovary, survival rates are over 90%. Survival drops to less than 6% for women diagnosed at stage IV when the cancer has spread and formed metastasis at distant sites.

Figure I-1: Statistics of ovarian cancer survival in correlation with stage on time of diagnosis. Data from Anglia Cancer Network of women diagnosed between 2004-2008. (http://info.cancerresearchuk.org/cancerstats/types/ovary/survival/#trends)

Thus, detecting the disease early can affect longterm survival. Population based screening trials might offer a good tool at discovering early stage disease before clinical presentation. A large trial is currently ongoing to assess the effects of epithelial ovarian cancer screening on overall mortality. Preliminary results show that screening is successful at detecting disease in symptomless women (Menon, Gentry-Maharaj et al. 2009).

One of the difficulties with EOC is heterogeneity of the disease. Ovarian cancer can be divided broadly into type I and type II tumours (Shih Ie and Kurman 2004). Type I tumours are slow growing and include the clear cell, endometrioid and mucinous subtypes as well as low grade serous and malignant Brenner tumours. Type II tumours include high grade serous and undifferentiated tumours which exhibit aggressive growth and are the most commonly diagnosed tumours (75%) accounting for 90% of cancer deaths (Shih Ie and Kurman 2004; Sharma, Gentry-Maharaj et al. 2012).

Table I-1: Summary of classification of epithelial ovarian cancer subtypes and clinical behaviour.

Type I	Origin/Precursor lesions	Clinical Presentation
Low grade serous	Ovarian epithelium	Usually discovered at an early stage, good prognosis
Mucinous	Ovarian epithelium	Mostly diagnosed at the early stages with a good prognosis
Endometrioid	Ovarian epithelium/endometriosis	Diagnosis usually at stages III and IV with spread of disease
Clear cell	Ovarian epithelium/endometriosis	Diagnosis usually at stages III and IV with spread of disease
Malignant Brenner	Benign brenner tumours	Very rare with good prognosis
Type II	**Origin/Precursor lesions**	**Clinical Presentation**
High grade serous	Probably fallopian tube epithelium and/or ovarian surface epithelium	Fast growing with late stage diagnosis and metastasis, poor diagnosis
Undifferentiated	Not known	
Carcinosarcoma	Not known	

I.1.1 Origin of epithelial ovarian cancer

The heterogeneity of epithelial ovarian cancer leads to the assumption that there are different tissue origins for the different EOC subtypes. The ovarian surface epithelium (OSE) was long considered the origin of most serous epithelial ovarian cancers (EOCs) (Auersperg, Edelson et al. 1998). However, recent histopathological examinations of fallopian tube sections of BRCA1/2 patients undergoing prophylactic surgery have identified early serous carcinomas at the fimbrial end of the fallopian tube (Medeiros, Muto et al. 2006). Furthermore, gene expression analysis showed that serous ovarian tumours resemble normal fallopian tube epithelium (Marquez, Baggerly et al. 2005). These observations suggest that a proportion of serous epithelial ovarian cancers originate from the epithelium at the fimbrial end of the fallopian tubes.

Morphological examination of the endometrioid subtype indicates a resemblance to the endometrial epithelium and the mucinous subtype shows similarity to the endocervical epithelium. Furthermore, endometrioid and clear cell subtypes of epithelial ovarian cancer have been shown to be associated with endometriosis (Sainz de la Cuesta, Eichhorn et al. 1996). These observations led Dubeau to postulate that a high proportion of epithelial ovarian cancers arise from ectopically located müllerian epithelium (Dubeau 2008).

In summary, the debate about the cell of origin remains unsolved. However, it is most likely that the cell of origin is as heterogeneous as the disease itself and that different sites of origin give rise to the different subtypes of epithelial ovarian cancer.

I.1.2 Epithelial ovarian cancer risk factors and the microenvironment

A family history of ovarian cancer is an important risk factor for EOC development. Most of these cancer cases are due to mutations in the *BRCA1/2* genes, which is the most important risk factor for the development of hereditary ovarian cancer (Edmondson and Monaghan 2001). However, 90% of ovarian cancers are sporadic and other risk factors need to be considered.

In 1971 Fathalla proposed the incessant ovulation hypothesis in which he made the connection between repeated ovulation and the occurrence of EOC. He based his theory on observations of hens housed under artificial light conditions to maximise egg production. Seventeen out of 19 hens developed adenocarcinoma of the ovary compared to no tumour development in control hens kept under normal conditions (Fathalla 1971). It was hypothesised that the frequent ovulation poses a risk factor for ovarian cancer development. Follicle growth and subsequent rupture during ovulation is followed by migration and proliferation of the OSE to repair the site of ovulatory rupture. The processes involved show similarities to inflammation and wound healing in response to tissue damage. Epidemiological studies show a protective effect of the oral contraceptive pill (OCP) use and pregnancy on the development of ovarian cancer (Shu, Brinton et al. 1989;

Rosenberg, Palmer et al. 1994; Riman, Dickman et al. 2002). The risk for developing EOC decreases further when OCP is used over a long period of time (Rosenberg, Palmer et al. 1994). This also applies to *BRCA1/2* mutation carriers that exhibit a significantly reduced risk of developing ovarian cancer upon prolonged OCP use (Iodice, Barile et al. 2010). Both pregnancy and OCP use reduce the number of ovulations that occur during a woman's reproductive years, and so the protective effect associated with these two lifestyle factors has been postulated to be in keeping with Fathallas model.

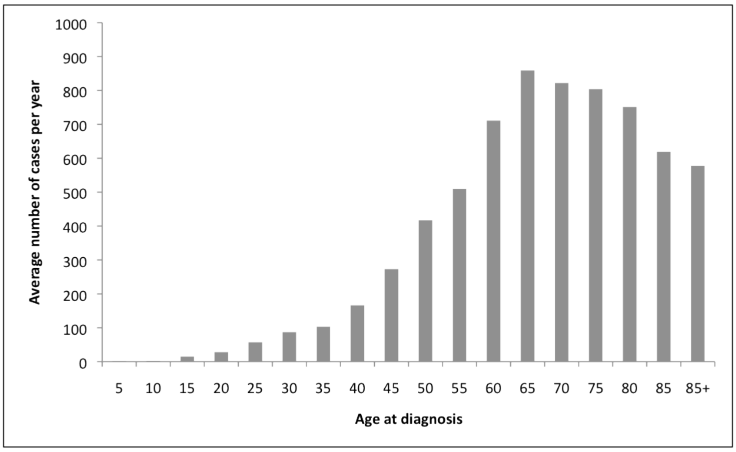

Figure I-2: Incidence of epithelial ovarian cancer within different age groups in the UK between 2006-2008. The risk of developing EOC increases with age. The highest incident of ovarian cancer is in women above the age of 65. Data was obtained from Cancer Research UK. (http://info.cancerresearchuk.org/cancerstats/types/ovary/incidence/uk-ovarian-cancer-incidence-statistics#age).

The risk of ovarian cancer development increases with age (Figure I-2). This observation led to the hypothesis that an ageing microenvironment might be associated with the development of EOC. An *in vitro* experiment has shown that senescent fibroblasts (representing the ageing microenvironment) have an enhancing effect on the tumourigenic behaviour of transformed epithelial ovarian cancer cell lines; thus indicating a role for the ageing microenvironment in the neoplastic transformation of ovarian epithelial cells (Lawrenson, Grun et al. 2010). However, in ovarian cancer the interactions between tumour epithelial cells and their surrounding microenvironment remain poorly understood and more research is needed to better understand the role of the tumour microenvironment in the initiation, development and progression of EOCs.

I.2 Studying Epithelial Tumours

In epithelial tumours the majority of research to date has focused on the malignant epithelial cell population in the tumour. In most tumour types, the tumour epithelial cells are derived from the normal tissue epithelia of that organ. Previous studies have focused on identifying the somatic molecular events that lead to malignant transformation of epithelial cells, as exemplified by Vogelsteins' stepwise genetic transformation model for colorectal carcinoma (Fearon and Vogelstein 1990). These studies have given significant insights into tumourigenesis and have revealed novel opportunities for treatment and tumour detection in many tumour types. A large number of genes have been discovered which play an important role in the development of multiple carcinomas, including *p53, CMYC,* and the *Ras* family of oncogenes. For ovarian cancer, tumour studies including the recently published cancer genome atlas (TCGA) catalogue of nearly 500 primary ovarian tumours have shown that around one-third of ovarian serous carcinomas harbour alterations of the *BRCA1* or *BRCA2* genes (Spellman and al. 2011). Other histological subtypes of ovarian cancer also harbour distinct somatic changes, for example endometrioid ovarian cancers have been linked to the hereditary non-polyposis colon cancer (HNPCC) syndrome and frequently show mutation or LOH of the mismatch repair (MMR) genes (Prat 2012). Clear cell ovarian cancers frequently harbour mutations in *ARID1A* (Jones, Wang et al. 2010).

However, a comprehensive understanding of tumour development cannot be achieved by epithelial-centric approaches because this approach disregards the fact that tumours are extensively heterogeneous and contain many different cellular populations (Dvorak 1986). Tumour initiation and progression are synergistic processes involving the neoplastic epithelial cells and the surrounding microenvironment. Without a supporting tumour microenvironment tumour growth would be restricted to 2-3mm due to insufficient supply of oxygen and nutrients (Folkman 1995). Epithelial tumours contain a large amount of other cell types that make up the tumour stroma which, in many tumours, greatly outnumber the malignant epithelial cells. The neoplastic epithelial cells alter the microenvironment and attract endothelial cells to form new blood vessels needed for oxygen and nutrient supply (Kalluri and Zeisberg 2006). Furthermore mesenchymal stem cells and immune cells locate within the stroma. The predominant cells within the stroma are the tumour supporting fibroblasts, often referred to as cancer associated fibroblasts (CAFs). Therefore a tumour should be considered a three dimensional "organ" exhibiting a complex interplay of different cell types supported by the extracellular matrix (ECM) (Figure I-3). To fully understand tumour development it is necessary to unravel the interactions of the different cell types during tumour initiation and progression.

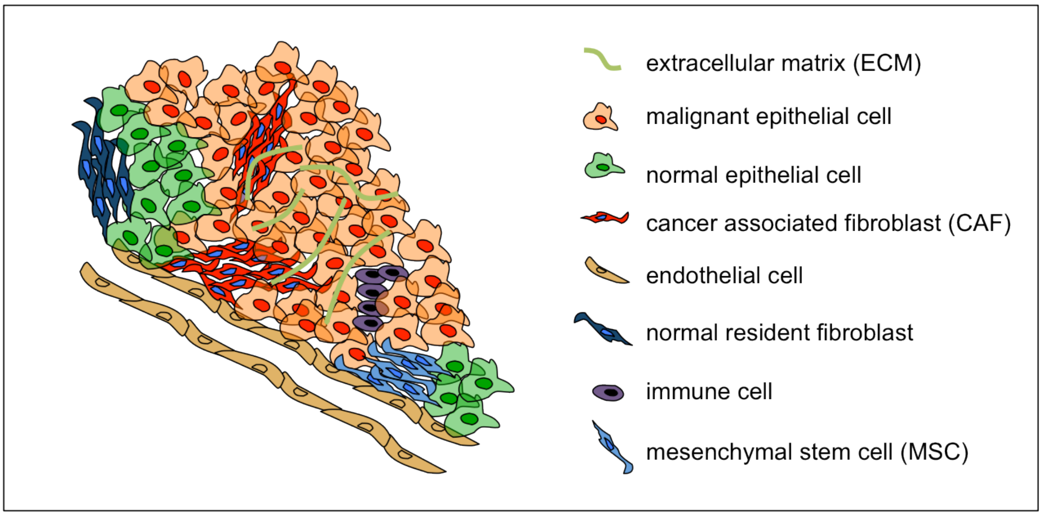

Figure I-3: Schematic view of an epithelial tumour. The tumour is comprised of the malignant epithelial cells, which are supported by the cells of the tumour microenvironment. The predominant cells within the tumour stroma are cancer associated fibroblasts (CAFs). These cells provide structural support as well as the production and secretion of growth promoting factors enhancing tumour progression. Endothelial cells are recruited into the tumour stroma and form new blood vessels to supply the tumour with oxygen and nutrients. Immune cells home into the stroma in response to inflammatory signals. Mesenchymal stem cells are recruited into the tumour microenvironment and locate within the stroma. The extracellular matrix (ECM) provides structural support for the growing tumour and its microenvironment and plays an important role in cell-cell interactions.

I.3 Models of epithelial ovarian cancer

The lack of effective therapies for ovarian cancer may be largely due to a shortfall in appropriate biological models of disease. Over the years, several models of ovarian cancer have been established. Xenograft models have been developed for several ovarian cancer cell lines from different primary tumours. The injection of cells intraperitoneally into nude mice results in the formation of xenografts representing the different histological subtypes of ovarian cancer corresponding to the tissue of origin (Shaw, Senterman et al. 2004). However one limitation is that typically the tumours represent advanced stages of disease and are not suitable to study the early stages of carcinogenesis.

I.3.1 Rodent models of epithelial ovarian cancer

The main disadvantage of xenograft models is that they can only be performed in immuno-compromised mice, which disregards the effects that an active immune system might have on tumour development. To overcome this limitation, cells from a model organism can be cultured and transformed *in vitro* and then reintroduced into the animals. Alternatively transgenic mouse models can be generated in which expression of mutant alleles or floxed constructs are driven throughout the whole organism or in a tissue specific manner. Using both approaches the immune system of the organism remains intact, and genetic elements can be selected that best reflect the somatic genetic aberrations detected in human tumours. Hence mouse ovarian surface epithelial (mOSE) cells have been used to study tumour development in mice with an intact immune system. Multiple combinations of oncogenes have been introduced into mOSE cells leading to *in vivo* tumour growth. The introduction of two oncogenes (*C-myc*, *K-ras* or *AKT*) into *p53* deficient mice led to tumour formation *in vivo* (Orsulic, Li et al. 2002).

For the ovary the main challenge has been the difficulties in identifying an ovarian (or fallopian) specific promoter. MISIIR (müllerian inhibiting substance receptor type II) was initially thought to be specific to OSE and the introduction of the SV40 early region under control of this promoter into mice resulted in the development of poorly differentiated tumours. Tumour growth was observed in approximately 50% of transgenic mice (Connolly, Bao et al. 2003). However subsequent studies suggest that MISIIR promoter expression is not specific to ovarian surface epithelia.

In another study, the Cre-loxP system was used to introduce inducible expression/knockdown of oncogenes/tumour suppressor genes. The Cre-loxP system is a site-specific recombination technique that allows targeted deletions of DNA sequences. The recombinase (cre) catalyses the recombination between two *loxP* sites resulting in the deletion of the DNA sequence flanked by *loxP* (Sauer 1993).

Flesken-Nikitin et al (2003) used this system to inactivate p53 and Rb in the mOSE and observed tumour formation. The histology of the resulting tumours showed mostly well-differentiated serous tumours or poorly differentiated neoplasms (Flesken-Nikitin, Choi et al. 2003). In another study, Dinulescu et al were able to develop mice with endometrioid ovarian carcinomas by altering Pten and K-ras expression (Dinulescu, Ince et al. 2005). Interestingly, this study also showed that altering one gene individually led to mice bearing pre-neoplastic lesions in the ovary. These lesions closely resemble endometriosis supporting the pathological and epidemiological evidence linking endometriosis and endometrioid ovarian cancer.

A rat model of epithelial ovarian cancer led to the identification of the tumour suppressor gene *lot1*. Abdollahi and coworkers compared the gene expression profiles of normal and malignant rat OSE cells and identified the tumour suppressor *lot1* (Abdollahi, Godwin et al. 1997). A subsequent analysis of frozen human epithelial ovarian cancer sections revealed an undetectable expression of the lot1 mRNA in 39% of cases (Cvetkovic, Pisarcik et al. 2004). They further identified that the gene region is subject to frequent loss of heterozygosity (LOH) in cancer and confirmed loss of heterozygosity (LOH) within the lot1 locus in 36% of ovarian tumour specimens.

Although rodent models are useful tools to model epithelial ovarian cancers they have some significant limitations. Rodent ovaries and human ovaries are morphologically different. Mouse ovaries are surrounded by the bursal membrane that is absent in human ovaries. This is an especially important fact to consider when modelling dissemination of EOC cells. Furthermore, rodent cells have been shown to immortalise spontaneously in tissue culture, which is extremely rare for human cells. Human cells exhibit higher natural barriers for transformation than rodent cells (Hahn and Weinberg 2002) which strongly suggests that human ovarian surface epithelial cells represent the most relevant model of this disease.

I.3.2 *In vitro* models of human OSE transformation

To overcome the limitations of rodent models, human ovarian surface epithelial (OSE) cells have been isolated and established in culture (Adams and Auersperg 1981; Auersperg, Siemens et al. 1984; Kido and Shibuya 1998). The isolation of normal ovarian surface epithelial cells by Auersperg and colleagues in 1984 offered the opportunity to induce mutations associated with ovarian cancer development to mimic early stages of transformation. Human OSE can bypass replicative senescence following co-transfection of SV40 and the catalytic subunit of human telomerase (hTERT) without inducing tumour growth in mice (Kusakari, Kariya et al. 2003; Liu, Yang et al. 2004). Malignant transformation could be induced by transfecting the cell lines with activated *H-ras*, *ERBB2* or *K-ras* alleles and tumour growth could be observed in mice. These models recapitulated the transformation from normal OSE cells to a malignant phenotype *in vitro.* The *in* *vitro* culturing of cells however, bears the risk of introducing genetic changes by adaptation of the cells to the tissue culture environment.

I.3.3 *In vitro* models of human epithelial ovarian cancer

The establishment of epithelial ovarian cancer cell lines from human tumours has historically been invaluable for studying the disease *in vitro.* Cell lines have been isolated both from the ascites of ovarian cancer patients and from primary solid tumour tissues. Isolation of primary EOC cell lines is challenging due to the tumour heterogeneity and it can take up to a year to establish an "immortal" EOC cell line (van den Berg-Bakker, Hagemeijer et al. 1993). This is further explored in chapter 3. Newly isolated cell lines are subjected to investigations designed to confirm the epithelial phenotype and malignant behaviour of the newly derived cell isolate, including:

(1) Immortality

In 1961 it was discovered that normal human cells exhibit a limited lifespan in culture resulting in growth arrest and senescence, called the Hayflick limit (Hayflick and Moorhead 1961). Cell lines are termed immortal when they are not subject to the Hayflick limit. Growth curves for newly established cell lines can be performed to determine growth characteristics. In contrast to normal primary cell lines that have a limited *in vitro* and *in vivo* lifespan, malignant cells able to bypass the Hayflick limit and have the potential to grow indefinitely *in vitro*.

(2) Immunohistochemistry

Immunohistochemistry is performed to verify the expression of epithelial markers by the new cell line. Due to the heterogeneity of epithelial ovarian tumours it is necessary to confirm a homogenous population of epithelial cells without contamination of stromal cell types e.g. fibroblasts, endothelial cells, pericytes and immune cells. Most EOC cell lines express cytokeratin 7, 8 and 18 as well as further epithelial markers like BerEp4 (EpCAM) and are negative for fibroblast markers (FSP) and endothelial cell markers e.g. von willenbrand Factor VIII.

(3) Anchorage independent growth

Anchorage independent growth assays test for the ability to evade anoikis, which is a feature of malignant cells but not normal cells. Cell lines that form colonies in semi-solid medium show tumourigenic behaviour.

(4) Invasion assay

The invasive ability of the newly established cell lines can be assessed using an *in vitro* invasion assay. The capability of cells to invade through a basement membrane (matrigel coated tissue culture insert) towards a chemoattractant is measured. If cells show invasive potential they exhibit another feature of tumourigenic behaviour.

(5) Karyotyping

Karyotyping gives an insight into the genetic status of the primary cell line. Cancer cells are often genomicly unstable, undergoing substantial chromosomal alterations including aneuploidy, interstitial alterations and translocations. Several studies have shown that ovarian cancers can have particularly large numbers of chromosomal alterations (Spellman and al. 2011).

(6) *In vivo* tumour growth in SCID mice

Tumour cells can be injected into mice to assess their ability to form tumours *in vivo*. Cells can be injected subcutaneously, intraperitoneally or orthotopically. The formation of tumours can be monitored and the development of metastasis can be observed. Tumour formation in mice is another feature of tumourigenic behaviour.

Several epithelial ovarian cancer cell lines have been established over the years (DiSaia, Morrow et al. 1975; Buick, Pullano et al. 1985; van den Berg-Bakker, Hagemeijer et al. 1993; Provencher, Lounis et al. 2000; Ouellet, Zietarska et al. 2008). These cell lines have been useful in advancing our understanding of epithelial ovarian cancer biology. The use of primary epithelial ovarian cancer cell lines also led to the discovery of the widely used clinical biomarker for EOC, CA125. Using hybridoma technology it was possible to generate and isolate a monoclonal antibody, which reacts with 6 out of 6 epithelial ovarian cancer cell lines while not binding to normal ovarian cells (Bast, Feeney et al. 1981). It was subsequently shown that CA125 reacts with 80% of EOCs (apart from the mucinous subtype) (Kabawat, Bast et al. 1983) and could also be detected in the serum of more than 80% of epithelial ovarian cancer patients (Bast, Klug et al. 1983). It was further shown that the serum level of CA125 correlated with disease progression. These observations made CA125 a promising biomarker for the detection of EOC and the monitoring of disease. Today CA125 is used to observe response to chemotherapy and detect recurrence of disease. However, 20% of all

EOCs do not exhibit CA125 expression and it is therefore not possible to use this marker alone for the early detection of EOC (Bast, Badgwell et al. 2005).

EOC cell lines are also widely used to identify potential oncogenes/tumour suppressor genes and for functional analysis of newly identified candidate genes. Some chromosomes have been found to be frequently deleted in ovarian cancer. By reintroducing the lost chromosome into EOC cell lines it has been possible to detect potential tumour suppressor genes on chromosome 6 and 18 (Dafou, Ramus et al. 2009). Subsequent analysis of candidate genes on chromosome 18 by gene expression microarray profiling identified *EPB41L3* as a potential ovarian tumour suppressor gene. Functional analysis using *in vitro* 2D and 3D models revealed growth suppression and induction of apoptosis in EOC cell lines after introduction of a functional copy of EPB41L3 (Dafou, Grun et al. 2010).

A further use of primary EOC cell lines is the testing of novel drugs. Established EOC cell lines are frequently used in the first line of investigation into the effectiveness of newly developed anti-cancer drugs. While they have been useful in the past in identifying effective novel drugs the use of the standard *in vitro* cell culture system has its limitations. Traditional 2D tissue culture methods are commonly used for high throughput screening of candidate therapeutic agents. However, the results frequently fail to translate into clinical studies. It has been shown that cells cultured on standard 2D tissue culture plastics are more sensitive to drugs compared to the same cells grown as three-dimensional (3D) spheroids (Nederman 1984). This may be due to hindered penetration of the substance into the heterogeneous 3D structures which exhibit nutrient gradients, areas of differently proliferating cells plus hypoxic and necrotic areas. These features however, are reflective of the primary tumour and need to be taken into consideration when modelling the disease *in vitro.* Therefore, this limitation of traditional *in vitro* models needs to be addressed and more representative models of disease are necessary.

I.3.4 Three dimensional tissue culture models

Traditional 2D culture models of homogenous cell populations are widely used to model disease *in vitro*. However, they fail to recreate the three-dimensional (3D) architecture and dynamic cell-cell and cell-extracellular matrix interaction *in vivo*. To overcome these limitations of standard 2D cultures, scientists have explored establishing *in vitro* 3D models of disease. Pioneering work by Mina Bissell and colleagues has shown the importance of 3D culturing to model normal epithelial and tumour cell phenotypes *in vitro*. The group was able to achieve a reversion to a normal phenotype of a breast cancer cell line grown in 3D by treatment with a β-integrin antibody. This effect could not be detected in 2D cultures (Weaver, Petersen et al. 1997). This study showed the importance of 3D models in recreating a human disease *in vitro* and the significance of an intact extracellular matrix in regulating tumour cell behaviour.

Several methods have been used to achieve 3D culture growth. As early as in the 1970s Sutherland et al created multicellular spheroids (MCS) using the Spinner flask culture method (Sutherland, Inch et al. 1970). Constant stirring of the cells in culture led to aggregation of cells and formation of MCS. His group went on to test the effects of radiation and cytotoxic agents on MCS. They found radiation resistant cells within the hypoxic areas of the spheroids that develop during spheroid formation (Sutherland and Durand 1976), thus mimicking the *in vivo* tumour environment.

A further development of the Spinner flask is the Rotary Cell Culture System (RCCS). This method was developed by NASA and keeps the cells in constant rotation while reducing shear forces, therefore facilitating spheroid formation (Cherry 1993; Goodwin, Prewett et al. 1993). Studies have reported the formation of spheroids that closely resemble tissues *in vivo* (Unsworth and Lelkes 1998; Hammond and Hammond 2001).

Another method used to develop MCS is to treat tissue culture plastics to prevent attachment of cells, thus inducing spheroid formation. Early studies used an agar base to prevent attachment and achieved formation of spheroids in tumour cell cultures but not in normal cell lines. Comparison of growth rates between 2D and 3D cultures with the *in vivo* tumour showed that 3D cultures better reflect the *in vivo* state (Yuhas, Li et al. 1977). Recently other substrates such as agarose and polyHEMA (poly-2-hydroxyethyl methacrylate) have been used to prevent cell attachment (Ivascu and Kubbies 2006) and multicellular spheroids were successfully established from normal ovarian cell lines (Lawrenson, Benjamin et al. 2009).

Embedding cells into an ECM matrix is another commonly used method of establishing cell growth in 3D. Collagen gel or Matrigel is frequently used to generate the matrices. These approaches have been successful in establishing 3D models of the interactions of luminal epithelial cells and myoepithelial cells (Gudjonsson, Ronnov-Jessen et al. 2002). A drawback of this approach however is the pre-determined composition of the gel, which may not accurately reflect the *in vivo* environment of the examined tissue.

A recent study used the hanging droplet approach to generate MCS of epithelial ovarian cancer cell lines. Cells are grown on an inverted microplate in a hanging droplet that leads to spheroid formation. Gene expression comparison of 3D MCS, 2D cultures and xenografts of the same cell lines revealed that 3D *in vitro* cultures are more representative of the *in vivo* conditions than traditional 2D cultures (Zietarska, Maugard et al. 2007).

Furthermore, using three-dimensional culture methods it has been possible to generate multicellular spheroids with heterogeneous cell populations. These more closely resemble the *in vivo* state were tumours exhibit areas of slow proliferating, apoptotic and necrotic cells as opposed to the homogenous cell populations found in standard 2D cultures (Kim 2005). Hence 3D cultures offer a greater potential to model disease *in vitro*.

Table I-2: Overview of different methods for three-dimensional *in vitro* cultures.

3D Method	Advantages	Disadvantages
Spinner Flask	• Large amount of MCS can be generated • Movement of medium aids transport of nutrients and waste product removal	• Spheroids of different sizes • Shear forces might be detrimental for some cell types
RCCS (explored in chapter 3)	• Reduced shear forces • Good transport of nutrients and removal of waste products	• Expensive and difficult to handle • Only few spheroids per vessel
Coating of tissue culture plastic (explored in chapter 4&5)	• Cost effective method • Mass culture of spheroids • Easy to manipulate	• Spheroids of different sizes • Not all cell lines form spheroids spontaneously
ECM/Collagen gel	• Polarity of cells can be recreated *in vitro* • Offers very good support for cell growth	• Fixed composition of ECM components • Might not resemble environment of tissue origin • Difficult to manipulate
Hanging droplet (explored in chapter 4)	• Uniformly sized spheroids	• Small spheroid sizes • Delicate to handle

I.3.5 Heterotypic three dimensional models

A further improvement of the previously described 3D models are heterotypic 3D models. By introducing different cell types within a 3D culture it is not only possible to recreate the *in vivo* 3D architecture but also the complex interactions between different cell types within a tumour. Over the past decades it has become increasingly apparent that the stroma plays an important role in tumour initiation, maintenance and development (explored later on in my thesis). When modelling epithelial tumours *in vitro* it is therefore advantageous to also include cells of the stromal microenvironment.

Early heterotypic 3D models have focussed on the interactions of skin epithelial and fibroblast cells. Three-dimensional co-cultures of rat epithelial dermal cells and rat fibroblast cells using collagen gels led to the formation of skin grafts. These could be grafted onto the donor animal and persistent wound closure was achieved (Bell, Ehrlich et al. 1981). A further study using collagen gels to model the 3D interactions of human foreskin fibroblasts and human epidermal cells *in vitro* showed that fibroblasts could regulate the invasive behaviour of transformed dermal cells. Human foreskin fibroblasts led to invasion of a transformed dermal cell line. This behaviour could be prevented by substitution of the fibroblast cell line (Kaur and Carter 1992).

Three-dimensional heterotypic models have also been applied to the field of cancer research. In 1997 Zhau and colleagues established a heterotypic model of human prostate cancer by co-culturing prostate fibroblasts and an epithelial prostate cancer cell line using a rotary culture system. They were able to show that the growth and differentiation response of the epithelial cells to androgen treatment resembled the response observed *in vivo* (Zhau, Goodwin et al. 1997).

Several studies investigated the interactions of mammary myoepithelial cells and luminal epithelial cells *in vitro* and were able to show the formation of polarised luminal cores covered by myoepithelial cells in 3D heterotypic cultures; thus recapitulating *in vivo* features (Runswick, O'Hare et al. 2001; Gudjonsson, Ronnov-Jessen et al. 2002). The addition of myoepithelial cells derived from breast cancer patients to luminal cell cultures however did not result in polarisation and lumen formation of mammary luminal cells (Gudjonsson, Ronnov-Jessen et al. 2002). These models were further developed by the addition of normal or tumour associated mammary fibroblasts. Normal mammary fibroblasts included in 3D heterotypic models of luminal and myoepithelial cells did not interfere with the formation of polarised luminal structures surrounded by myoepithelial cells. In these models normal fibroblasts covered the myoepithelial cells. Addition of cancer associated fibroblasts however prevented formation of organised structures and cells were found intermingled (Holliday, Brouilette et al. 2009).

In 2001 Kunz-Schughart and colleagues established a heterotypic model to recapitulate stromal and epithelial interaction of scirrhous breast cancers *in vitro*. This group has shown the potential of epithelial breast cancer cells to induce expression of αSMA in adjacent fibroblasts, which reflects the *in vivo* situation. However, only tumour derived fibroblasts but not normal skin fibroblasts responded with αSMA expression upon direct co-culture with epithelial breast cancer cells (Kunz-Schughart, Heyder et al. 2001). A further study of stromal and epithelial interactions in a breast cancer model demonstrated the ability of normal breast fibroblasts to inhibit growth of a non-tumourigenic and a malignant epithelial breast cell line. Cancer associated fibroblasts were also able to inhibit growth of the non-tumourigenic cell line while no growth inhibition could be observed in co-cultures with malignant epithelial cells (Sadlonova, Novak et al. 2005).

Heterotypic 3D models have also been applied to ovarian cancer research. The early stages of metastasis to the omentum were modelled *in vitro* utilising a heterotypic 3D model. Omental fibroblasts were embedded into a collagen gel and layered with omental mesothelial cells to recreate the *in vivo* structure of the omentum *in vitro*. Adhesion of an epithelial ovarian cancer cell line to this structure was then examined and reduced adhesion was observed upon addition of a MMP-2 inhibitor (Kenny, Kaur et al. 2008).

I.4 Tumour microenvironment

The importance of the microenvironment in tumour progression was recognised as early as 1889 when Paget formulated the seed and soil hypothesis after he observed preferential sites of metastasis in human breast cancer cases (Paget 1989). The ability of neoplastic cells to form metastases lies not only in the malignant cell itself but also requires a permissive environment. The important role of the microenvironment is further supported by findings that many humans carry benign neoplasms that never develop into cancer. Neoplastic lesions have been found in sections of the prostate in 44% of male patients in their forties (Sakr, Haas et al. 1993) and similarly, occult papillary carcinoma were found in 35% of sectioned thyroids. Due to the high incidence of occult papillary carcinomas of the thyroid these findings were even designated as normal (Harach, Franssila et al. 1985). These examples clearly indicate a role for the microenvironment in controlling malignant growth and it has therefore been proposed that the tissue phenotype is dominant over a cellular genotype.

While the microenvironment is able to suppress tumour development the reverse is also likely to be true. Altered signalling of the microenvironment has been shown to promote tumour development and will be described more closely in the following paragraph.

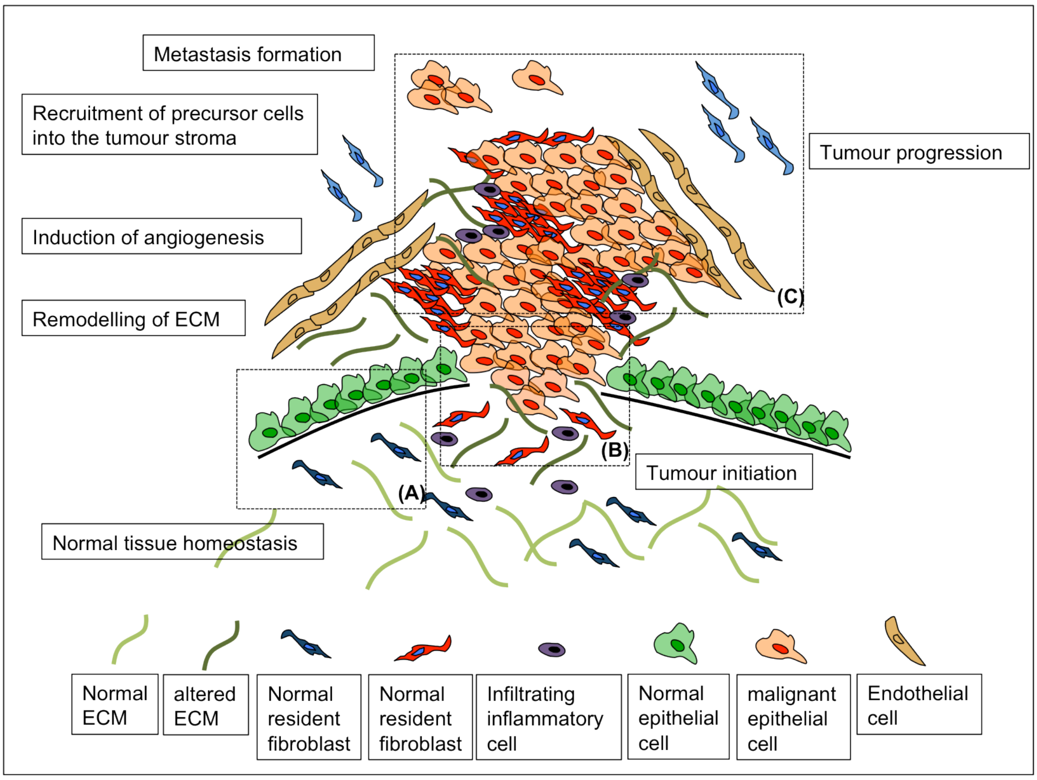

Figure I-4: Schematic view of tumour development. (A) Normal tissue homeostasis: Signalling between stromal cells, epithelial cells and the extracellular matrix (ECM) regulates cell behaviour ensuring correct tissue function. The basement membrane is intact. (B) Tumour initiation: Altered signalling between neoplastic epithelial cells and the stromal microenvironment induces tumour formation. Stromal cells become activated, the ECM is changing and supporting neoplastic cell growth. Inflammatory cells locate within the stroma. Ultimately the basement membrane is degraded. (C) Tumour progression: Malignant epithelial cells grow further and recruit a supporting stroma. Angiogenesis is induced to insure nutrient and oxygen supply of the growing tumour. The ECM is remodelled to support tumour growth. Inflammatory cells infiltrate the tumour microenvironment. Eventually, metastases are formed at distant organs.

I.4.1 Tumour development

(1) Normal tissue homeostasis

In normal tissues cell proliferation and differentiation is tightly controlled by complex signalling between the different cell types and the extracellular matrix (ECM). The proteinaceous ECM is produced by stromal and epithelial cells, provides a three-dimensional physical support structure and facilitates interaction between different cell types. Interactions occur via direct cell-cell contact as well as in a paracrine manner by secretion of soluble factors. For example epithelial cell polarity is tightly controlled by cell-cell interactions via adherence and tight junctions and is essential for the maintenance of normal tissue homeostasis (Figure I-4 A). The importance of the microenvironment has been underlined by studies highlighting its potential in directing cell development. In 1975 Mintz and co-workers injected mouse embryonal carcinoma cells into normal blastocysts and observed the development of normal mice (Mintz and Illmensee 1975). They found tumour cells involved in several tissues performing functions of normal cells thus indicating that a normal microenvironment has a profound influence on the behaviour of cells.

(2) Tumour initiation

The role of the microenvironment for tumour initiation is particularly apparent when studying chronic inflammation and cancer development as links between sustained inflammation and occurrence of cancer have been reported for several tumour types including gastric and liver cancer (Matysiak-Budnik and Megraud 2006; El-Serag 2012). Inflammatory cells found at the sites of wound healing express factors that promote cell proliferation, angiogenesis, ECM remodelling and possibly even promote genomic instability in nearby cells. Thus it is postulated that inflammation can induce somatic mutations within the epithelial cell population, which may then lie dormant until a secondary event leads to neoplastic formation (Coussens and Werb 2002).

A pioneering study by Olumi and coworkers explored the effects of different fibroblast populations on tumour formation in mice. Normal prostate fibroblasts or cancer associated fibroblasts were admixed with an initiated non-tumourigenic prostate epithelial cell line and co-injected into mice. Tumour formation was only observed in mice co-injected with CAFs (Olumi, Grossfeld et al. 1999). Interestingly CAFs did not induce tumour formation in non-initiated prostate epithelial cells after co-injection into mice. These observations indicate that tumour formation is a synergistic event requiring genetic changes in the epithelial cell component in conjunction with a promoting tumour stroma (Figure I-4 B).

(3) Tumour progression and metastasis

Cancer associated fibroblasts, the predominant cell type within the tumour stroma, have been shown to enhance tumour growth in *in vivo* and *in vitro* model systems. Orimo and coworkers have shown a promoting effect of CAFs on the growth of a human breast cancer cell line using a co-implantation mouse model. Tumour volume was significantly increased in combination with CAFs compared to normal fibroblasts. They further identified stromal derived factor 1 (SDF1) which is secreted by CAFs as the main mediator of tumour growth promotion (Orimo, Gupta et al. 2005).

Progression of tumours towards invasion and metastasis has also been linked to stromal contribution. The observation that myofibroblasts are often found at the invasive front of carcinomas supports this theory (Figure I-4 C). Additionally, a study by Karnoub and colleagues, demonstrated that bone marrow derived mesenchymal stem cells (MSCs) have a pro-oncogenic influence on breast cancer metastasis in a tumour xenograft model (Karnoub, Dash et al. 2007). This group also demonstrated that bone marrow derived human MSCs locate into the tumour stroma of a breast cancer model and promote metastasis through the secretion of CCL5. The contribution of MSCs to the tumour microenvironment is further described in the following paragraphs and explored in chapters 4 and 5.

I.4.2 Cancer associated fibroblasts - myofibroblasts

CAFs can be referred to as "activated fibroblasts", "myofibroblasts" or "reactive stroma". They express markers distinct from normal fibroblasts but similar to fibroblasts found at sites of wound healing (Serini and Gabbiani 1999; Mueller and Fusenig 2004). Based on these observations cancers have been described as "wounds that never heal" (Dvorak 1986). Myofibroblasts found at sites of wound healing often express proteins like α-smooth muscle actin (αSMA), vimentin, tenascin c and secrete SDF-1 (Figure I-5) (Sappino, Schurch et al. 1990; Orimo, Gupta et al. 2005). Myofibroblasts located within the tumour stroma have been shown to express similar proteins (Ronnov-Jessen, Petersen et al. 1995).

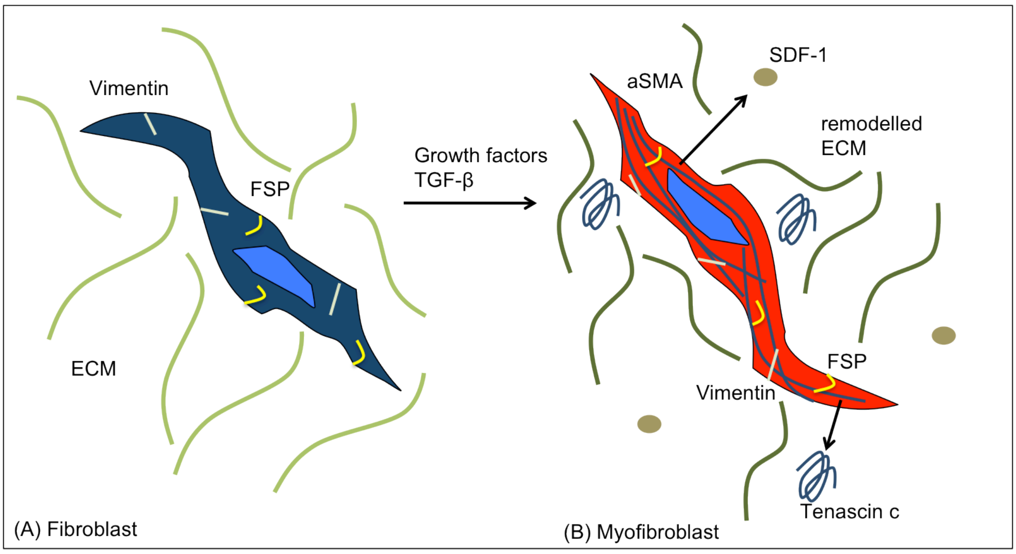

Figure I-5: Fibroblast activation. (A) Normal fibroblasts express markers like Vimentin and fibroblast specific protein (FSP) and produce extracellular matrix proteins. **(B)** Myofibroblasts (cancer associated fibroblasts; activated fibroblasts) show expression of α-smooth muscle actin (αSMA) in addition to FSP and Vimentin. They further produce different ECM proteins like Tenascin c and also secrete stromal derived factor 1 (SDF-1).

But not all CAFs show the same expression patterns and different combinations of markers have been described (Sugimoto, Mundel et al. 2006). Based on the aforementioned influences of CAFs on tumour development these cells pose an interesting and promising target for novel anti-cancer therapies. However, the interactions between stromal and epithelial cells within a tumour remain poorly understood. In particular the recruitment of stromal cells into the tumour microenvironment and the subsequent conversion into tumour supporting fibroblasts remains unclear. Several different cell types have been proposed as the cell of origin of CAFs (Figure I-6), including:

(1) Resident fibroblasts

A popular theory claims that normal resident fibroblasts can serve as the precursor cells of CAFs (Kalluri and Zeisberg 2006; Orimo and Weinberg 2006; Mueller, Goumas et al. 2007). This theory is supported by studies showing that treatment of resident fibroblasts with tumour conditioned medium or TGF-β can lead to the expression of myofibroblast markers like αSMA (Ronnov-Jessen and Petersen 1993; Kojima, Acar et al. 2010) and to a tumour promoting phenotype of the resulting myofibroblasts.

(2) Epithelial to mesenchymal transition

Another proposed origin of CAFs is epithelial to mesenchymal transition (EMT) of the epithelial cancer cells. EMT was first discovered during embryogenesis and describes the conversion of epithelial cells to mesenchymal cells during organ formation. This process goes in hand with loss of epithelial markers (keratins), increased mobility and the expression of mesenchymal markers (Vimentin, FSP, αSMA). EMT also plays an important role in tissue repair during wound healing and is thought to be involved in tissue fibrosis (Kalluri and Weinberg 2009).

Cancer cells are thought to be able to endogenously produce a tumour supporting stroma to encourage tumour growth. EMT has been observed in human mammary carcinomas and αSMA expression was confirmed in the resulting mesenchymal cells. Further *in vitro* evidence showed a tumour promoting effect of this αSMA expressing subpopulation (Petersen, Nielsen et al. 2003).

(3) Endothelial to mesenchymal transition

The discovery of endothelial to mesenchymal transition (EndMT) suggests that these cells can also serve as progenitor cell of CAFs. Using mouse endothelial cells it was possible to induce CAF features (FSP expression) after treatment with TGF-β. At the same time downregulation of the endothelial marker CD31 was observed suggesting a transition of an endothelial phenotype towards a fibroblastic phenotype (Zeisberg, Potenta et al. 2007).

(4) Mesenchymal stem cells

Mesenchymal stem cells (MSCs) have recently been implicated as a potential source of CAFs. MSCs are multipotent circulating bone marrow derived cells that can differentiate into osteocytes, chondrocytes, myocytes and adipocytes. It has been shown that MSCs locate preferentially into the tumour stroma (Studeny, Marini et al. 2002). Further studies reported transdifferentiation of human MSCs into αSMA expressing myofibroblasts after treatment with TGF-β or conditioned medium from different tumour cell lines (Emura, Ochiai et al. 2000; Karnoub, Dash et al. 2007; Mishra, Mishra et al. 2008; Spaeth, Dembinski et al. 2009).

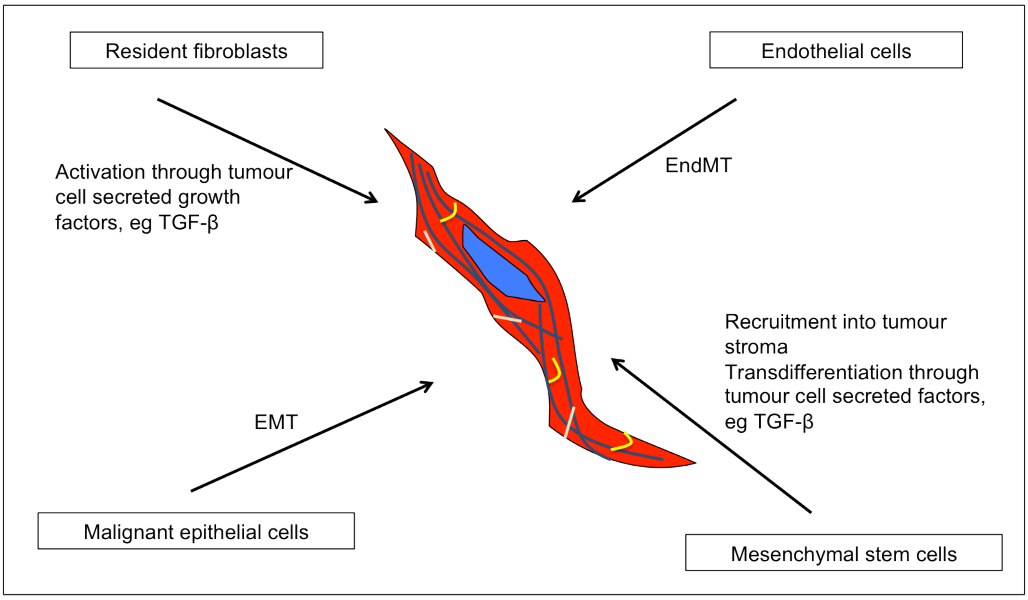

Figure I-6: Overview of potential precursor cell types of cancer associated fibroblasts.

Taking these reports together it seems likely that the cancer associated fibroblast population is heterogeneous with fibroblasts being recruited from several sources (Sugimoto, Mundel et al. 2006). It is also very likely that the tumour cells recruit supporting stroma from different sources during tumour formation, corresponding with the stage of tumour development and progression. CAFs are an attractive target for anti-cancer therapy since they are more genetically stable and are therefore less able to evolve drug resistance, which is a common problem with malignant epithelial cells. TGF-β has been reported to stimulate the generation of fibroblasts into CAFs (De Wever and Mareel 2003). The effects of TGF-β however are very context-dependent and range from tumour suppressive to tumour promoting. Thus, TGF-β signalling would be very difficult to target therapeutically. It is clear that it is essential to better understand the recruitment mechanism of CAFs by epithelial cancer cells and to identify the signals by which the CAFs are directed to form parts of the tumour stroma. Understanding the pathways involved in the differentiation of CAFs from CAF precursor cells will hopefully lead to the development of novel therapies targeting the recruitment of cells into the tumour stroma, hence weakening the support network neoplastic epithelial cells rely on.

I.4.3 Implications for treatment

The potential for targeting the supporting tumour microenvironment with anti-cancer therapies is a promising strategy, which is being explored widely. Several drugs targeting cells within the tumour stroma have been developed and are currently used in therapy or undergoing clinical trials. The angiogenesis inhibitor bevacizumab is an approved inhibitor of VEGF-A and prevents signalling between tumour cells and endothelial cells thus inhibiting angiogenesis (Ferrara, Hillan et al. 2004). In a mouse model of pancreatic ductal adenocarcinoma it was shown that the combinational treatment with a conventional chemotherapeutic drug and a small molecule inhibitor targeting the tumour stroma improved response rates (Olive, Jacobetz et al. 2009). The small molecule inhibitor IPI-926 inhibits hedgehog signalling between malignant epithelial cells and supporting stromal cells and leads to the depletion of desmoplastic stroma within the tumour. This in turn is thought to aid distribution of the chemotherapeutic agent and hence improve its effect. The inhibitor IPI-926 is currently undergoing phase 2 clinical testing. A summary of some drugs targeting the tumour microenvironment can be found in Table I-3.

Table I-3: Examples of some drugs currently in praxis or clinical trials that target the tumour microenvironment.

Drug name	Target and function	Reference
Bevacizumab	Antibody to VEGF-A; inhibits angiogenesis; approved for treatment of breast and ovarian cancer	(Ferrara, Hillan et al. 2004)
Sorafenib (BAY 43-9006, Nexavar™)	Multiple kinase inhibtor (Raf kinase, VEGFR, PDGFR); anti-tumour activity in xenograft models; approved for treatment of liver and kidney cancer	(Wilhelm, Carter et al. 2004)
AMD070	CXCR4; blocks tumour stroma interactions by inhibiting CXCR4 (specific receptor for SDF1); clinical trials	(Burger and Peled 2009)
IPI-926	Hedgehog signalling is inhibited; small molecular inhibitor; clinical trials	(Olive, Jacobetz et al. 2009)

With the discovery of carcinomas *in situ* that lie dormant for several years in organs including the breast, prostate and thyroid and may never develop into malignant cancers, it is obvious that the microenvironment must play a crucial role in controlling and suppressing malignant progression. Verified by functional studies showing the effect of a normal microenvironment on the behaviour of malignant cells it is now clear that the tumour environment holds the key in controlling cancer development, which has been postulated by Mina Bissel since the 1980s. She proclaims that by unravelling the interactions between the different cell types within a tumour it is ultimately hoped to develop therapies aiming at restoring signalling to a normal tissue microenvironment and thus controlling malignant cell growth, converting cancer to a chronic disease (Bissell and Hines 2011).

I.5 Aims of the Thesis

Advances in the treatment of epithelial ovarian cancer have been slow. This is in part due to our lack of understanding of the biology of the disease. The overarching theme of my thesis is to develop relevant *in vitro* models of EOC that can be used to advance our knowledge of cancer biology and aid in the development of novel therapeutics. Three-dimensional cell culture models are a promising tool for creating *in vitro* models of disease that more closely resemble the *in vivo* state than traditional monolayer cultures. Furthermore, cancer cell lines that have been cultured *in vitro* for a prolonged time, are likely to have undergone culture induced genomic changes and do not represent the primary tumour accurately. One aim therefore, described in chapter 3, was to establish 3D models of novel primary epithelial cancer cell lines and compare the characteristics of these cells to traditional 2D culturing methods.

To create cell culture models that are even more representative of the *in vivo* tumour it is necessary to incorporate cell types that are usually found within the tumour microenvironment. In chapter 4 I describe the establishment of heterotypic 3D models of epithelial ovarian cancer. I go on to describe interactions of stromal and epithelial cells and the 3D structure of heterotypic 3D spheroids.

Finally, the study aimed to identify potential precursor cell types of cancer associated fibroblasts in epithelial ovarian cancer. Mesenchymal stem cells and normal resident fibroblasts have been implicated as the source of cancer associated fibroblasts before. In chapter 5 I describe the potential of these cell types to transdifferentiate and express markers associated with tumour stromal fibroblasts.

.

II Material and Methods

II.1 Cell culture methods

II.1.1 Establishing primary ovarian cancer cell lines

At University College London Hospital (UCLH) fresh tumours were collected with informed consent from patients under the approval of the UCL/UCLH ethical committees. The tumour specimen were cut into 1mm small pieces and cultivated in medium 199 and MCDB 105 (1:1 ratio) (Sigma) at 37ºC and 5% CO_2. The medium was supplemented with 15% foetal bovine serum (FBS) (Lonza) and 200mM L-Glutamin (Invitrogen). Following 1-2 weeks of incubation, colonies were picked using either paper cloning discs (Sigma) or cloning cylinders (Sigma). When cells reached confluency they were sub-cultured according to standard trypsinisation protocols using 0.25% Trypsin-EDTA (Invitrogen). Frozen stocks were prepared by resuspending pelleted cells in FBS containing 1% di-methyl-sulfoxide (DMSO, Sigma). The ampoules were placed within a Mr. Frosty (Jencons) in an -80ºC freezer overnight before transferring into liquid nitrogen for long term storage.

Complete Medium: 250ml Medium 199
250ml Medium 105
75ml FBS (15%)
6ml Glutamine (200mM final conc.)

II.1.2 Establishing primary ovarian cancer associated fibroblast cell lines

Fresh epithelial ovarian tumours were collected at University College Hospital. With the help of a pathologist an area containing predominately stromal cells was identified and a piece was dissected and transferred to a tissue culture plate. Several approaches to isolate fibroblasts from the tumour tissue were tested. (Castello-Cros and Cukierman 2009)

Firstly, a piece of the tissue was transferred into a tissue culture dish and minced into very small pieces. Complete medium was added and the cells were incubated at 37ºC and 5% CO_2 for several days. Cell growth was monitored closely and medium was replaced regularly. This approach resulted in mixed populations of epithelial and stromal cells. Fibroblasts were isolated via subcloning using paper cloning discs or cloning rings (both Sigma). Differential trypsinisation was also used to isolate fibroblasts from a mixed plate. The cells were washed with PBS before adding 0.25% Trypsin-EDTA (Invitrogen) and incubated for 1min at 37°C. When the fibroblasts started to detach while the epithelial cells were still attached the trypsin was removed with the fibroblasts and transferred onto a new dish and complete medium was added. The cells were then left to incubate and cell growth was observed while replacing the medium every 2-3 days.

Another way of isolating fibroblasts from tumour tissue is to use their ability to migrate out of the tissue. A grid was scratched into the surface of a tissue culture plate using sterile scalpel blades. The tumour tissue was minced and a small piece of tissue was placed onto the scratched surface of the culture dish and allowed to attach for a few minutes before adding culture medium. Fibroblast growth was observed under an inverted microscope and cells were subcultured when they reached ≥ 50% confluency.

Primary normal cell lines are subject to replicative senescence and immortalisation is necessary to keep them in culture for prolonged times. Homogenous fibroblast populations were immortalised using lentiviral or retroviral hTERT infection.

II.1.3 Culturing mesenchymal stem cells

Mesenchymal stem cells (MSCs) were obtained from the Texas A&M Health and Science Centre and cultured in complete culture medium (CCM) containing α-MEM (Invitrogen) and MSC qualified FBS (Invitrogen). The medium was also supplemented with L-Glutamin, Penicillin/Streptomycin and Gentamicin (all Invitrogen). To retain the differentiation ability of the MSCs, cells were always kept at low densities. 60 cells/ cm^2 were expanded for 10 – 15 days before freezing in special medium containing DMSO (Sigma) for long term storage.

<u>Complete culture medium:</u> 500ml α-MEM
100ml MSC qualified FBS
6ml L-Glutamine
6ml Penicillin/Streptomycin
60μl Gentamicin

Freezing medium: 65ml α-MEM
30ml MSC qualified FBS
5ml DMSO
1ml Penicillin/Streptomycin

II.1.3.1 Quality control assays

(1) Colony formation

To establish the ability of single cells to form colonies, cells were plated at a clonal density and left to grow for 2 – 3 weeks. 100 cells were seeded into a well of a 6-well plate or a P100 and cultured at 37ºC/5% CO_2 with complete culture medium for 2 – 3 weeks while refeeding once a week. The appearance of colonies was checked regularly under an inverted microscope. After the incubation period the medium was taken off and the cells were fixed with 100% Methanol for 5min before washing with phosphate buffered saline (PBS). The colonies were stained with coomassie brilliant blue stain (BDH) for 5min. Excess stain was removed by washing with water and stained colonies were counted.

1 x PBS: 8g NaCl
0.2g KCl
1.44g Na_2HPO_4
0.24g KH_2PO_4
pH 7.4
add distilled water to 1l

Coomassie Brilliant Blue Solution: 2g Coomassie Brilliant Blue
1l distilled water

(2) Adipocyte and Osteocyte differentiation

50.000 cells were plated into each well of a 6-well plate and cultured until confluent. The culture medium was replaced and the cells were washed twice with PBS before adding 2ml of adipocyte/osteocyte differentiation medium (both Invitrogen). 2ml of complete culture medium was used as a control. The cells were left to incubate for 21 days and medium was replaced every 4 days. At the end of the incubation time the medium was removed and the cells were washed with PBS before fixation in buffered formalin for 1 hour at room temperature.

Adipocyte staining: Oil-Red-O working solution was prepared by mixing 3 parts of stock solution with 2 parts of PBS. After mixing well, the solution was left to stand for 10min before filtration through a 0.45μm syringe filter. The flow through was left to stand for another 10min before it was ready to use. The fixed cells were washed with PBS before adding 2 ml Oil-Red-O (Sigma) working solution to each well. After 20min of incubation the stain was removed and the wells were washed with PBS until the background was clear. The cells were examined microscopically for adipocyte differentiation.

Osteocyte staining: After fixation cells were washed with deionised water and 2ml of Alizarin Red (Sigma) was added and incubated for 20min. The cells were then washed with deionised water until the background was clear and examined microscopically for osteocyte differentiation.

Oil-Red-O stock solution:	2.5g Oil-Red-O
	500ml Isopropanol
Oil-Red-O working solution:	3x Oil-Red-O stock solution
	2x PBS
	filter through sterile filter unit
Alizarin Red S solution:	1g Alizarin Red S
	100ml distilled water
	filter through sterile filter unit

II.1.4 Culturing immortalised ovarian surface epithelial cells and immortalised normal ovarian fibroblasts

Immortalised ovarian surface epithelial (IOSE) cells and immortalised normal ovarian fibroblasts (INOFs) were isolated and established in our lab and culture conditions were optimised (Lawrenson, Benjamin et al. 2009; Lawrenson, Grun et al. 2010). IOSE cells were cultured in medium 199 and medium 105 (both Sigma) at a 1:1 ratio. The medium was supplemented with 15% FBS, 34μg protein/μl bovine pituitary extract (BPE) (both Invitrogen), 5μg/μl Insulin, 10ng/μl epidermal growth factor (EGF) and 0.5μg/μl hydrocortisone (all Sigma).

INOF cells were cultured using the same medium as for the primary epithelial ovarian cancer cell lines (II.1.1).

II.1.5 Gene delivery

To manipulate cell lines it might be necessary to add a gene of interest. This can be achieved with the following techniques.

II.1.5.1 Transfection

To transfect cells FuGENE® 6 (Roche) was used according to manufacturers recommendations. Briefly a 3:1 ratio of transfection reagent to DNA was achieved by adding 18µl of reagent to 582µl of serum free medium without touching the walls of the sterile microfuge tube. The mixture was mixed by vortexing for 1 second and incubated at room temperature for 5min. 6µg of DNA was added and the tube was vortexed for another second and then incubated for at least 15min at room temperature. The transfection-DNA complex was added dropwise to the target cells without the need to remove the culture medium. To achieve even distribution the plate was swirled around carefully and returned to the incubator. Selection of transfected cells was started after 2-3 days.

II.1.5.2 Viral Infection

(1) Production of lentiviral supernatant

A second generation self inactivating (SIN) lentiviral system was used containing three plasmids. The packaging vector pCMV-8.91 contains the sequences *gag*, *pol*, *tat* and *rev* coding for the capsid protein, the reverse transcriptase and integrase, the transactivator and the rev protein promoting nuclear export and stabilisation of the mRNA. The envelope vector pMD.G codes for the *vsv* envelope protein that is necessary for the virus to enter the host cell. The third vector pSIN contains the gene of interest and the expression enhancing woodchuck hepatitis post-transcriptional element (WPRE) flanked by the long terminal repeats (LTRs) which contain regulatory regions.

The human kidney cell line 293T was used to produce the virus. A confluent P100 plate of cells was split 1:7 one day prior to transfection. The next day the cells were washed carefully with PBS and 8ml of Opti-MEM® (Invitrogen) was added. To transfect cells 3µl of Fugene per µg of DNA was used. The total amount of DNA was 5µg consisting of 2µg gene of interest DNA, 1.5µg pCMV-8.91 and 1.5µg of pMD.G. Briefly, 15µl of Fugene was added to 35µl of Opti-MEM® without touching the wall of the tube, mixed and incubated at room temperature for 5min.

Appropriate amounts of DNA were also mixed together and brought to a total volume of 50µl with Opti-MEM®. Both mixtures were combined and incubated at room temperature for 20-30min. The solution was then added dropwise to a P100 dish and the cells were returned to the incubator. After 5h the Opti-MEM® was removed and 10ml of normal culture medium (DMEM, 10% FBS, 1x Penicillin/Streptomycin; all Invitrogen) was added. The cells were then left in the incubator to produce virus. After 48h of incubation the virus containing medium was taken off and filtered (0.45µm, Millipore) to remove any cell contaminations. The viral supernatant was stored in 1ml aliquots at -80°C. The virus producing cells were re-fed with 10ml of normal culture medium and left to incubate for another 12h before repeating the virus harvesting. Any virus left on the plates was eradicated by washing the plates with Virkon (VWR) before disposing them for incineration. Every item that came in touch with the viral supernatant was disposed in the same way. Any spill was also cleaned very carefully using Virkon and water.

Gene of interest Vectors: pSIN-GPF (Chris Boshoff's Lab)
LeGo-T2 (Lentiviral Gene Ontology Vectors, Kristoffer Weber, www.lentigo-vectors.de)
Lenti-hTERT-EGFP (Akimov, Ramezani et al. 2005)

(2) Production of retroviral supernatant

The pVPack vectors from Stratagene have been used to produce retroviral supernatant. The packaging vector pVPack-GP encodes for *gag* and *pol* and the vector pVPack-10A1 for the envelope protein. The vector p.Babe.hygro.hTERT contains the sequence for the gene of interest (hTERT: human telomerase reverse transcriptase) and an antibiotic resistance gene (hygro: hygromycin resistance).

The human kidney cell line 293T was chosen to produce the viral supernatant. 2µg of each vector were combined and used to transfect the 293T cells. FuGENE® 6 was used as the transfection agent as described above (II.1.5.1). Transfection was performed in the evening and the medium was replaced with normal growth medium the following morning. The cells were left to incubate for 48 hours before harvesting the first batch of viral supernatant. The supernatant was filtered through a 0.45µm syringe filter, aliquoted, snapfrozen using dry ice and isopropanol (VWR) and stored at -80°C. After an additional 24 hours the second batch of viral supernatant was harvested, filtered, aliquoted and snapfrozen as described above.

(3) Infection

Target cells were split one day prior to infection to achieve 50%-70% confluency. On the day of infection the culture medium was removed and 3ml of viral supernatant per P100 plate was added. 3ml of serum free medium containing 16μg/ml polybrene (Sigma) was added to achieve a final polybrene concentration of 8μg/ml. The cells were returned to the incubator over night. The next morning the viral supernatant was removed and standard growth medium added. To select successfully infected cells one of the following methods was used.

Antibody selection: If the viral genome contains an antibiotic resistance it is possible to select successfully infected cells by using the appropriate antibiotic. The optimal concentration of antibiotics has to be evaluated for each individual cell line and each individual antibody. Kill curves have to be performed using various concentrations of antibiotics. Briefly, cells were plated into each well of a 6-well plate and left to grow over night. The next day the medium was removed and the cells were re-fed with different concentration (1-100units/ml) of the antibiotic hygromycin B (Calbiochem). The cells were left to grow for 10 days while the medium was replaced regularly. After 10 days the cells were fixed in 10% methanol (VWR), washed in PBS and stained using Coomassie Brilliant Blue (Sigma) to determine the lowest concentration of antibiotic to kill all cells in a well. This concentration was then used to select successfully infected cells. 30units/ml of hygromycin was added to the normal growth medium and infected cells were cultured for a couple of weeks. Colonies of infected cells were picked and transferred to a P60 (Greiner) dish for expansion.

FACS sorting: Cells infected with fluorescent proteins can be selected using fluorescence activated cell sorting (FACS). This method provides the opportunity to separate a heterogeneous cell population according to their fluorescent characteristics. Briefly, a confluent plate of infected cells is trypsinised as described above (II.1.1) and resuspended in PBS to an appropriate cell number ($0.5\text{-}2x10^{6}$cells/ml). The cell suspension is pipetted up and down to ensure it is a single cell suspension and kept on ice until sorting. Uninfected cells serve as a reference. The sorting is performed by the scientific support services of the Wolfson Institute for Biomedical Research. Selected cells were collected in the appropriate medium supplemented with gentamicin to prevent contamination and transferred to a tissue culture dish. Cells were then expanded and stocks of positively infected cells were frozen.

II.2 Characterisation of cell lines

II.2.1 Anchorage dependent assays

The doubling times of all cell lines were determined by two week growth assays. 10^5 cells were plated in P60 cell culture dishes (Greiner). The assay was performed in triplicates and when cells reached confluence, cultures were passaged accordingly. The population doublings were calculated using the following formula:

$$PD = \log [\text{total cell number} / \text{initial cell number}] / \log 2$$

II.2.2 Anchorage independent assays

Soft agar assays measure the ability of a certain cell type to grow anchorage independent in semi-solid medium. A base layer is prepared using complete medium and 0.6% noble agar (Sigma) solution. After the base layer becomes solid the top layer is added. The top layer contains complete medium and 0.3% noble agar solution and a certain number of cells optimised for each cell line. After the top layer hardens the plates are incubated at 37ºC/5%CO_2 for three weeks and colony growth is measured at several timepoints. Colonies were visualised by adding staining solution and left over night at 37ºC/5%CO_2. Red stained colonies over approximately 50 cells were counted. The colony forming efficiency (CFE) was calculated based on the following formula: CFE = number of colonies counted/number of cells plated x 100%.

3% agar solution: 0.33g noble agar (Sigma)
100mg bactopeptone (Sigma)
add 10ml of distilled water

6% agar solution: 0.66g noble agar (Sigma)
100mg bactopeptone (Sigma)

staining solution: 1mg/ml p-iodonitrotetrazilium violet (Sigma) in methanol

II.2.3 Migration assays

Migration assays measure the ability of different cell types to migrate through a porous membrane towards a chemoattractant. 30,000 cells in serum free medium were plated in triplicates in 24-well thincerts (Greiner) with a membrane pore size of 8µm. The inserts were placed in 24-well plates containing 10% FBS as a chemoattractant and incubated at 37ºC/5%CO_2 for 24h. After incubation time, the remaining non-migrated cells were removed from the insert. To analyse the number of cells migrated through the membrane, the QCM™ 24-well cell invasion assay kit (Millipore) was used. The detection was performed according to manufacturers' protocol and relative fluorescence units were measured using a Varioskan Flash (Thermo Scientific) plate reader and SkanIt software (Thermo Scientific).

II.2.4 Invasion assays

Invasion assays determine the capability of cells to invade through a basement membrane model. The following assays were used and each assay was performed in triplicates:

1) 24-well invasion chambers coated with Matrigel™ (BD Bioscience) were used to assess the invasive ability of cancer cells. The invasion assay was performed according to manufacturers' instructions. 30,000 cells were plated per invasion chamber in 500µl serum free medium. The chambers were placed in a 24-well plate containing 750µl 1%BSA in serum free medium as a chemoattractant and incubated at 37ºC/5%CO_2 for 20h. After the incubation time non-invading cells were removed and invaded cells were stained using the Diff-Quick Staining kit (BDBioscience). The membrane containing the stained cells was excised and mounted on a microscope slide using DPX mounting medium (BDH). Invaded cells were counted using a 100x magnification.

2) The QCM™ cell invasion kit from Millipore was used and the assay was performed according to manufacturers instructions. 125000 cells were plated in 24-well inserts comprising an ECMatrix™ and incubated at 37ºC/5%CO_2 for 24h. Non-invaded cells were removed from the insert and the invaded cells were identified using the fluorimetric detection method according to manufacturers' protocol. The relative fluorescence units were read on a Varioskan Flash plate reader with SkanIt software.

II.2.5 Heterotypic migration and invasion assay

Standard migration and invasion assays as described above (II.2.3, II.2.4) were modified. Instead of the chemoattractant 90,000 fibroblasts or mesenchymal stem cells (MSCs) were plated into the wells of a 24-well plate and left to grow for 24 hours. The migration and invasion chambers were then placed on top of the fibroblasts/MSCs and assays were performed as described above using the Millipore assay.

II.2.6 2D and 3D Proliferation assay

Thiazolyl blue tetrazolium bromide (MTT) (Sigma) was used to determine the proliferation rate of cell lines in 2D cultures. The assay was performed in 24-well plates (Greiner). To measure proliferation the culture medium was taken off and replaced with 500µl of a 1:10 MTT dilution (stock solution 5mg/ml) in serum free medium. After 4 hours of incubation at 37ºC/5%CO_2 the MTT solution was removed and 500µl of dimethyl sulfoxide (DMSO) (Sigma) was added to solubilise the dye. Absorbance was measured at 570nm with a background substraction at 650nm using the Varikosan Flash plate reader.

MTT stock solution: 250mg MTT
50ml serum free medium

AlamarBlue® (Invitrogen) was used to determine the proliferation rates of cell lines grown in 2D or 3D. The active ingredient of alamarBlue® is converted into a fluorescent molecule by viable cells. For 2D proliferation assays 4,000 cells were plated per well of a 12-well plate and for 3D proliferation assays cell numbers were optimized at 10,000 per well. 10% of alamarBlue® was added to each well and fluorescence was measured every 24 hours using a Varioskan plate reader (Thermo). As a control cell free medium with 10% alamarBlue® was used.

II.2.7 Characterisation of marker expression

II.2.7.1 Immunofluorescence/-histochemistry staining

Live cell staining: Cells were cultured on round glass-coverslips (VWR) and prior to staining, coverslips were washed with PBS/1% bovine serum albumin (BSA, Sigma). The cells were then fixed using ice-cold 3% formaldehyde (BDH) for 10min, rinsed well in PBS, and permeabilised for 5min at room temperature in PBS/0.5%BSA/0.5%Triton-X-100 (Sigma). The cells were then washed thoroughly with PBS and incubated with PBS/1%BSA for 30min to block unspecific binding sites. Antibodies were diluted in PBS/1%BSA and applied for 1hour after which the coverslips were washed with PBS/1%BSA and the secondary antibody was added for 30min. The remaining antibody was washed off and Evans blue (Sigma) was added and left to incubate for 10min. The coverslips were washed again and transferred onto microscope slides with mounting medium containing DAPI (Vectashield) and sealed with a square coverslip. The slides were incubated for 30min before images were captured using a fluorescence microscope (Olympus BX61) with the Cytovision software.

Primary antibodies			
Name	Abbreviation	Description	Dilution
Cytokeratin 7	Ck7	Epithelial marker	1:1000
Epithelial Antigen	BerEp4	Epithelial marker	1:1000
Pan-cytokeratin	AE1/AE3 (DAKO)	Epithelial marker	1:1000
Fibroblast surface protein	FSP (Sigma)	Fibroblast marker	1:1000
Anti Smooth muscle actin	αSMA (Dako)	Myofibroblast marker	1:1000
Cancer antigen 125	Ca125 (Dako)	Tumour marker	1:1000
Vimentin	Vimentin (cruk)	Epithelial/fibroblast cells	1:500
Secondary antibodies			
Alexa Fluor 488 IgG (Invitrogen)		goat anti-mouse	1:400
Alexa Fluor 488 IgM (Invitrogen)		goat anti-mouse	1:400

Immunocytochemistry/Immunohistochemistry: Paraffin embedded tissue sections and formalin fixed sections of multicellular spheroids (MCS) were sectioned and stained either at University College London Hospital Clinical Diagnostics Unit or at the Histology Service at Cancer Research UK (CRUK).

II.2.7.2 Western blot analysis

Cells were grown until 80% confluent before washing twice with ice-cold PBS. 100μl lysis buffer was added to P100 dishes and cells were lysed and collected using a cell scraper (Greiner). The whole cell lysate was transferred into a 1.5ml microfuge tube and cell debris was removed by centrifugation at 13.000rpm for

30min at 4°C. Protein concentration was determined using a Bradford assay (Pierce) and samples were normalised using lysis buffer. For SDS-gelelectrophoresis samples were denatured and reduced in Laemmli Buffer (Sigma) and boiled at 105°C for 5min. 10μg of each sample was run onto 8-16% precise protein gels (Pierce) at 150V for 45min. The BioRad system was used to blot the proteins onto a polyvinylidene fluorid (PVDF) membrane. The membrane was soaked in methanol before setting up the blot and transfer buffer was used during electroblotting at 100V for 1hour. The membrane was then blocked in TBS-T/2% BSA for 1hour or over night before incubation with the first antibody diluted in TBS-T for 1 hour. The antibody was removed by washing the membrane in TBS-T three times for 15min. The appropriate secondary horseradish peroxidase coupled secondary antibody was diluted in TBS-T and applied for 1hour. After the incubation time the membrane was washed again in TBS-T three times for 15min. To visualise the protein bands the enhanced chemiluminescence liquid (Pierce) was added and the membrane was exposed to chemiluminescence detection film.

Primary antibodies			
Name	Abbreviation	Description	Dilution
Anti Smooth muscle actin	αSMA (Dako)	Myofibroblast marker	1:1000
actin	actin (Sigma)	loading control	1:5000
Secondary antibodies			
Anti-mouse IgG HRP-coupled (Sigma)		1:5000	

II.3 3D cultures

II.3.1 Rotary cell culture system

The rotary cell culture system (RCCS, Synthecon) was used to promote cell aggregation in three-dimensional (3D) multicellular spheroids (MCS). The culture vessels were used according to manufacturers' instructions. 200,000 cells/ml were seeded into a 10ml disposable vessel and cultured rotating constantly at 5%Co_2/37ºC. Gas exchange takes place through an integral gas diffusion membrane.

To facilitate cell growth Hillex® II H112-170 microcarriers (SoloHill Engineering, Inc.) coated with cationic trimethyl ammonium and gelatin coated FACT III microcarriers (SoloHill Engineering, Inc.) were tested. The beads were autoclaved and resuspended in medium before incubating for 1h at 37ºC. Microcarriers were then added to the culture vessel at 5mg/ml for Hillex® and 10mg/ml for FACT III. Furthermore, ECM Gel from Engelbreth Holm-Swarm mouse sarcoma (Sigma) was used. The ECM gel was defrosted in the fridge overnight. 1ml of the gel was diluted 1:2 in Medium199 (Sigma) and used for a 10ml 3D vessel. The gel was added to the vessel just before inoculating with 200,000 cells/ml and the cells were grown for approximately 4 weeks to form MCS. To re-feed rotation was stopped for approx 20min until cells settled at the vessel bottom. The medium was then removed carefully to not destroy or remove any MCS before adding fresh complete medium. After the spheroids reached the desired size they were fixed in formalin and sent of to cancer research united kingdom (CRUK) histology service for processing into paraffin blocks.

II.3.2 Poly-HEMA coated tissue culture plastics

Poly-2-hydroxyethyl methacrylate (PolyHEMA, Sigma) was suspended in 95% Ethanol and dissolved by heating at approximately 60ºC. PolyHEMA solution was used to coat tissue culture plates to prevent cells from attaching. Tissue culture plates/flasks were coated twice and left until completely dry. Before use, plates were washed with PBS to remove any excess ethanol. Cells were then plated at appropriate densities and re-fed regularly. To re-feed cultures, flasks were left at an angle for cells to gather in one corner. The medium was removed carefully and replaced by fresh culture medium. After 1 - 3 weeks MCS were harvested and fixed in formalin. The agarose pellets were sent to Histology Service at Cancer Research UK or Histology Service at University College Hospital for embedding into paraffin.

Poly-HEMA: 1.5% polyHEMA
1 litre 95% Ethanol

II.3.3 Hanging droplet cultures

To achieve formation of same size spheroids the hanging droplet approach was chosen. An appropriate number of cells was placed into each well of a Nunc® MicroWell® 72 well MiniTray (Sigma) using 35μl medium per well. The tray was then inverted carefully leaving the cells suspended in a drop of medium. To avoid rapid evaporation of the culture medium, the tray was kept in a humid environment. To achieve that, the tray was placed together with an open P60 containing sterile water in a P150 tissue culture dish (Greiner) and incubated at 37°C/5%CO_2. To re-feed the cultures, the trays were inverted carefully and the desired amount of medium (usually 10-20μl) was added. Spheroid formation was observed under an inverted microscope. At the end of the incubation time the spheroids were transferred for subsequent analysis using a pipette with wide opening to not destroy any spheroids.

II.3.4 Heterotypic 3D cultures

II.3.4.1 Cell labelling

Cells were labelled using the fluorescent proteins tdTomato (red) and green fluorescent protein (GFP). The protein tdTomato is a tandem dimer with an excitation of 554nm and an emission of 581nm. GFP has an excitation peak at 488nm and the emission peak at 509nm. A mutant version of GFP leads to enhanced fluorescence (EGFP) with the excitation peak shifted to 490nm and the emission peak kept at 509nm. Lentiviral vectors expressing these fluorescent proteins were used to produce lentiviral supernatant (II.1.5.2(1)) and target cells were infected with the produced virus as described above (II.1.5.2).

II.3.4.2 3D cultures

Single cells suspensions of labelled stromal and epithelial cells were prepared and cell numbers determined using a hematocytometer. Both cell types were seeded onto the polyHEMA coated tissue culture plastics at a ratio of 3:1 stromal:epithelial cells (e.g. 375,000 stromal cells: 125,000 epithelial cells). Where the two cell types required different culture media both were used and mixed at a 1:1 ratio. Cultures were re-fed every couple of days as described above (II.3.2).

For production of same size heterotypic 3D cultures the hanging droplet method was used as described above (II.3.3). In this approach 12,000 stromal cells were plated first to allow formation of a stromal core. After 1 week of spheroid formation 4,000 epithelial cells were added to each spheroid and incubation went on for 1 day up to 1 week. To analyse the heterotypic cultures, spheroids were transferred using a pipette with a wide opening.

II.3.5 Characterisation of 3D cultures

II.3.5.1 Preparation of MCS for H&E staining and immunohistochemistry

Spheroids were grown as described above (II.3.4.2), fixed in formalin and sent for paraffin embedding to University College Hospital Histology Services. Immunohistochemistry was performed at the Advanced Diagnostics Laboratory at University College Hospital.

II.3.5.2 Confocal microscopy

Spheroids grown on polyHEMA coated tissue culture plastics were harvested and fixed in formalin as described before (II.3.2). Spheroids obtained using the hanging droplet approach were used for confocal microscopy without prior fixation step. A drop of 2% agarose was applied to a glass microscope slide and the spheroids were put into the middle. Anti-fade mounting medium (Vectashield) was added and a coverslip applied. The coverslip was sealed using clear nail varnish to prevent drying and to allow oil microscopy.

II.3.5.3 Flow cytometry

Sample Preparation: Cultures for flow cytometry were spun to collect the spheroids. To prepare a single cell suspension, the spheroids were resuspended in 1 ml of accutase (eBioscience) and incubated for approximately 30min at 37°C. To aid spheroid dissociation the suspension was pipetted up and down several times during incubation. The single cell suspension was transferred to a 1.5 ml microfuge tube and spun to collect cells. The enzyme containing supernatant was discarded and the cells resuspended in PBS and kept on ice until FACS analysis.

Analysis: The samples were analysed using a CyAn™ ADP flow cytometer (Beckman-Coulter). To choose the correct settings, each cell line expressing the fluorescent proteins was analysed separately and a protocol for each fluorescent protein combination was written taking into account only the high GFP/tdTomato expressing cells. The samples were then run in duplicates and 100,000 events per sample were collected. During analysis 5,500 live single cells were analysed.

II.4 Differentiation assays

II.4.1 Preparation of conditioned medium

Epithelial ovarian cancer cells and immortalised ovarian surface epithelial cells were plated at a density of $3x10^6$ cells per F175 (Corning) and left to grow for 24 hours. The cells were then washed with PBS twice and 15ml of serum free medium was added. After 48 hours of incubation the conditioned medium was harvested and cell debris was removed using a 0.45μm syringe filter (Millipore). The medium was aliquoted and snapfrozen using dry-ice (BOC) and isopropanol (VWR) and was stored at -80°C for subsequent use.

II.4.2 2D differentiation assay

To differentiate mesenchymal stem cells (MSCs) and immortalised normal ovarian fibroblasts (INOFs) into ‚cancer associated fibrobast (CAF) – like' cells 20,000 cells were seeded onto P145 tissue culture plates. To facilitate differentiation 10ml of the appropriate conditioned medium was added to 10ml of normal MSC/INOF culture medium. The normal culture medium was supplemented with additional FBS to keep the final serum concentration equal to the normal culture medium. Cultures were refed every four days. MSC cultures were passaged on day 17 and 26 only, whereas the faster growing INOF cultures were also subcultured when reaching 80% confluency. Samples for subsequent assays were prepared on day 17 and day 26.

MSC culture medium:	α-MEM	500ml
	MSC-qualified FBS	100ml
	L-Glutamine	12ml
	P/S	6ml

INOF culture medium:		
	199	250ml
	MCDB 105	250ml
	FBS	75ml
	L-Glutamine	6ml
	P/S	6ml

II.4.3 3D differentiation assay

To differentiate immortalised normal ovarian fibroblasts (INOFs) and mesenchymal stem cells (MSCs) in a three-dimensional environment, the polyHEMA approach was used. $2x10^6$ cells were seeded onto a polyHEMA coated F75 plate and left to grow in their normal growth medium for 24h. After 1 day of incubation, the medium was removed carefully as described above (II.3.2) and the cells were re-feed using normal growth medium and conditioned medium at a 1:1 ratio as described above (II.4.2). After 26 days of culture the spheroids and the medium was collected in a 50ml falcon tube (Greiner) and used for subsequent assays.

II.5 Fluorescence two-dimensional difference gel electrophoresis (2D-DIGE)

II.5.1 Sample preparation

Twenty-four hours before cell lysis of 3D multicellular spheroids (MCSs), the culture medium was replaced by serum free medium. The medium containing the MCSs was transferred to 50 ml tubes and centrifuged to collect the 3D aggregates. Spheroids were washed twice with ice-cold PBS before resuspending in 400μL 2D lysis buffer. For two dimensional cultures, cells were grown until 90% confluent before replacing the medium with serum free medium. After 24 hours, the medium was removed and the cells were washed twice with ice-cold PBS before cell lysis using 100μl 2D lysis buffer. Samples were homogenised using a 25G needle and the insoluble material was removed by centrifugation (12,000 x g/10 min/4°C). Protein concentrations were determined by Coomassie Protein Assay Reagent (Pierce) and a BSA standard curve.

Lysis buffer: 8 M urea
2M thiourea
4% CHAPS
0.5% NP40
10mM Tris-HCL pH 8.3

II.5.2 2D-Difference In Gel Electrophoresis

2D-DIGE analysis was performed in triplicate as described by Gharbi et al. (Gharbi, Gaffney et al. 2002). Samples were labelled randomly with NHS-Cy3 or NHS-Cy5 at 4 pmol dye/μg total protein. Equal amounts of protein from all samples were also mixed to create an internal standard, which was labelled with NHS-Cy2 at 4 pmol/μg protein (GE Healthcare). Cy3 and Cy5 labelled samples and the Cy2 labelled internal standard were mixed appropriately, reduced with Dithiothreitol (DTT, Sigma) to a final concentration of 65 mM and a carrier Ampholine/Pharmalyte mixture (1:1; pH 3-10) was added to a final concentration of 2% (v/v). 2D electrophoresis was carried out as described (Weeks, Sinclair et al. 2006) using 24 cm Immobiline Dry Strips pH 3-10 NL (GE Healthcare) and 12% homogenous sodium dodecyl sulfate polyacrylamide gel electrophoresis (SDS-PAGE) gels that were bonded to low-fluorescence glass plates. Ettan Gel Tanks (GE Healthcare) were used to run the gels at 16ºC and 2 watt/gel over night until the dye front had run out of the gel.

Gels were scanned between glass plates using a TyphoonTM 9400 variable mode imager and captured using ImageQuant software (both GE Healthcare). Low-resolution scans were initially made to give maximum pixel values within 5-10% for each Cy dye channel and below saturation, prior to high-resolution (100 μm) scans. Images were analysed using DeCyderTM software v5.0 (GE Healthcare) according to the software guidelines. Only spots displaying an average 2-fold increase or decrease in abundance (from triplicates measurements), matching across all gel images and with p-values ≤0.01, were selected for mass spectrometry-based identification. Gels were post-stained with Colloidal Coomassie Blue (CCB) and the stained images matched to the fluorescent images in DeCyder (Weeks, Sinclair et al. 2006). A pick list of spots of interest was then generated from the CCB image and spots were excised using an Ettan spot picker (GE Healthcare).

II.5.3 Protein identification by Matrix assisted laser desorption ionization time-of-flight mass spectrometry (MALDI-TOF MS) peptide mass fingerprinting

In-gel tryptic digestion was performed to extract peptides from the gel pieces for identification using mass spectrometry. The gel pieces were washed twice using 25mM ammonium bicarbonate / 50% acetronitrile before drying in a SpeedVac for 10 min. Reduction of samples was achieved in 10mM dithiothreitol / 25mM ammonium bicarbonate at 50°C for 45 min. The samples were then alkylated in 50mM iodoacetic acid / 25mM ammonium bicarbonate for 1 h at room temperature and in the dark. Samples were then washed again twice in 25mM ammonium bicarbonate / 50% acetronitrile before drying in a SpeedVac. Proteolysis of proteins was achieved using 30ng of modified Trypsin (Promega) in 25mM ammonium bicarbonate for 16 h at 37°C. The supernatant containing the protein was collected and peptides were extracted using 5% trifluoroacetic acid / 50% acetronitrile (Gharbi, Gaffney et al. 2002). The extracted peptides were vacuum-dried and resuspended in 5 mL water plus 0.1% formic acid. 0.5 mL of sample was then mixed with matrix (saturated aqueous solution of dihydroxybenzoic acid), spotted onto a stainless steel MALDI target and air dried. MALDI-TOF mass spectrometry was performed using an Ultraflex TOF/TOF instrument (Bruker Daltonics) in the reflectron mode. Prominent peaks in the mass range m/z 700–5000 were used to generate a peptide mass fingerprint, which was searched against the updated NCBI database using MASCOT version 2.0.02 (Matrix Sciences). Identifications were accepted when: (i) ≥ 6 peptide masses matched a particular protein; ii) sequence coverage was 20%; (iii) the search score was higher than the threshold score at p=0.05; (iv) the predicted protein mass agreed with the gel-based mass.

<u>**12.5 % homogenous SDS-PAGE gel:**</u>

40ml Acrylamide/bis
25ml 1.5M Tris-HCl pH 8.8
1ml 10% SDS
33.5ml distilled Water
50µl TEMED
500µl 1-% Ammonium Persulfat

Loading buffer: 50mM Tris pH 6.8

10% (v/v) glycerol

2% (w/v) SDS

0.1% (w/v) bromophenol blue

2% β-mercaptoethanol

1 x SDS-electrophoresis running buffer: 25mM Tris

192mM Glycine

0.1% SDS

II.5.4 SDS-PAGE and Western blot

(A) To validate the identified proteins a 12.5% polyacrylamide gel was run under denaturing conditions to separate the whole protein lysate. The samples were denatured for 5min at 105ºC with SDS-loading buffer (see II.5.2) before being loaded onto the gel. The gel was run in a Hoeffer gel rig at 10mA over night. A polyvinylidene fluoride (PVDF) membrane (Amersham) was soaked in methanol and the gel was electroblotted onto the membrane using the BioRad system according to manufacturer's instructions. The transfer was performed at 350mA overnight. After transfer the membrane was incubated for 1h in 5% BSA blocking buffer to prevent unspecific binding. The primary antibodies were diluted appropriately (see table) in TBS-T and the membrane was incubated for 1h at room temperature. Unbound antibody was removed by washing the membrane three times in TBS-T. The diluted horseradish peroxidase coupled secondary antibody was added and incubated for 1h before washing off any excess antibody with TBS-T. Visualisation was achieved using enhanced chemoluminescense (ECL) substrate (Pierce) according to manufacturer's instructions. The membrane was wrapped in cling film and fixed in an x-ray cassette and exposed to chemiluminescence detection film.

Transfer buffer: 195 mM glycine

25 mM Tris

20% (v/v) methanol

TBS-T: 50 mM Tris pH 8

150 mM NaCl

0.1% Tween-20

Blocking buffer: 5% BSA

In TBS-T

Primary Antibody	
Antigen	Dilution
Prohibitin (Santa Cruz Biotechnologies)	1:5000
Annexin IV (abcam)	1:5000
VDAC1 (abcam)	1:5000
Secondary Antibody	
Anti-rabbit IgG HRP-coupled (Amersham)	1:5000

III Establishment of three-dimensional models of ovarian cancer and endometrial cancer

III.1 Introduction

To understand the biology of epithelial ovarian cancer (EOC) it is vital to develop *in vitro* models that are representative of the disease. Standard 2D cell culture methods have been widely accepted as a tool to model cell behaviour *in vitro.* Homotypic monolayer cultures have been the methods of choice for functional analysis of potentially important biological factors and genes and are the standard test system for the development of novel drugs. However, they disregard any 3D structure and interactions with the microenvironment that tumours exhibit *in vivo.* In 2D cultures cells are easy to maintain and large numbers of homogenous cell populations can be rapidly produced. Tumours however, are heterogeneous and contain fast and slow proliferating cells, necrotic and hypoxic areas, gradients in oxygen, cellular waste products and nutrients. These important features of tumours cannot be reproduced in standard 2D cultures.

Given this, I chose to improve existing *in vitro* models of EOCs by establishing 3D cultures of primary epithelial ovarian cancer cell lines to mimic *in vitro* the *in vivo* 3D architecture and tumour heterogeneity. Because of the access during surgical procedures to other gynaecological tissues, I also developed primary 3D cultures of endometrial cancers. Although endometrial cancer is not the primary focus of my PhD thesis, the rationale is that the development of an endometrial cancer model in parallel would both serve as a control for comparing cancer cell line models established in 3D versus 2D, and develop a novel tool for future research in endometrial cancer. To verify that 3D models are an improvement on conventional monolayer models, the same cells cultured in 2D and 3D were directly compared to the original tumour tissue using haematoxylin and eosin staining to assess morphological features; immunofluorescence/histochemistry was also performed to analyse marker expression. I considered the many 3D approaches that can be used such as polyHEMA coating, spinner flasks and rotary systems (I.3.4). The RCCS is a small bioreactor that was first developed by NASA to study cells in microgravity (Figure III-1). The vessel containing the cell suspension is kept in constant rotation, which prevents attachment of cells to the vessel wall and leads to spheroid formation (Navran 2008). The advantage of the RCCS over the spinner flask methods is the reduced shear forces within the vessel. Spinner flasks use a fishing swivel that keeps the medium in constant rotation to maintain cells in suspension and facilitate spheroid formation. However, the constant stirring introduces turbulences in the medium and high shear forces have a damaging effect on cells (Unsworth and Lelkes 1998). The RCCS further assists spheroid formation by keeping the cells in close proximity, induced by the steady rotation of the wall vessel, resulting in the formation of single spheroids. The polyHEMA method on the other hand is a static system that facilitates spheroid formation by preventing attachment of cells to a plastic surface. This leads to the establishment of many spheroids of different sizes. Equal distribution of nutrients and removal of waste products cannot be achieved in a static system compared to the RCCS. Thus, in the present study, I chose the Rotary Cell Culture System (RCCS) to establish cell growth of primary epithelial cancer cell lines in 3D.

Figure III-1: The rotary cell culture system (RCCS). Cell culture vessels are attached to the wall and kept in constant rotation to establish spheroid formation. Gas exchange takes places via a membrane at the back of the vessel. Image from www.exomed3D.com.

To carry out the experiments I decided to establish new primary cancer cell lines to ensure that the cell lines were early passage and as closely related to the primary tumour as possible. Most of the cancer cell lines available within the research community have been maintained and passaged *in vitro* for a long time. Culturing cell lines always carries the risk of accumulating additional genetic alterations over time and selection for a subset of tumour cells that can grow in an unnatural environment. *In vivo,* tumour cells grow in a 3D architecture embedded in a dynamic microenvironment, the tumour stroma. The standard method for establishing primary cancer cell lines, however, is to isolate them from the tumour microenvironment and grow them attached to a specially treated plastic surface. By doing this, tumour cells have to adapt to the new surroundings and inevitably undergo gene expression changes and somatic alterations (Masters 2000).

I hypothesised that culturing gynaecological cancer cells under 3D conditions better mimics the behaviour and biological properties of these cells *in vivo*. To test my hypothesis I compared 3D spheroids of newly established cell lines with traditional 2D cultures and with the primary tumours. Furthermore, immunohistochemistry and proteomic profiling were used to determine further differences between 3D and 2D culture methods.

III.2 Results

III.2.1 Establishing 3D cultures of primary gynaecological cancer cell lines

III.2.1.1 Establishment of primary cancer cell lines

To establish primary cancer cell lines, endometrial and ovarian tumour tissues were collected at University College London Hospital (UCLH) under approval of UCLH/NHS trust ethics committee. Either a piece of tumour was dissected from the tumour specimen or a brushing using a sterile cytobrush of the tumour was taken and transferred to the lab under sterile conditions. Tumour tissue was placed in a cell culture dish, minced and cell growth was observed after a couple of days in culture. Tumour cells obtained using the cytobrush method were transferred to a tissue culture dish and left to grow for about a week before re-feeding. The resulting colonies of cells were passaged to establish homogenous populations of epithelial cells using standard 2D adherent tissue culture methods. In many cases however, the resulting population was mixed and contained epithelial cells as well as fibroblasts (Figure III-2 A).

Stromal contamination is a major obstacle in obtaining a homogenous epithelial cancer cell line since fibroblasts will eventually outgrow the epithelial cells (Yuan, Kim et al. 1997; Dunfield, Shepherd et al. 2002). To overcome this I tested two approaches: Differential trypsinisation utilizes the fact that fibroblasts detach earlier from the culture dish than epithelial cells. The plate containing the mixed population of stromal and epithelial cells is incubated with trypsin and monitored closely to determine when fibroblast cells start to detach while epithelial cells remain attached. The detached fibroblasts can then be removed from the plate. This process might be repeated if stromal cells are still detected. In my experience however, this method was not ideal since many of the primary epithelial cells were quite delicate and detached easily upon treatment with trypsin. This resulted in a sparse population of epithelial cells left in culture. Yet primary epithelial cells prefer close contact to neighbouring cells to proliferate and hence growth arrest was common after differential trypsinisation. I therefore chose to isolate large epithelial colonies using the ring cloning method. By targeting large colonies of epithelial cells and transferring them to small tissue culture dishes (P60; 6-well plate) I successfully isolated the epithelial sub-population of the tumour specimen.

The resulting morphologies of epithelial cells varied greatly between each sample. I observed round morphologies, swirly colonies, cells exhibiting a stromal morphology and classic cobblestone growth (Figure III-2 B).

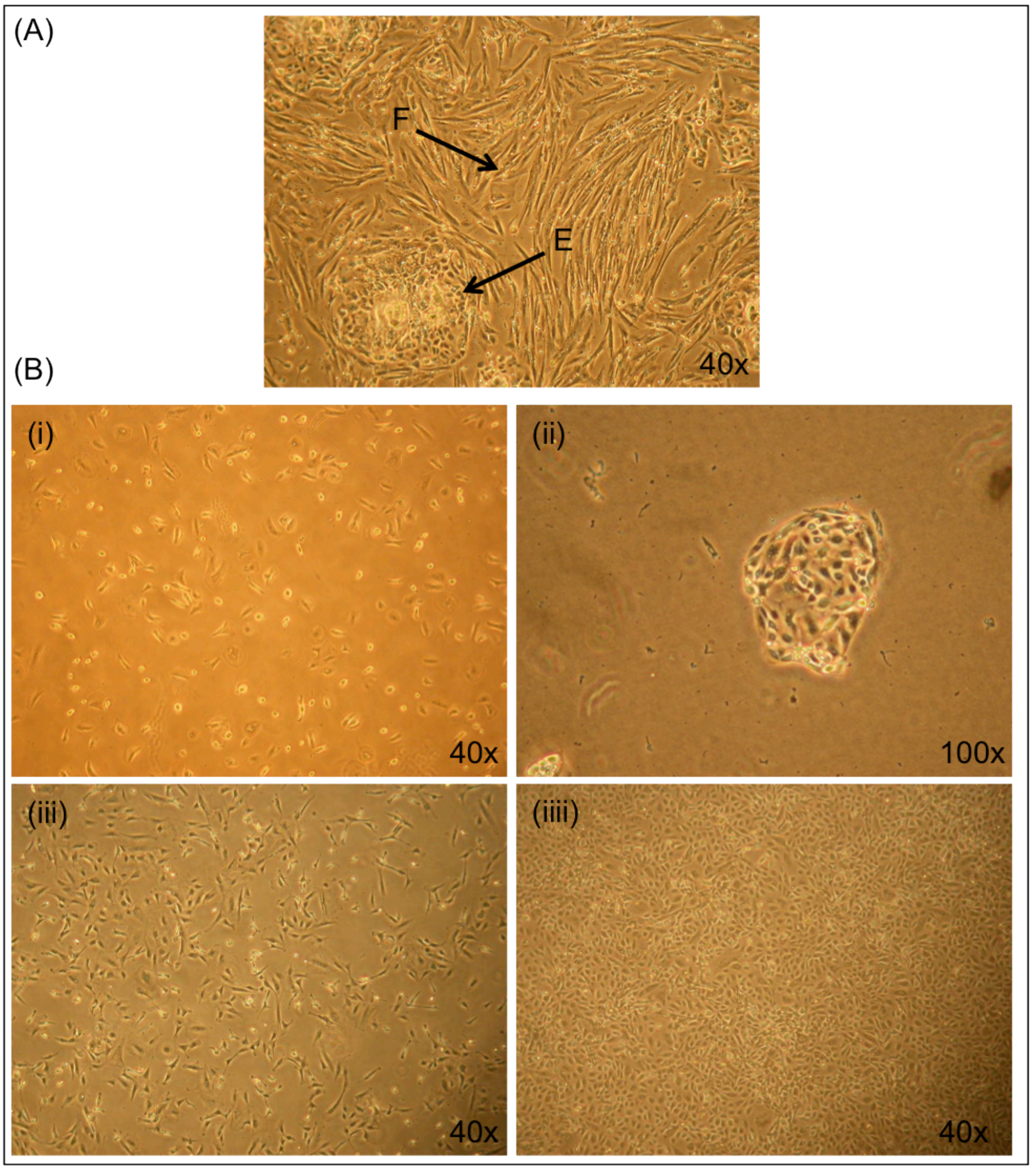

Figure III-2: (A) Example of fibroblast contamination (B) Different morphologies observed (i) rounded cells (ii) swirly colonies (iii) fibroblast like (iii) cobblestone

From the newly established cell lines four lines showed good growth abilities and were taken forward for further characterisation: OV-TRL12B was derived from a 59 year old patient with a poorly differentiated squamous cell carcinoma arising within a mature cystic teratoma of the ovary. The cell line showed growth in small colonies, which only merged upon reaching confluency. The cell line EN-TRL67T was derived from a 52 year old lady with a history of cervical cancer. The previous cancer was treated with radiotherapy and now an endometrioid adenocarcinoma of the endometrium was discovered. The resulting cell line exhibited growth in large colonies with very dense areas of small cells in the middle and larger cells at the periphery. EN-TRL71T was derived from 71 year old lady diagnosed with a serous papillary carcinoma of the endometrium. The cell line showed a classical epithelial morphology, and growth appeared to be very slow compared to the other cell lines. OV-TRL90T was derived from a 56 year old patient with ovarian cancer. The tumour exhibited the morphology of a moderately to poorly differentiated endometrioid adenocarcinoma. The cell morphology of the resulting cell line was very different from the other observed morphologies. Cells were very small and appeared dark. Even at low densities (less than 40% confluency), many cells could be seen growing in suspension (Figure III-3, Table III-1).

Table III-1: Summary of patient clinical data

	Patient age	Tumour site	Histology	grade
OV-TRL12B	59	Ovary	Poorly differentiated squamous carcinoma in a background of a mature cystic teratoma	3
EN-TRL67T	52	Uterus	endometrioid adenocarcioma of endometrium	2
EN-TRL71T	71	Uterus	serous papillary carcinoma of endometrium	high
OV-TRL90T	56	Ovary	Moderately/poorly (50%) differentiated endometriod adenocarcinoma	3

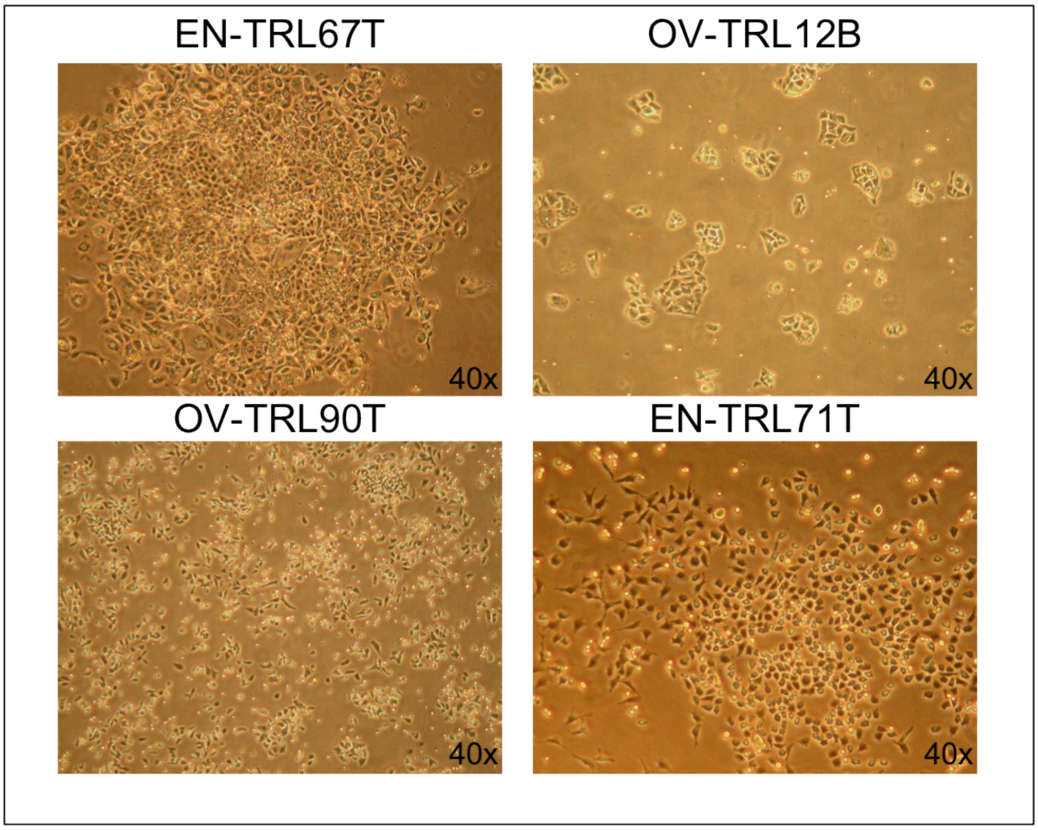

Figure III-3: Images of primary cell lines under phase microscopy. OV-TRL12B was established from a squamous carcinoma arising from an ovarian teratoma; EN-TRL67T was derived from an endometrial carcinoma; OV-TRL90T was established from an endometrioid ovarian carcinoma; EN-TRL71T was derived from an endometrial tumour.

III.2.2 Phenotypic characteristics of cell lines

Due to the many different morphologies observed it was then necessary to confirm the epithelial origin of the growing cell lines. The cells were stained for the epithelial markers cytokeratin 7 (ck7) and BerEp4. Ck7 is an intermediate filament, which is expressed in many epithelial cell lines. BerEp4 is also known as EpCAM and is an epithelial cell adhesion molecule, which is expressed in most epithelial cells and carcinomas. The cancer antigen 125 (Ca125) is expressed in almost all epithelial ovarian carcinomas and is used to monitor the response to anti-cancer treatment. It is however not very specific as it is not expressed in all EOCs and can be expressed by the normal epithelial ovarian tissue as well as in other benign conditions and endometrial cancer. Fibroblast specific protein (FSP) was used to rule out fibroblastic contamination.

BerEp4 was expressed in three out of the four cell lines tested. OV-TRL90T showed only very faint staining for this marker and hence was considered negative for BerEp4. This cell line also showed no expression of the other markers tested. The cell lines EN-TRL67T and OV-TRL71T also showed expression of the second epithelial marker ck7 and for the tumour marker Ca125, whereas OV-TRL12B was negative for both markers (Figure III-4). Additionally OV-TRL12B showed some positive staining for FSP whereas the other cell lines showed very weak staining and were considered negative for this marker. The results for the FSP staining were compared to the established EOC cell lines IGROV and TOV21G and a human fibroblast cell line 1BR. Both EOC cell lines showed some reactivity with FSP but compared to the fibroblast cell line the observed staining was weak. The results confirm the epithelial origin for OV-TRL12B, EN-TRL67T and EN-TRL71T. The cell line OV-TRL90T showed no positive staining for any marker tested, hence the epithelial origin of this cell line could not be evaluated.

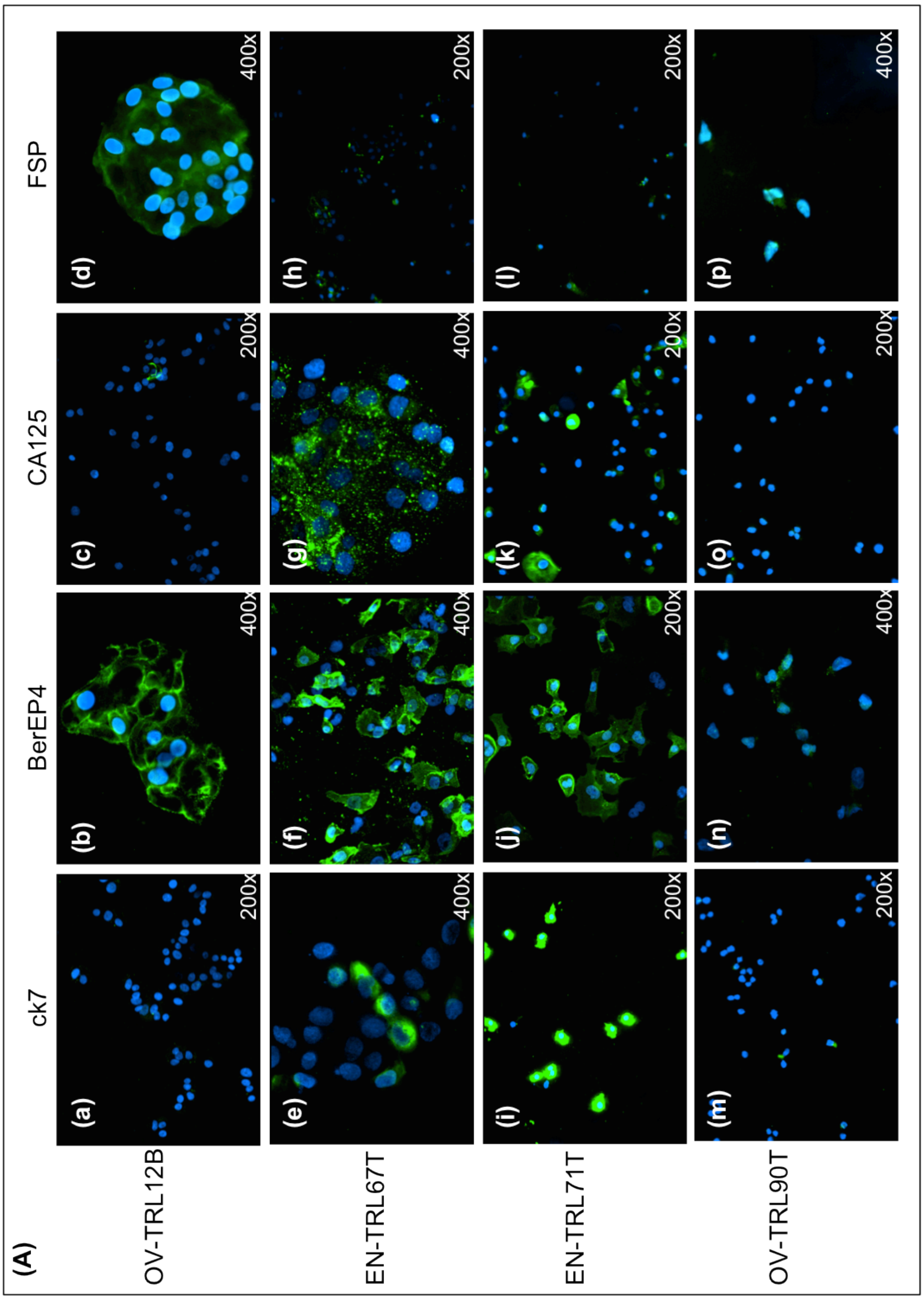

Figure III-4: Characterisation of primary cell lines. (A) Immunofluorescent staining. The cells were grown on glass coverslips until desired confluency before fixation. The cells were then stained with ck7, BerEp4 and Ca125. To visualise the staining a green fluorescent labelled secondary antibody was used and the nucleus was counterstained using DAPI staining (blue). Three of the four cell lines showed staining for the epithelial marker BerEp4 (b, f, j) whereas OV-TRL90T showed only very weak staining for this marker (n). This cell line was also negative for ck7 and Ca125 (m,o). EN-TRL67T and EN-TRL71T showed some positive staining for the tumour marker Ca125 (g, k), which was not expressed by OV-TRL12B (c). Strong expression of ck7 was detected for EN-TRL71T (i) and also EN-TRL67T showed some positive ck7 staining (e). OV-TRL12B was negative for this marker (a). OV-TRL12B showed some positive staining for FSP (d), whereas all other cell lines showed only weak or no staining for this marker (h, l, p).

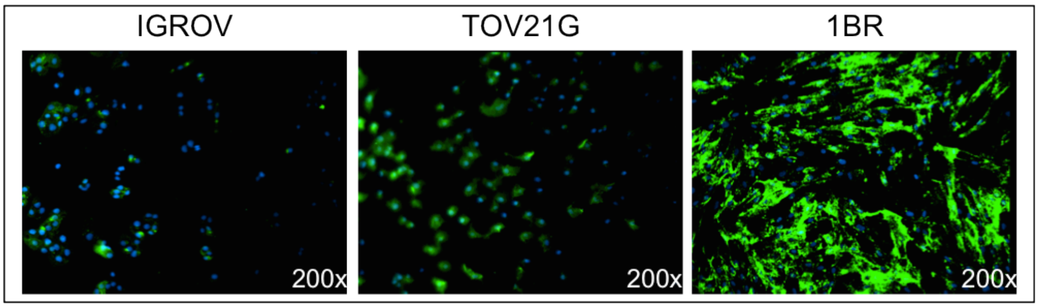

Figure III-5. Control for FSP staining. Epithelial ovarian cancer cell lines IGROV and TOV21G showed some positive staining for the fibroblast specific protein. The human skin fibroblast cell line 1BR serves as a positive control.

Tumour cells should not undergo replicative senescence but should be immortal when grown in culture. To test this feature I performed anchorage dependent growth assays in standard 2D cultures. After more than 50 days in culture all cell lines still showed logarithmic growth (Figure III-6) and no signs of senescence could be observed. Signs of senescence would include a large flattened morphology of cells and decreased growth rates. The mean population doubling time for OV-TRL12B was 3.87 days (+/- 0.034), for EN-TRL67T 3.53 days (+/- 0.032), for EN-TRL71T 6.77 (+/-0.073) and for OV-TRL90T 2.71 (+/- 0.012) days. Most published population doubling times range between 1 and 3 days (Kruitwagen, Poels et al. 1989; Yuan, Kim et al. 1997; Han, Papadopoulos et al. 1999; Ouellet, Zietarska et al. 2008) showing that cell line EN-TRL71T is an exceptionally slow growing cell line compared to established ovarian and endometrial cancer cell lines. The doubling times of the other three cell lines compare better to previously reported doubling times and the slightly slower growth rates might be explained by slight experimental variations in determining population doubling times.

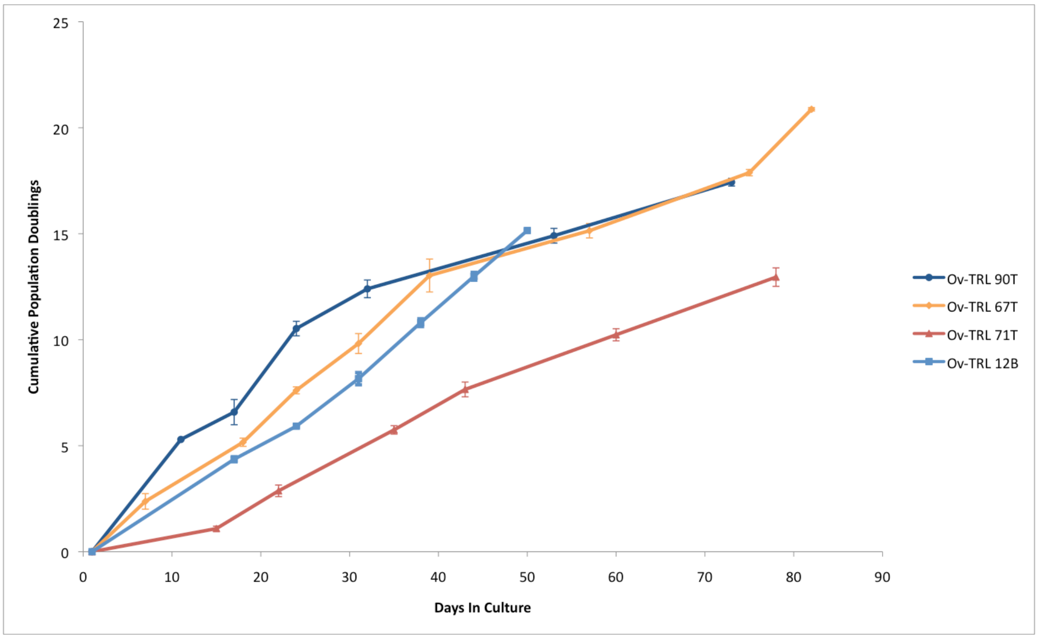

Figure III-6: Characterisation of primary cell lines: Growth curves. 10000 cells were plated in triplicates, counted and subcultured when they reached confluency to determine the population doublings. After more than 2 month in culture all cell lines still showed logarithmic growth and so growth curves were stopped. The population doubling times were 3.87 days for OV-TRL12B, 3.53 days for EN-TRL67T, 6.77 for EN-TRL71T and 2.71 days for OV-TRL90T.

III.2.3 Neoplastic phenotyping of cell lines

After the epithelial nature and the *in vitro* lifespan of the cell lines were determined I went on to analyse the neoplastic phenotype of these lines. Tumour cell lines show phenotypic characteristics that indicate a transformed phenotype. One characteristic is their ability to invade through a basement membrane. Another feature is the ability of cells to form colonies in semi-solid medium. I evaluated the *in vitro* malignant phenotype of the four primary cell lines using invasion assays and anchorage independent growth assays. All cell lines except EN-TRL71T were able to invade through a basement membrane (Figure III-7b) and formed colonies in soft agar after three weeks (Figure III-7a). These data suggest that the cell lines OV-TRL12B, EN-TRL67T and OV-TRL90T exhibit a malignant phenotype. OV-TRL12B showed the highest invasion and foci formation rates, which suggests a more aggressive phenotype compared to the other cell lines. However EN-TRL71T showed no evidence of malignant behaviour.

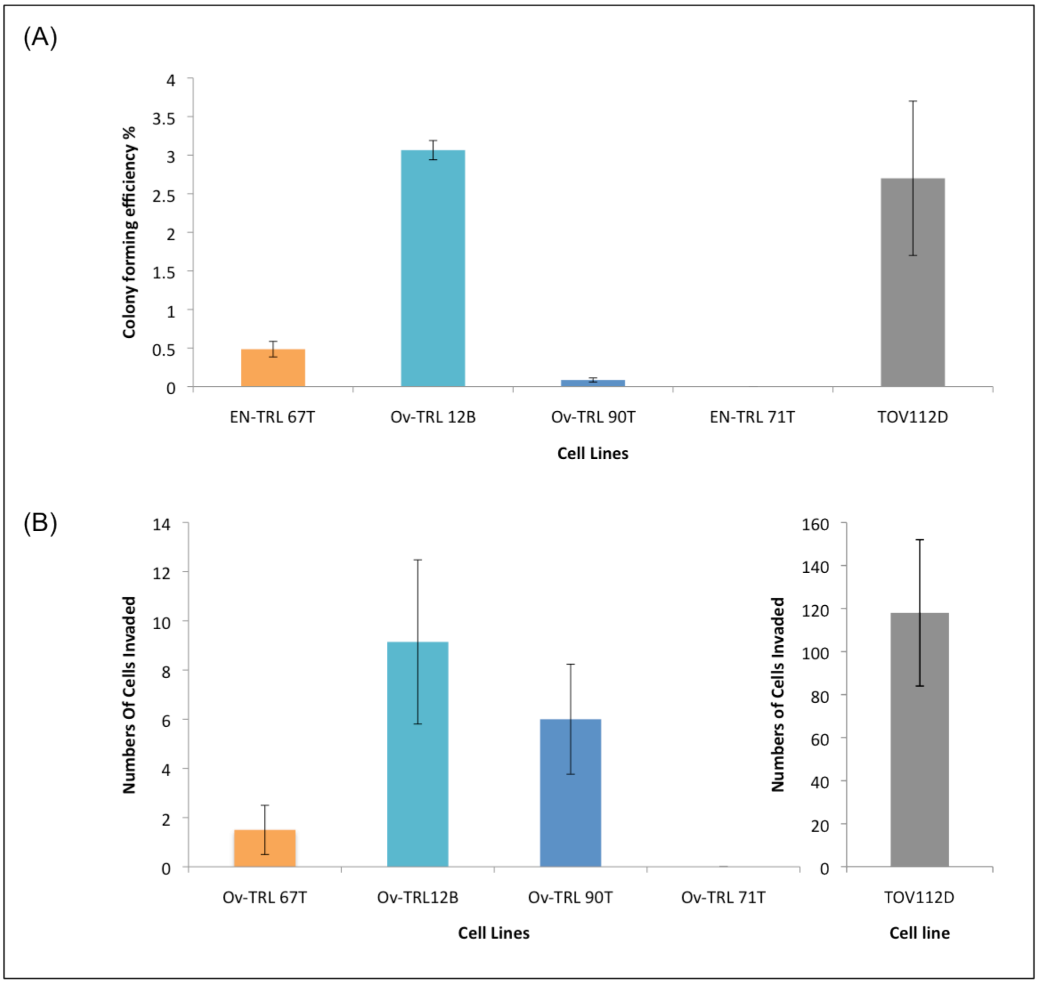

Figure III-7: Tumourigenic characteristics of primary cell lines. (A) Colony Forming Efficiency (CFE%) of cell lines in soft agar. Appropriate numbers of cells were plated in semi-solid medium (0.3% noble agar) on top of a base layer comprising 0.6% noble agar. After three weeks of incubation, colonies were fixed, stained and counted. EN-TRL67T showed a colony forming efficiency (CFE) of 0.5%, OV-TRL12B of 3%, OV-TRL90T of 0.1% and EN-TRL71T showed no colony formation in soft agar. The cell line TOV112D serves as a reference (Ouellet, Zietarska et al. 2008). **(B) Invasion assay.** 30.000 cells were placed in an insert containing a matrigel covered membrane on top of a well containing a chemoattractant. After 20h the number of invaded cells was determined by staining and counting cells on the bottom side of the membrane. OV-TRL71T showed no evidence of invasion, whereas all other cell lines were able to invade through a Matrigel basement membrane. The reference cell line 112D was plotted in a separate graph since the experiment was performed in a slightly different way and the scale of the Y-axis is disproportionate between the two experiments (Ouellet, Zietarska et al. 2008).

III.2.4 Establishment and characterisation of 3D cultures

To test the ability of the newly established primary cancer cell lines to form multicellular spheroids (MCSs) in a 3D culture I chose to use the rotary cell culture system (RCCS) (Figure III-1). The reasons for this are outlined in the introduction to this chapter. An appropriate number (II.3.1) of cells was placed into each vessel of the RCCS and kept in constant rotation to facilitate spheroid formation. MCS formation was examined for the cell lines OV-TRL12B, EN-TRL67T and OV-TRL90T. Due to the slow growth characteristics and non-tumourigenic behaviour of cell line EN-TRL71T I chose not to take this cell line forward.

MCSs formed readily for cell lines OV-TRL12B and EN-TRL67T. Passage 28 of the OV-TRL12B cell line led to spheroid formation after one week while passage 18 of the EN-TRL67T cell line resulted in MCS formation within two weeks. One large spheroid was detected in each vessel and reached a maximum diameter of 4mm during 4 week cultures, after which they tended to dissociate. This was likely to be due to shear forces caused by the constant rotation of the culture medium.

3D cultures of OV-TRL90T did not result in the formation of a large single spheroid but in numerous small aggregates of cells. Many single cells could also be observed floating in the medium, probably due to the cell line's tendency to grow in suspension (III.2.1.1).

Taken together the results from the primary cell line characterisation experiments and the spheroid formation ability I decided to only take OV-TRL12B and EN-TRL67T forward for further characterisation. The epithelial nature of both cell lines was confirmed and both exhibit immortal anchorage dependent growth. Furthermore, malignant features could be detected and spheroid formation in 3D cultures was successful.

To optimise 3D culture conditions I investigated whether the addition of microcarrier beads coated with cationic trimethyl ammonium (HillexII) or gelatin (cationic type 1 porcine collagen Factor III) improved cell growth in 3D. Both coatings have been shown to facilitate the attachment and growth of mammalian cells. I also tested whether the addition of a gel comprising components of the extracellular matrix (ECM) provided a support network that enhanced 3D growth. However, none of these support matrices improved the size or stability of MCSs (Figure III-8). Moreover cells tended to form spheroids between themselves rather than attaching to microcarriers or incorporating carriers into their 3D structure. The resulting spheroids were smaller in size than cells grown on their own. This suggests that microcarriers limited spheroid development rather than promoting MCS formation. Only the addition of ECM promoted the formation of ECM-cell spheroids. The gel facilitated growth of the cancer cell line but spheroids without any support material showed similar growth rates, hence I chose to use the RCCS without any supporting material for further studies.

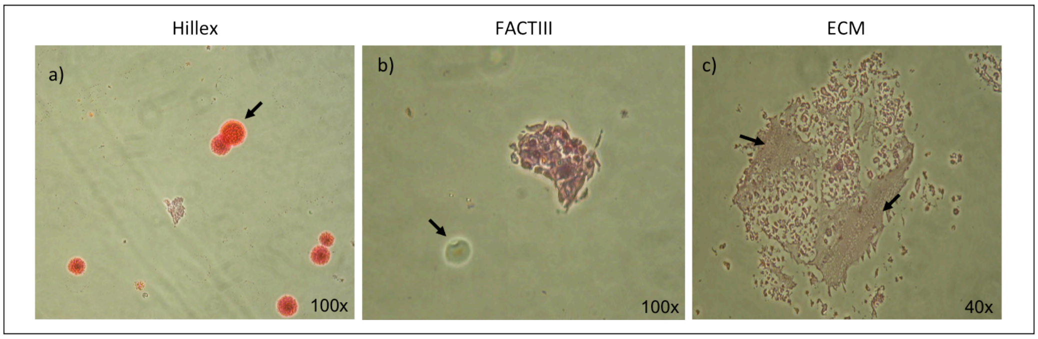

Figure III-8: Optimisation of culture conditions in the Rotary Cell Culture System (RCCS). a) 200,000 cells/ml were mixed with 5mg/ml Hillex® II H112-170 microcarriers and incubated for 4 weeks before fixation and analysis. The picture shows the beads (arrows) alone in culture with no cells attached. b) 10mg/ml FACT III microcarriers were added to 200,000 cells/ml and incubated for 4 weeks before fixation and analysis. No cells were found attached to the beads (arrows) but spheroids were formed without microcarrier involvement. c) ECM gel was diluted 1:2 and 1ml was added to a 10ml vessel containing 200,000 cells/ml. The culture was left to grow for 4 weeks before fixation and analysis.

III.2.4.1 Phenotypic comparison of multicellular spheroids and primary tumours

To examine if the 3D spheroids offer a good representation of the primary tumour I compared the morphological characteristics of the MCSs with the primary tumour from which the cell lines were derived.

Cell aggregates from 3D cultures were formalin fixed, paraffin embedded, sectioned and haematoxylin and eosin stained to examine histological features. Sections of the primary tumour were also stained and the morphological characteristics were compared.

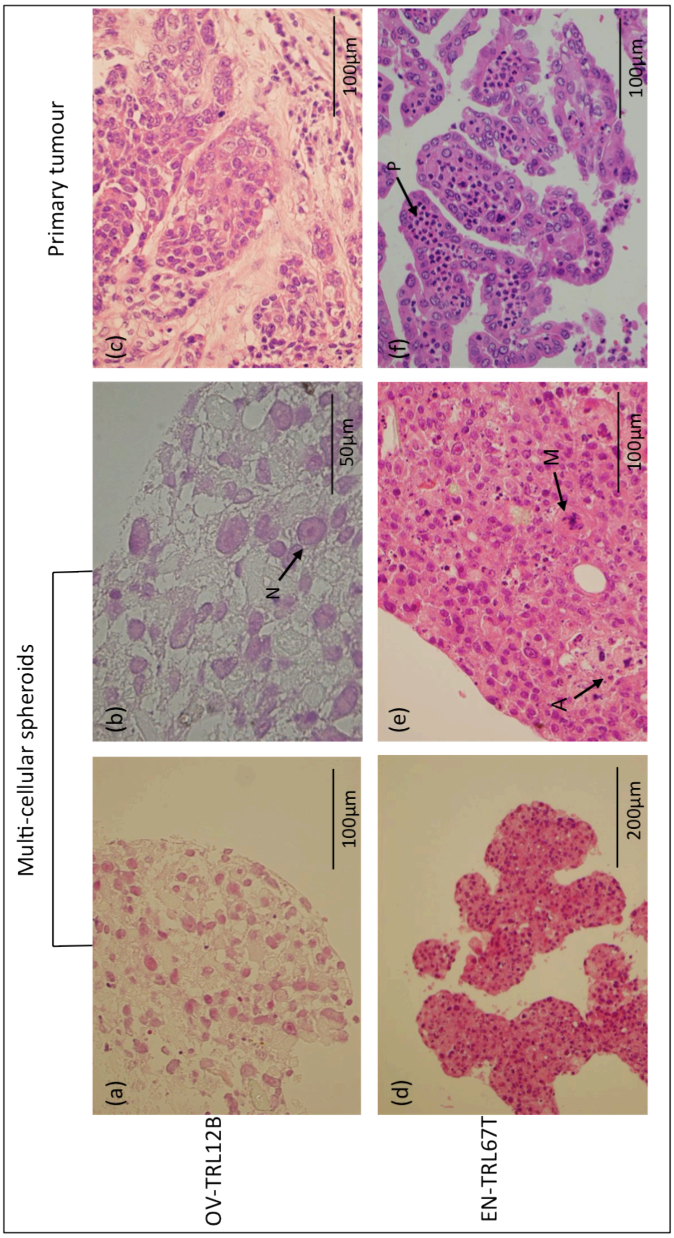

Figure III-9: H&E staining to compare morphology of cell lines grown in 3D to the primary tumour. 3D cultures of the OV-TRL12B cancer cell line (a & b) showed cell clusters composed of sheets of cells showing variation in cell size. At higher magnification, nuclear pleomorphism and prominent nucleoli (N) were seen. Histology section of the original tumour (c) showed poorly differentiated squamous carcinoma infiltrating stroma, forming sheets and nests of cells. Tumour cells showed similar cytological features with variation in cell size nuclear pleomorphism and prominent nucleoli, as the 3D culture; (d-f) 3D cultures of the EN-TRL 67T cancer cell line (d & f) showed papillary formation of the cell clusters. Tumour cells showed nuclear pleomorphism, increased mitotic activity and atypical mitoses (M). Foci of apoptosis (A) and nuclear debris were present. Histology section of the original endometrial adenocarcinoma (f) showed a papillary architecture and prominent neutrophil polymorph (P) infiltration of stroma. The tumour cells showed similar architectural and morphological features although apoptosis was more prominent in the 3D culture.

The primary tumour cells of cell line OV-TRL12B infiltrated the stroma as nests, sheets and trabeculae. The cells had a variable amount of eosinophilic cytoplasm, pleomorphic nuclei and showed mitotic activity. There was also focal keratinisation and areas of necrosis (Figure III-9c). Compared to the original tumour the 3D MCS grew in similar sheets and cell clusters. The cells varied in size and had pleomorphic nuclei with prominent nucleoli; foci of apoptotic cells were also present (Figure III-9a, b).

The primary tumour of the cell line EN-TRL67T showed papillary architecture. Extensive areas of necrosis were present and the tumour cells were pleomorphic with abundant eosinophilic cytoplasm and mitotic activity (Figure III-9f). 3D MCSs grew in clusters, which resembled the papillary structure of the primary tumour. The cells were pleomorphic with enlarged nuclei, prominent nucleoli and mitoses. There were also foci of apoptosis with cell degeneration and karyorhexis (Figure III-9d, e).

III.2.4.2 Immunohistochemistry

H&E staining shows histological features but does not enable analysis of marker expression. Therefore, to more quantitatively and qualitatively compare 2D cultures with 3D cultures and the primary tumour, I profiled protein expression of selected markers.

Examination of epithelial marker of cells grown in 3D showed a similar pattern of ck7 and BerEp4 expression as the same cells grown in 2D. Analysis of the immunohistochemical staining was evaluated by taking the percentage of positive stained cells and the intensity of the stain into account (Figure III-10). I also compared the expression of several functional and tumour associated markers between 2D and 3D cultures and the primary tumours from which both cancer cell lines were derived. These included the ovarian tumour marker CA125; the apoptotic marker BCL2; the proliferation marker Mib-1; the cell cycle control protein P53; and the steroid hormone receptors PR and ER. In general, the levels of expression for these markers were similar between cells from 2D and 3D cultures and from the primary tumours. The only notable exception was for Mib-1, which was highly expressed in 2D cultures of EN-TRL67T, but showed weak expression in cells from 3D cultures and the primary tumour (Table III-2).

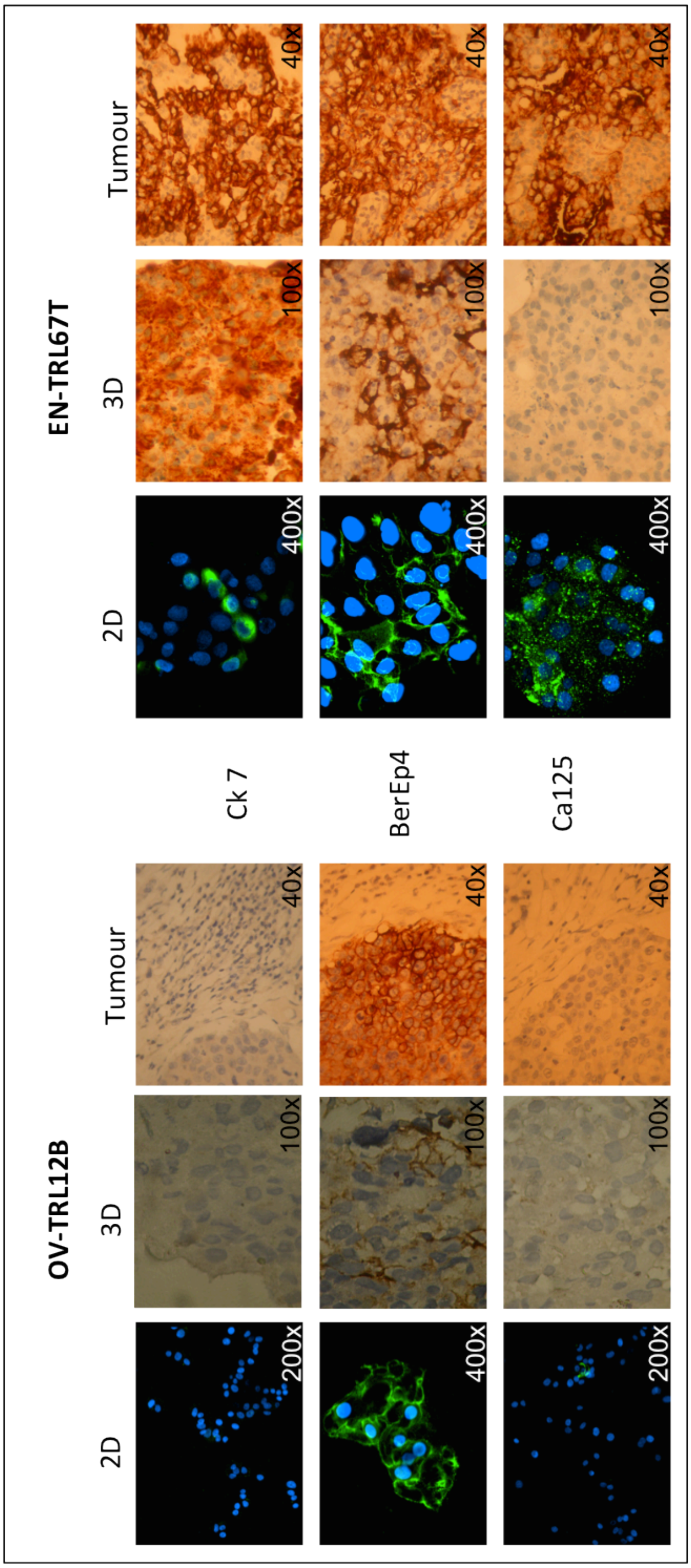

Figure III-10: Comparison of 2D and 3D culture by immunohistochemistry. Immunohistochemistry analysis of OV-TRL12B and EN-TRL67T cell lines grown in 2D, in 3D and the corresponding original tumour for the marker ck7, the epithelial antigen BerEp4 and the epithelial tumour marker Ca125.

Table III-2: Comparison of 2D and 3D culture by immunohistochemistry. Summary of the immunohistochemical staining for several markers. Shading of the boxes is graded according to the percentage of positive stained cells and the staining intensity.

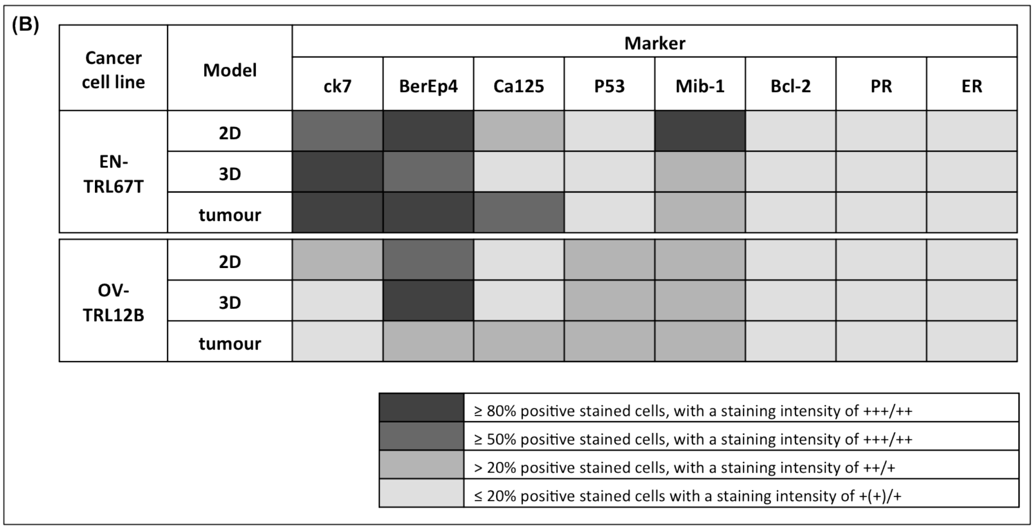

III.2.5 Proteomic comparison of cell lines grown in 2D and 3D

To expand the comparison of 2D and 3D culture conditions to a molecular level I went on to analyse the protein profiles of the cell lines OV-TRL12B and EN-TRL67T grown in 2D and 3D. The different culture conditions might lead to molecular changes resulting in differences in the protein profiles. I therefore prepared whole cell protein lysates of both cell lines grown in 2D and 3D. The samples were run in triplicates using two-dimensional difference gel electrophoresis (2D-DIGE) (Figure III-12a). Differentially expressed protein spots were analysed using the DeCyder™ software. For OV-TRL12B, 176 protein isoforms were found that were >2-fold differentially expressed between cells grown in 2D and 3D at a significance level of $p<0.01$ (t-test). For EN-TRL67T, 78 proteins were differentially expressed between the 2D and 3D cultures. Of these, 57 (29%) were common to both the ovarian and endometrial cancer cell lines.

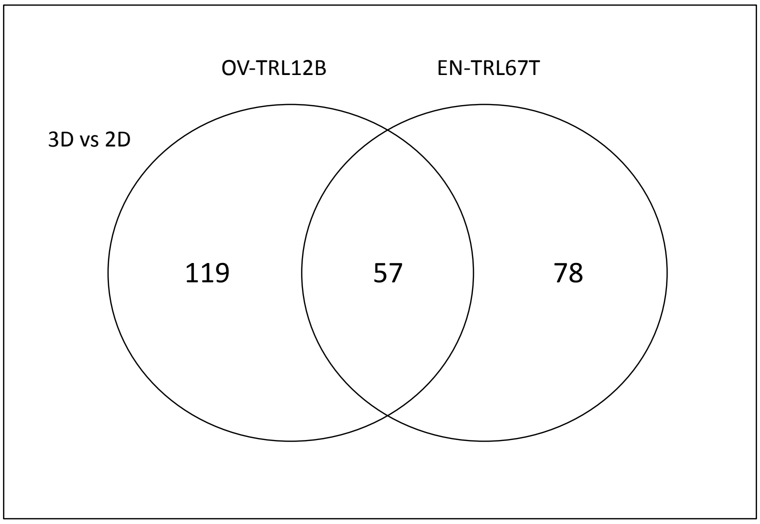

Figure III-11: Venn diagram of differentially expressed proteins. The diagram shows numbers of proteins that are differentially expressed in 3D versus 2D cultures for the cell lines OV-TRL12B and EN-TRL67T. Of all changes 57 were common between both cell lines.

Mass spectrometry with subsequent NCBI database search using MASCOT (II.5.3) was used to identify differentially expressed proteins. The identity of 22 proteins could be determined (Table III-3). Of these, 20 proteins were either up or down regulated in the 3D versus 2D cultures of both cell lines. The biggest change was seen for the proteins Peroxiredoxin 1 (PRDX1), voltage dependent anion channel protein 1 (VDAC1) and Prohibitin. PRDX1 expression was 41.7-fold upregulated in 3D cultures of EN-TRL67T cells and 5.3-fold upregulated in OV-TRL12B 3D cultures ($p=2.6x10^{-6}$, $p=0.0032$). VDAC1 was 6.9-fold upregulated in 3D cultures compared to 2D cultures for cell line EN-TRL67T and 14.2-fold upregulated for cell line OV-TRL12B ($p=4.3x10^{-5}$; $p=4x10^{-5}$). Prohibitin was 6-fold upregulated in EN-TRL67T 3D cultures and 4.6-fold in OV-TRL12B 3D cultures ($p=2.5x10^{-5}$, $p=3.3x10^{-5}$).

The identified proteins could be separated into groups. Metabolic enzymes were found to be downregulated in 3D cultures. Proteins involved in the apoptotic program, protection against oxidative stress and negative regulation of cell proliferation were all upregulated in 3D cultures compared to 2D cultures. The identified structural proteins were downregulated in the 3D cultures and heat shock proteins also appeared to be downregulated in 3D compared to 2D cultures. And finally proteasome related proteins were found to be downregulated in 3D cultures.

For three of the identified proteins, annexin IV, prohibitin and VDAC1, Western blotting was used to validate the altered expression observed between 2D and 3D cultures (Figure III-12b). Annexin IV was found to be significantly upregulated in 3D cultures of cell line EN-TRL67T (3.6 fold, $p=3.9x10^{-5}$) but no significant change was seen for cell line OV-TRL12B. Western blot analysis confirmed these findings. High levels of annexin IV were detected in 3D cultures of EN-TRL67T whereas 2D cultures showed weaker expression. The cell line OV-TRL12B exhibited very low levels of annexin IV expression for both culture conditions. Prohibitin expression was significantly upregulated in 3D cultures of both cell lines as described before. This was verified by western blotting which showed higher expression of Prohibitin in 3D culture lysates. Expression rates of Prohibitin appeared at the same level for both cell lines. Finally VDAC-1 has been shown to be significantly upregulated in the 3D culture condition of both cell lines (see above). Western blotting for this protein showed similar expression rates for both cell lines and confirmed a higher abundance of VDAC1 in 3D cultured cells. Furthermore, western blot analysis showed that β-actin was less abundant in 3D cultures of both cell lines than in 2D cultures. It appeared that β-actin is downregulated in 3D cultures of both cell lines.

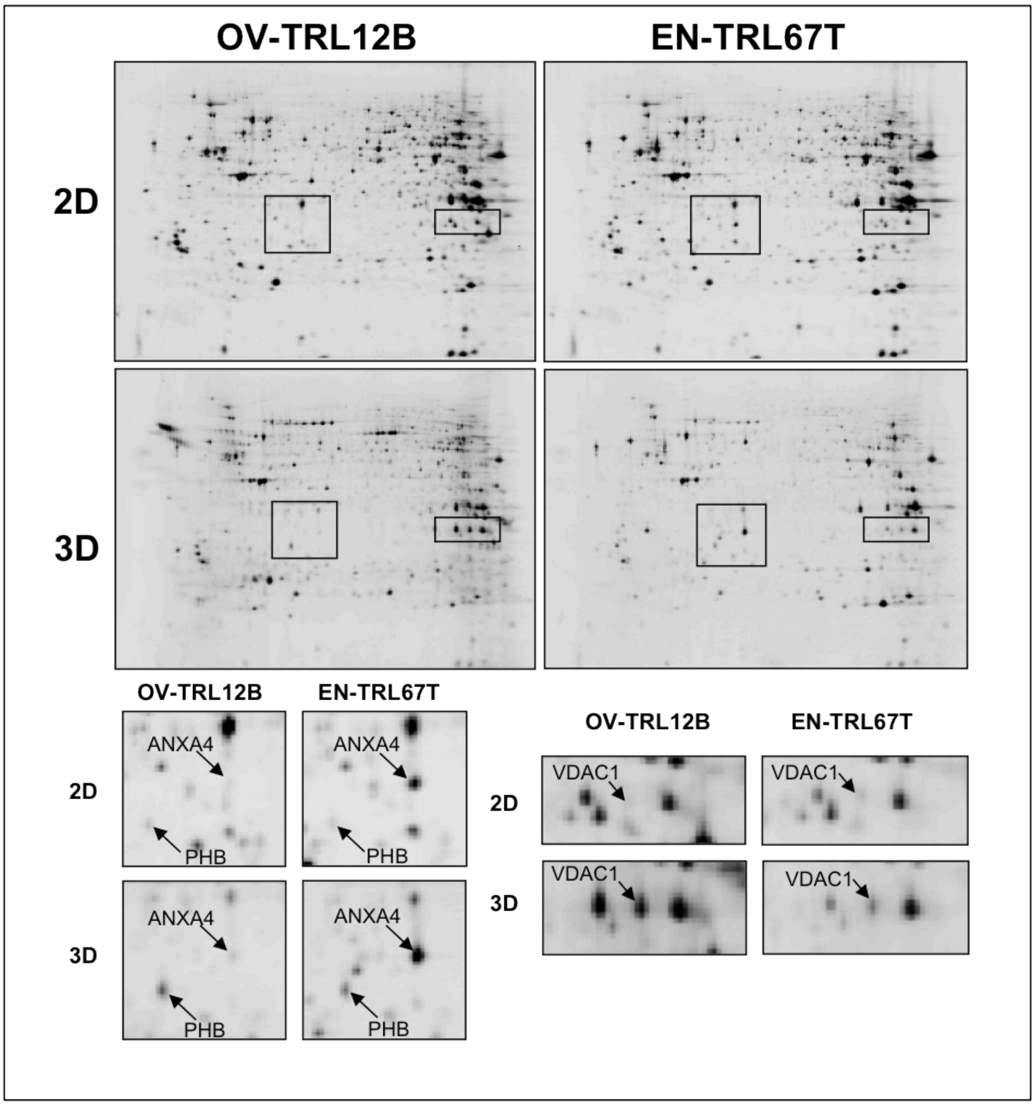

Figure III-12: Two dimensional difference gel electrophoresis (2D-DIGE) analysis of the cancer cell lines OV-TRL12B and EN-TRL67T grown in 2D and 3D cultures. (a) Examples of the 2D gels from both cell lines grown in different culture conditions. The further validated proteins are marked and a magnification of these spots is shown (ANXA4: AnnexinIV; PHB: Prohibitin; VDAC1: voltage dependent anion channel 1).

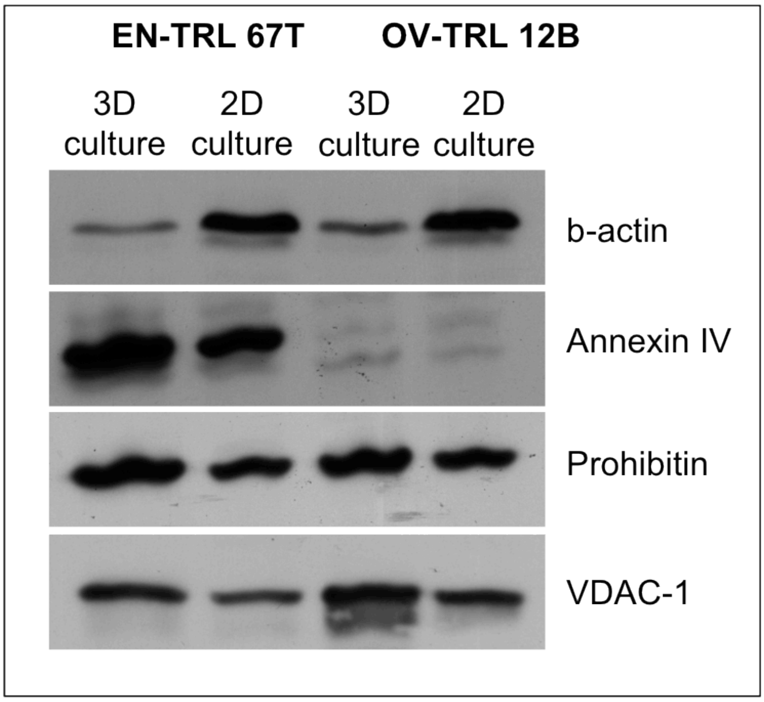

Figure III-13: Western Blot. Three proteins identified as being differentially expressed between 2D and 3D cultures of OV-TRL12B and EN-TRL67T cancer cell lines by 2D-DIGE, validated by Western blotting analysis on total cell lysates from 2D monolayer and 4 week 3D cultures.

Table III-3: Differentially expressed proteins identified between 2D and 3D cultures of OV-TRL12B and EN-TRL67T cancer cell line.

Protein Nomenclature	EN-TRL67T 3D v 2D		OV-TRL12B 3D v 2D		Known or predicted function
	Ratio	p-value	Ratio	p-value	
Isoform alpha-enolase of Alpha-enolase ENO1	-1.3	0.044	-4.2	7.50 x 10-7	Phosphopyruvate hydratase activity/Plasminogen activator activity /DNA binding/Lyase activity /Magnesium ion binding /Regulation of transcription,DNA-dependent /Transcription /Glycolysis /growth control, hypoxia tolerance/allergic responses
Adenosylhomocysteinase AHCY	-1.3	0.0054	-4.7	0.0002	Adenosylhomocysteinase activity/Hydrolase activity/One-carbon compound metabolism
Phosphoglycerate kinase 1 PGK1	-1.1	0.18	-2.9	4.90 x 10-5	ATP binding/Phosphoglycerate kinase activity /Transferaseactivity /Glycolysis/Phosphorylation
Fructose-bisphosphate aldolase A ALDOA	-1.8	0.0017	-3.3	2.00 x 10-5	Fructose-bisphosphate aldolase activity /Lyase activity/Fructose metabolism/Glycolysis/Striated muscle contraction carbohydrate degradation; glycolysis; d-glyceraldehyde 3- phosphate and glycerone phosphate from d-glucose
L-lactate dehydrogenase B chain LDHB	-1.3	0.0068	-3.2	0.0001	Oxidoreductase activity /L-lactate dehydrogenase activity /Tricarboxylic acid cycle intermediate metabolism/Anaerobic glycolysis
Triosephosphate isomerase 1	-1.1	0.38	-2	8.90 x 10-5	Metabolism/Pentose-phosphate shunt/Fatty acid biosynthesis /Gluconeogenesis /Glycolysis
GSTP1	-1.5	0.0026	-2.7	4.10 x 10-5	Transferase activity/Glutathione transferase activity/Metabolism/Central nervous system development
Heat shock protein HSPA5	2.2	0.00016	-1	0.52	ATP binding, Protein binding, bridging
Heat shock 70kDa protein 8 isoform 2 variant	-1.2	0.0074	-2.3	6.70 x 10-5	ATPase activity, coupled/Unfolded protein binding/ATP binding/Protein folding/ Response to unfolded protein
Proteasome activator complex subunit2 PSME2	-2.1	0.0005	-2.2	0.0017	Proteasome activator activity /Immune response
PSME1 29 kDa	-1.8	0.0012	-2.9	0.0013	Proteasome activator activity /Immune response

Protein Nomenclature	EN-TRL67T 3D v 2D		OV-TRL12B 3D v 2D		Known or predicted function
	Ratio	p-value	Ratio	p-value	
Voltage-dependent anion-selective channel protein1	6.9	4.30 x 10-5	14.2	4.00 x 10-5	Voltage-gated anion channel porin activity/Voltage-gated ion-selective channel activity /Apoptogenic cytochrome c release channel activity /Anion transport/Apoptotic program
VDAC1	3.3	0.0003	2.8	2.50 x 10-5	Voltage-gated anion channel porin activity/Voltage-gated ion-selective channel activity /Apoptogenic cytochrome c release channel activity /Anion transport
Prohibitin PHB	6	2.50 x 10-5	4.6	3.30 x 10-5	Transcriptional activator activity /Transcriptional repressor activity /Negative regulation of transcription/Regulation of cell cycle /DNA metabolism /Histone deacetylation/ Negative regulation of cell proliferation
Peroxiredoxin-6 (PRDX6)	-1.7	0.0081	-2.8	0.0002	Peroxidase activity/Phospholipase A2 activity /Hydrolase activity /Oxidoreductase activity/Phospholipid catabolism/Response to oxidative stress /Lipid catabolism
Peroxiredoxin-1 (PRDX1)	-1.1	0.2	-3.1	0.0001	Oxidoreductase activity/Peroxidase activity/Skeletal development/Cell proliferation
PRDX1 19 kDa	41.7	1.60 x 10-6	5.3	0.0032	Oxidoreductase activity/Peroxidase activity/Skeletal development/Cell proliferation
SOD2	3.1	0.0001	2.7	1.20 x 10-5	destroys radicals which are normally produced within the cells and which are toxic to biological systems
Vimentin 50 kDa protein VIM	-2	2.20 x 10-6	-2.9	0.0001	Protein binding/Structural constituent of cytoskeleton/ Structural molecule activity
Tubulin, beta polypeptide TUBB	-2.1	3.00 x 10-5	-2.7	0.0002	Structural molecule activity I/GTP binding/Unfolded protein binding/GTPase activity/Microtubule-based movement/ Natural killer cell mediated cytotoxicity /Protein polymerization/ Cytoplasm/ Tubulin
Annexin IV ANXA4	3.6	3.90 x 10-5	1.7	0.024	Calcium ion binding/Calcium-dependent phospholipid binding/Phospholipase inhibitor activity
protein DKFZp686J13123 TKT	1	0.48	-3.4	2.40 x 10-5	Calcium ion binding/Transferase activity/Transketolase activity

III.3 Discussion

I have described establishing primary ovarian and endometrial cancer cell lines and then using these cell lines to set up a three-dimensional (3D) model of ovarian and endometrial cancer using the rotary cell culture system (RCCS). Traditionally, two dimensional culture methods have been used to establish and maintain cell lines; however, they fail to address important characteristics of cancer tissues *in vivo.* The 3D architecture of organs cannot be recreated in a 2D culture nor can the complex interactions between cells (e.g.: adherens junctions, gap junctions) over their whole surface area be modelled. Therefore it has become increasingly apparent that more relevant *in vitro* models are necessary to study disease behaviour, i.e. response rates of potential novel drugs.

Here I chose to use novel primary cancer cell lines to keep culture induced phenotypic and genotypic changes to a minimum and to use cell lines that are closely related to the primary tumour tissue. Cell lines were isolated from endometrial and ovarian tumours and primary cancer cell lines were established. The *in vitro* lifespan and the epithelial nature of those cell lines were evaluated and the tumourigenic behaviour assessed. Of the established cell lines 2 lines were taken forward. The ovarian cancer cell line OV-TRL12B and the endometrial cancer cell line EN-TRL67T exhibited an extended *in vitro* lifespan. Cell lines still showed logarithmic growth after more than 40 days in culture. Both cell lines stained positive for epithelial markers (ck7 or BerEp4) and showed signs of a malignant phenotype in invasion and anchorage independent assays; thus these cell lines have been established as 3D models and compared to the primary tumour from which the lines originated.

Epithelial tumours *in vivo* exhibit a complex 3D architecture, containing multiple different cell types as well as the extracellular matrix (ECM). As early as in 1977 Emerman et al have shown that culturing mouse mammary epithelial cells in 3D on floating collagen membranes leads to the production of the milk protein casein (Emerman, Enami et al. 1977). The same effect is not seen if cells are cultured on 2D tissue culture dishes. Another study has shown that culturing normal human mammary cells in a 3D environment containing ECM can lead to the formation of acini-like structures with polarized, growth arrested epithelial cells growing around a central lumen (Petersen, Ronnov-Jessen et al. 1992). A research paper by Weigelt and coworkers also showed the importance of the 3D architecture on cell behaviour. They showed that malignant mammary epithelial cells grown in 3D cultures respond differently to drugs targeting HER2 positive cells than cells grown in 2D monolayer cultures (Weigelt, Lo et al. 2009). These studies clearly show the need for models of disease that are closely related to the *in vivo* situation.

Models for endometrial cancer include a study of Park et al were a 3D *in vitro* model of the human endometrium was used to study invasion of endometrial cancer cell lines (Park, Choi et al. 2003). In another study a 3D *in vitro* model of the omental microenvironment has been generated by embedding omental fibroblasts and mesothelial cells in collagen to examine ovarian cancer metastasis. The authors observed that the addition of ovarian cancer cells resulted in 3D aggregates that resembled metastasis to the omentum as found in patients with ovarian cancer (Kenny, Krausz et al. 2007). These models provide a valuable insight into the behaviour of endometrial and ovarian cancer cells in a three dimensional environment. However, using gel-based substances as a tool to create a 3D environment generates a semi-solid system, which is not easily adaptable to new external stimuli and proliferation is restricted to the size of the surrounding gel matrix. Furthermore ECM gels contain predetermined ratios of ECM components like collagen and laminin, which do not necessarily reflect the ECM of the modelled tissue. Therefore, these gel-based systems are not readily adjusted to represent the ECM of the tumour tissue.

Here I decided to use the Rotary Cell Culture System (RCCS) to establish 3D models of ovarian and endometrial cancer. The RCCS facilitates spheroid formation by keeping the cells in constant rotation thus preventing attachment to a surface. Both cell lines form spheroids readily without the need of additional support by microcarriers or ECM gel. Morphological and histological assessment of primary tumour sections and spheroid sections showed striking similarities. Spheroids of the ovarian cancer cell line showed growth in sheets and cell clusters which closely resembled the growth of the primary tumour. The endometrial cancer cell line grew in clusters in a 3D environment, which is very similar to the papillary structure of the primary tumour tissue. Spheroids of both cell lines also exhibited areas of apoptosis, which are commonly found in primary tumours. This shows that 3D cultures are not homogenous cell populations but cells behave differently depending on their location within the 3D structure. This has also been observed in spheroid cultures of melanoma cells and colon carcinoma cells. Gosh et al observed actively proliferating cells at the periphery of melanoma cell spheroids whereas the cores where found to be necrotic (Ghosh, Spagnoli et al. 2005). The same was described for colon carcinoma spheroids (Freyer and Sutherland 1980). These observed regions of non-proliferating cells within the tumour spheroids are especially relevant for drug development. It has been shown that quiescent cells are more resistant to chemotherapeutic drugs than fast proliferating cells (Valeriote and van Putten 1975; Drewinko, Patchen et al. 1981; Siu, Arooz et al. 1999). Thus, the growth pattern of the cell lines in 3D cultures described here showed close morphological similarities to the original tumour.

Immunohistochemical comparison of several markers (ck7, BerEp4, Ca125, Bcl2, Mib-1, PGR, ER) between cell lines grown in 2D cultures, 3D spheroids and the primary tumour showed similar expression patterns for all samples. Only the proliferation marker Mib-1 showed strong expression in 2D cultures of the endometrial cancer cell line EN-TRL67T but weak expression in 3D spheroids and the primary tumour. This indicates a higher proliferative activity of these cells in 2D cultures compared to 3D cultures. 2D cultures consist of homogenous highly proliferating cell populations, which is substantially different to the *in vivo* situation. *In vivo* tumours exhibit areas of slow proliferating cells as well as highly proliferative regions. Thus 3D cultures reflect this characteristic better than traditional 2D cultures.

To further analyse the differences between the two culture methods proteomic profiling was performed. Proteomic and transcriptomic analysis has been widely used in tumour profiling and helped in our understanding of tumour biology (Webb and Simon 2010; Goncalves and Bertucci 2011; Reis-Filho and Pusztai 2011). Proteomic profiling detects differences in protein abundance between two biological samples whereas transcriptomic profiling identifies differences in gene expression rates. Changes in RNA abundance however do not necessarily transfer into a change in the corresponding protein expression (Chen, Gharib et al. 2002). This might be due to post-translational modifications and the resulting protein expression levels can only be detected using the proteomic approach.

I chose proteomic profiling to analyse differences in the protein profiles of cell lines grown in 2D and 3D. This revealed numerous differences in protein expression between the two culture methods. Interestingly 29% of all differently expressed proteins were common to both cell lines, suggesting common pathways involved in the establishment of a 3D architecture. However, large cell type specific changes also occurred, which might be due to inherent molecular features of the cells.

Proteins involved in apoptosis and protection against oxidative stress were found to be upregulated in 3D compared to 2D. PRDX1 and VDAC1 showed the biggest fold change in this group and were highly upregulated in 3D cultures compared to 2D cultures. VDAC1 is located in the membrane of mitochondria and regulates the traffic of many metabolites like calcium through the membrane into the cytosol. Therefore VDAC1 holds a key function in energy production and apoptosis (Shoshan-Barmatz, Israelson et al. 2006; Abu-Hamad, Arbel et al. 2009). PRDX1 belongs to a family of antioxidant enzymes and plays a role in protecting the cells from oxidative stress by inducing apoptosis (Morinaka, Funato et al. 2011). Another member of this family, mitochondrial superoxide dismutase (SOD2), was also found to be upregulated in 3D cultures. Overexpression of this protein has been shown to decrease proliferation and cell growth while increasing differentiation (Kinnula and Crapo 2004). Another protein, Prohibitin, that has been shown to negatively regulate cell proliferation was found to be highly upregulated in 3D cultures (Rizwani, Alexandrow et al. 2009). Furthermore, the downregulation of metabolic enzymes and enzymes involved in protein degradation (PSME1, PSME2) again indicate a slower proliferative activity of cells in 3D cultures.

Theses changes of protein expression further underline the findings that cell lines in 3D are less proliferative and exhibit apoptotic areas, which are not seen in 2D cultures. These are key characteristics of cell growth *in vivo*, which can be recreated within a three-dimensional environment.

Cytoskeletal proteins were also found differentially expressed. Vimentin and beta tubulin (TUBB) were downregulated in cells cultured in 3D and western blot analysis indicated a decreased expression of actin in 3D cultures. Vimentin is an intermediate filament, which is responsible for maintaining cellular integrity and is known to be involved in epithelial to mesenchymal transition (EMT). It is also found in the extracellular matrix (ECM) (Rosano, Spinella et al. 2006; Satelli and Li 2011). Beta tubulin (TUBB) is a component of the microtubules and involved in various cellular processes including organelle positioning and intracellular transport. It also forms part of the centrioles during mitosis (Janke and Bulinski 2011). The third component of the cytoskeleton is actin, which was not identified by 2D-DIGE as being differentially expressed. However, western blot analysis to verify identified proteins showed that actin, which was used as a loading control, seemed to be downregulated in cell lines cultured in 3D compared to traditional 2D cultures. Actin is a subunit of the microfilaments which are involved in processes like cell motility, muscle contraction and cell division (Schoenenberger, Mannherz et al. 2011).

The downregulation of structural proteins in 3D cultures compared to 2D cultures seems to be surprising since it was thought that the 3D architecture and the resulting cell-cell interactions would lead to an increase in structural proteins, especially proteins like vimentin which form part of the ECM and would be expected to be upregulated in 3D cultures. In a study comparing 2D cultures of normal ovarian surface epithelial (NOSE) cells with 3D cultures of the same cell line, widespread vimentin expression was observed in 3D spheroids whereas only focal staining was detected in 2D cultures (Lawrenson, Benjamin et al. 2009). However, in these experiments normal cells were used which produced a core of ECM when grown as spheroids. This is profoundly different from the spheroids tumour cells form using the RCCS. The downregulation of the cytoskeletal proteins was probably due to the extensive areas of necrosis/apoptosis found within the tumourspheroids. The disintegration of cells within the spheroids coincides with the degradation of cytoskeletal proteins and further emphasizes the vast differences between the two culture methods.

Finally annexin IV was found upregulated in 3D cultures. This protein is expressed almost exclusively in epithelial cells and is thought to serve as a marker for epithelial cell polarization (Ponnampalam and Rogers 2006). This indicates a more polarized phenotype of cells grown in a three-dimensional architecture. Differential expression of the proteins VDAC1, prohibitin and annexin IV was confirmed using Western blot analysis.

These findings are supported by studies were the expression profiles of cell lines grown in 2D were compared to 3D cultures. In 2003 Li et al found that gene expression varies greatly between smooth muscle cells cultured in 2D and 3D. They also found genes upregulated in 3D, which lead to decreased proliferation rates in those cultures compared to 2D methods (Li, Lao et al. 2003). A study using melanoma cells in a 3D models also found profound differences in the gene expression profiles between 3D and 2D culture methods (Ghosh, Spagnoli et al. 2005). These approaches have been taken a step further by Zietarska et al, who compared the gene expression profiles of 2D and 3D cultures with xenograft models from the same cell lines. The group used epithelial ovarian cancer cell lines to form multicellular spheroids using the hanging droplet method. In this approach cells are plated into each well of a multiwell plate, which is then inverted so that the cells grow in a hanging droplet and form multicellular spheroids. The resulting spheroids are smaller in size (about 500 µm) than spheroids in the RCCS but are uniformly sized and therefore a good tool if consistently sized replicates are needed. Zietarska and coworkers were able to identify a group of genes that distinguished the profiles of the 3D culture and xenograft model from the traditional 2D culture method. One of the genes upregulated in 3D and xenograft models was confirmed to be expressed in most EOC tissues, while no significant expression was detected in normal control tissue (Zietarska, Maugard et al. 2007). They concluded that 3D models better reflect the *in vivo* gene expression pattern than 2D cultures.

A recent study performed in our laboratory described 3D cultures of normal ovarian surface epithelial cells, which have been established using the non-adherent method (Lawrenson, Benjamin et al. 2009). This can be facilitated by coating tissue culture plastics with poly-2-hydroxyethyl methacrylate (polyHEMA) to prevent cells from attaching to the tissue culture surface. Morphological comparison and analysis of ECM proteins of cells cultured in 2D and 3D with primary ovarian surface epithelial cells also showed that 3D cultures better resemble the *in vivo* state than traditional 2D cultures.

III.4 Conclusions

Taken together these findings underline the hypothesis that 3D cultures better represent the *in vivo* characteristics of primary tumours than the traditionally used 2D culture methods. Cultures grown in 3D show reduced proliferation rates, central apoptotic areas and reproduce the three-dimensional architecture of tumours *in vivo*. This better reflects the heterogeneous conditions of primary tumours over the homogenous, fast growing 2D cultures.

Three-dimensional culture methods present an important improvement of traditional 2D culture systems by recreating a 3D architecture that better reflects the *in vivo* conditions. However, it disregards the interactions between different cell types within an organ/tumour and the communication between cells and the ECM. The importance of the ECM in directing cell behaviour has been shown using human mammary epithelial cells. By treating 3D cultures with an antibody that alters communication between cells and the ECM it was possible to achieve a reversion of the malignant phenotype (Weaver, Petersen et al. 1997). The tumour microenvironment also plays a crucial role in tumour development. Stromal fibroblasts are the predominant cell type within the microenvironment and it has been shown that co-injection of moderately malignant epithelial cells with transformed fibroblasts leads to an acceleration of epithelial tumour growth in mouse models (Camps, Chang et al. 1990). To better understand the biology of a tumour it is therefore crucial to not only focus on the malignant cell type itself, but to treat the whole tumour including the microenvironment as an entity and study the interactions of the different cell types. This might lead to a better understanding of tumour initiation, development and progression. To achieve this it is necessary to further develop these 3D models and incorporate different cell types found in the tumour microenvironment. To address this, the next chapter focuses on utilizing the established 3D models and adding stromal cells to generate heterotypic 3D cultures to create a model that reflects the *in vivo* disease even better.

IV Establishment of heterotypic three-dimensional models of epithelial ovarian cancer

IV.1 Introduction

In the previous chapter I showed that 3D cultures create a very good model of disease, which closely mimics cell behaviour *in vivo*. However, it is not only the 3D architecture which is important for an *in vitro* model that is representative of disease; probably even more important are the interactions of the different cell types within this 3D structure. Within an epithelial tumour there are large areas of stromal cells, the so called tumour stroma. The stroma predominantly contains so called "cancer associated fibroblasts" (CAFs) that are crucial in supporting tumour growth and homeostasis (I.4). Therefore it is necessary to further improve the 3D models by including different cell types that can be found in the tumour microenvironment to recreate the heterotypic cell-cell interactions *in vitro*.

In this chapter I describe attempts to isolate CAFs from epithelial ovarian tumours for subsequent use in heterotypic models of disease. Isolation of CAFs has proved a challenging area of research, and there are very few reports of the generation of CAFs in experimental model of ovarian cancer. For this reason, I chose to use mesenchymal stem cells (MSCs) to represent CAFs. I went on to develop heterotypic 3D models using MSCs representing CAFs and immortalised normal ovarian fibroblasts (INOFs) to represent stromal cells from a normal ovary. These cells were cocultured with ovarian epithelial cells in different states of transformation to create models of a normal ovary and ovarian cancer. I further evaluated the use of these models for possible subsequent assays to characterise the spheroids.

I further examined the use of different methods for 3D cultures. In the previous chapter I used the rotary cell culture system (RCCS) to produce spheroids. At the same time my colleagues showed how the use of polyHEMA coated tissue culture plastics can also produce 3D spheroids that accurately represent the disease (Lawrenson, Benjamin et al. 2009). They showed that the RCCS method produced spheroids with higher rates of apoptosis compared to spheroids grown on polyHEMA coated tissue culture plates. This might be due to the shear forces within the RCCS vessel produced by the constant rotation of the vessel. Together with the fact that only five samples can be cultured at any one time using the RCCS and the high price of the disposable vessels I decided to use the polyHEMA method to establish heterotypic 3D models. This method uses a polymer (polyhydroxyethylmethacrylate; polyHEMA) that becomes a hydrogel in solution. This gel is used to coat tissue culture plastics to prevent cells from attaching and this leads to aggregation of cells in suspension and subsequent spheroid formation. This method provides a relatively cheap and easy way to produce numerous different sized spheroids. For certain experiments however, like testing the efficiency of drugs, it is necessary to use same size spheroids. To achieve this I have tested the hanging droplet method to produce same size heterotypic spheroids. In this method cell suspensions are added to each well of a multiwell plate before the plate is inverted. This leads to droplets hanging from each well with the cells gathering at the bottom of each drop to form spheroids.

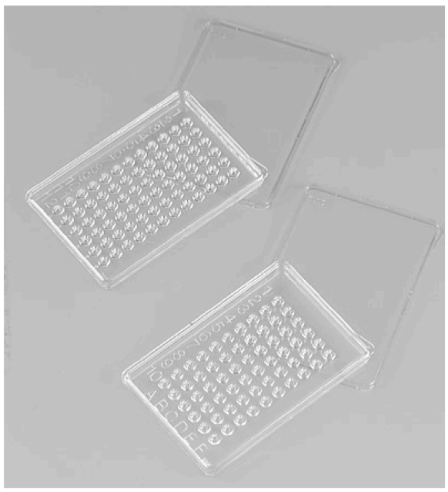

Figure IV-1: Multiwell plate. An example of a multiwell plate used to grow spheroids in hanging droplet cultures. Cells were resuspended at appropriate concentrations and 35μl of cell suspension was added to each well. The lid was then replaced and the plate inverted which led to droplets hanging from each well. The cells gathered at the bottom of each drop and aggregated to from spheroids. (Picture from sigmaaldrich.com)

I hypothesise that coculturing epithelial ovarian cancer cells with stromal cells in 3D will offer a very good representation of the *in vivo* tumour. I also wished to determine if MSCs affect the growth of epithelial cells differently than INOFs. To test this hypothesis and to evaluate downstream experiments I started by labelling the different cell types to be able to distinguish between them. H&E staining was performed to analyse morphological features of the heterotypic spheroids and compare them to standard homotypic spheroids. I then used flow cytometry to analyse the proliferation rates of both cell types within the spheroids and confocal microscopy to visualise spheroid structure and the location of the different cell types relative to each other.

IV.2 Results

IV.2.1 Isolation and establishment of cancer associated fibroblasts

Cancer associated fibroblasts from ovarian tumours have been isolated from epithelial ovarian tumours collected at UCH. Colonies of fibroblastic morphology have been separated from mixed populations using the ring/ or paper cloning method and plated on a P60 dish for expansion. Within these cultures I observed many cells with a large flattened morphology and with enlarged vacuoles indicating replicative senescence (Figure IV-2). It was therefore imperative to immortalise these cells at a very early passage to increase their lifespan. Retroviral delivery of hTERT was used to achieve immortalisation of fibroblast populations. The virus was produced as described (II.1.5.2) and cells were infected at passage 2 or 3. Selection of infected clones was achieved using 20U/ml of Hygromycin B. However, positively infected cells could not be selected. The Retrovirus used in this experiment is based on the murine leukaemia virus (MLV) and is only able to infect dividing cells (Yamashita and Emerman 2006). The fibroblast population however, contained high numbers of senescent cells indicating that most of the cells are not dividing. I therefore chose to use a lentivirus to deliver hTERT into the cells. The lentiviral system is based on the human immunodeficiency virus (HIV) and is able to efficiently infect non-dividing cells (Yamashita and Emerman 2006). In addition to hTERT this virus also carries GFP as a reporter (Akimov, Ramezani et al. 2005), which allowed selection of successfully infected cells using fluorescent microscopy. The use of the lentivirus did not improve infection rates and no immortalised ovarian cancer associated fibroblasts could be established in culture.

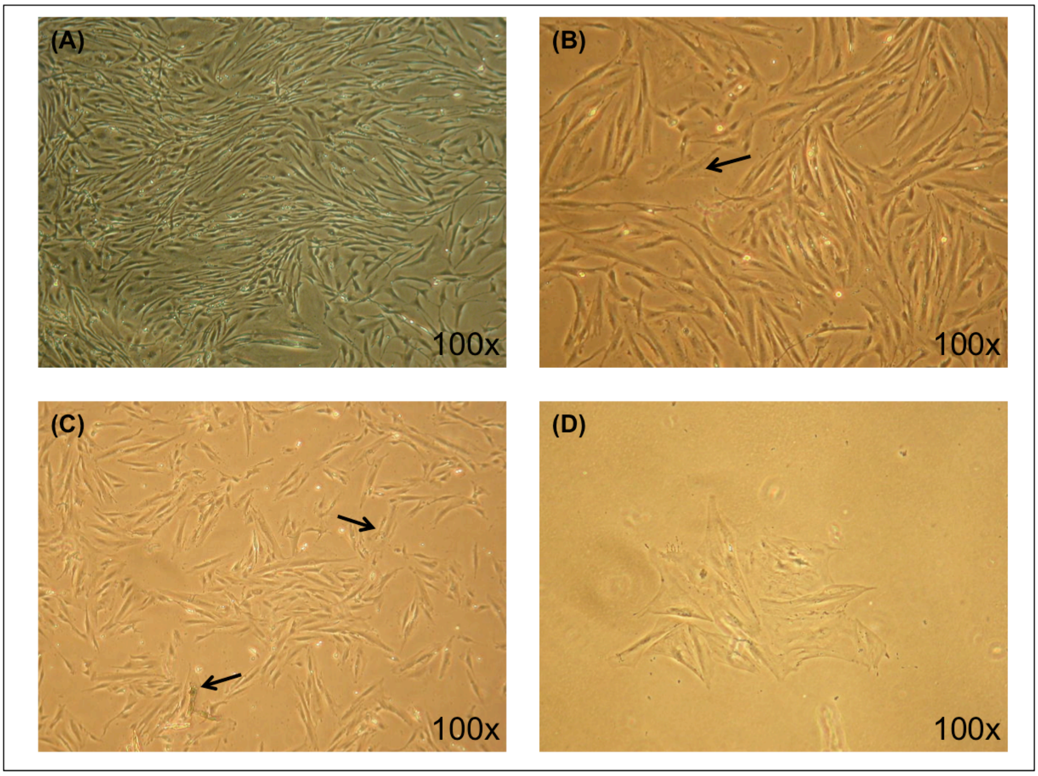

Figure IV-2: Light microscopy of stromal cell lines. (A) Healthy looking fibroblast population; (B) Fibroblasts still look healthy, but note the appearance of some flattened cells (arrow); (C) Cells start to look more senescent; lots of cells exhibit a flattened morphology (arrows); (D) Senescent cells

Other groups have isolated ovarian cancer associated fibroblasts and also found high rates of senescence within. Yang et al stained the microenvironment of epithelial ovarian tumours with senescent markers and showed that fibroblasts within EOCs are senescent (Yang, Rosen et al. 2006). Quiros et al established CAF cell lines from ovarian tumours and found that most of the cell lines exhibited a flat and spread morphology, which is consisted with my findings (Quiros, Valianou et al. 2008). However none of these groups have immortalised the cell lines for prolonged culture. In our lab normal ovarian fibroblasts have been successfully immortalised with hTERT; but for CAFs it might be necessary to inactivate the p16 pathway before delivery of hTERT as it has been shown before for other cell lines (Haga, Ohno et al. 2007). It has also been reported that early senescent fibroblasts contain high levels of p16 and that the introduction of Bmi-1 to suppress p16 leads to an extended lifespan (Itahana, Zou et al. 2003); thus inactivation of p16 might extend the lifespan of freshly isolated ovarian CAFs and aid successful introduction of hTERT to achieve immortalisation.

Due to the unsuccessful establishment of CAFs I chose to use mesenchymal stem cells to represent CAFs in the heterotypic 3D models. Mesenchymal stem cells have been implicated as a source of CAFs, which I explain in more detail in the next chapter.

IV.2.2 Establishment of heterotypic 3D models of ovarian cancer

The aim of this chapter was to create a model of ovarian cancer *in vitro.* I chose to use three different epithelial cell lines; an immortalised ovarian surface epithelial (IOSE) cell line to represent normal cells; a normal cell line overexpressing c-myc (IOSE19^{cmyc}) to represent an early transformed cell line and an epithelial ovarian cancer cell line (HEY) derived from a papillary cystadenocarcinoma of the ovary to represent an ovarian cancer cell line. An immortalised normal ovarian fibroblast (INOF) cell line was used to represent the normal stroma and because of the lack of ovarian CAFs, mesenchymal stem cells (MSCs) were used as a representation of the tumour stroma. The IOSE, IOSE19^{cmyc} and INOF cell lines have been established in the lab (Lawrenson, Grun et al. 2010); the MSCs were provided by the Texas A&M Health Science Centre College of Medicine Institute for Regenerative Medicine at Scott & White (through a grant from NCRR of the NIH, Grant # P40RR017447) and the HEY ovarian cancer cells were established in 1985 (Buick, Pullano et al. 1985) and was obtained from Gordon Mills lab at the MD Anderson Cancer Centre.

To distinguish epithelial from stromal cells in subsequent assays the cells were labelled with fluorescent proteins. The red fluorescent protein tdTomato (Shaner, Campbell et al. 2004) was used to label the epithelial cells whereas the stromal cells were labelled with GFP. Delivery of the fluorescent proteins was achieved using HIV based lentiviral systems (II.1.5.2) and cells successfully expressing the fluorescent proteins were isolated by fluorescence activated cell sorting (FACS). To achieve multicellular spheroid formation, cells were plated onto polyHEMA coated tissue culture plastics. As a reference each cell line was plated individually and incubated for 8 – 14 days. The spheroids were then embedded into paraffin, sectioned and stained with haematoxylin and eosin for structural analysis.

IOSE cells formed small spheroids with matrix deposits in the core and a single layer of cells covering the spheroid (Figure IV-3 (a)), which is consistent with previous observations for these cells. IOSE19^{cmyc} cells formed loose but bigger spheroids with an active morphology, indicated by the presence of mitotic figures. Pleomorphic nuclei were visible with prominent nucleoli (Figure IV-3(b)). HEY cancer cells formed cohesive spheroids with many mitoses present, which indicate a high proliferation rate. The cells had abundant cytoplasm and pleomorphic nuclei (Figure IV-3(c)). Normal ovarian fibroblasts deposited some matrix material at the centre of the spheroids. Spindle shaped cells grew at the periphery and high rates of apoptosis were visible at the core of the spheroids (Figure IV-3(d)). Similarly MSC spheroids showed a high level of apoptosis at the centre and flattened layers of cells at the periphery. There was also some hyaline material present at the core (Figure IV-3 (e)).

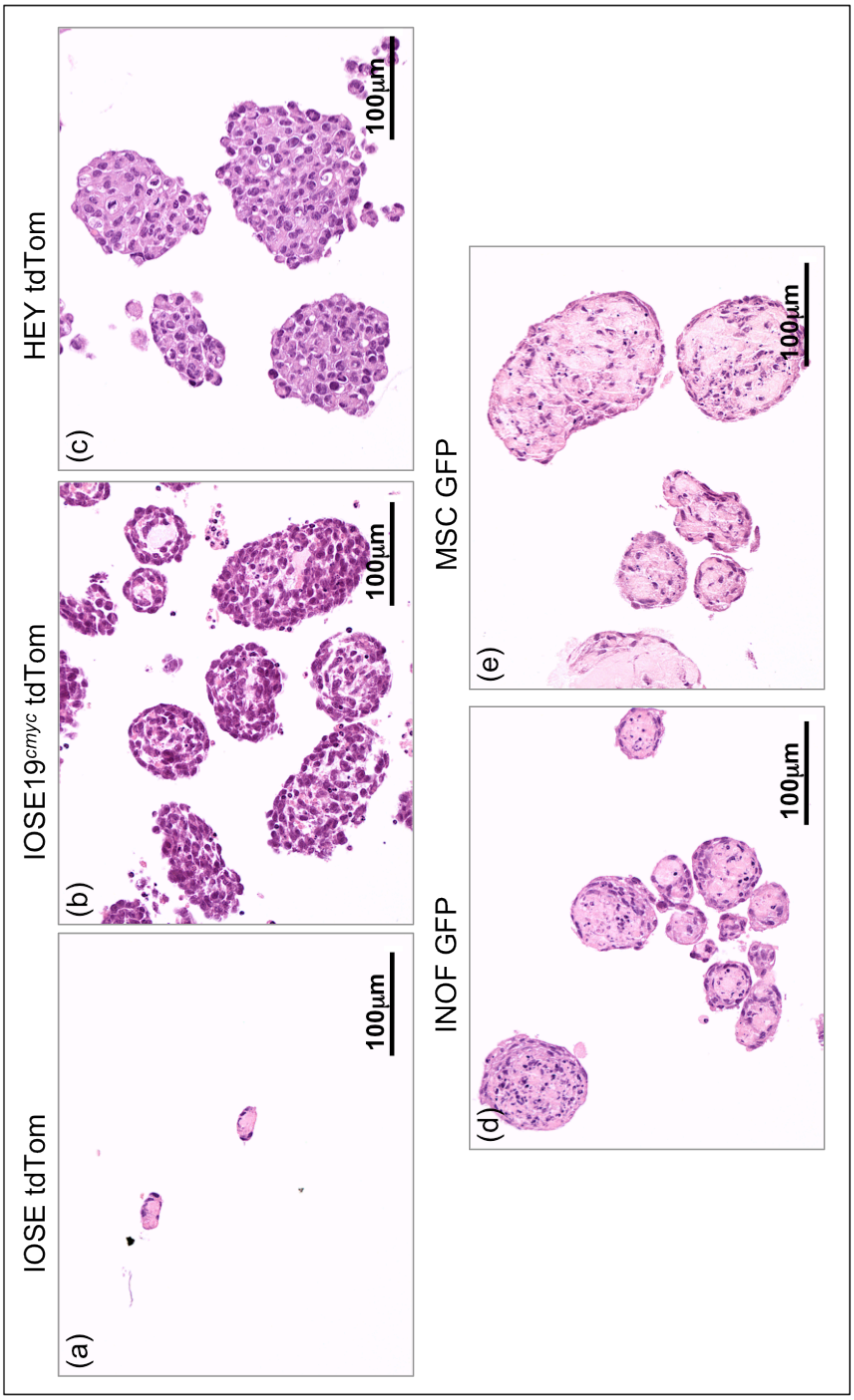

Figure IV-3: Haematoxylin and Eosin (H&E) staining of multicellular control spheroids grown in 3D. (a) Multicellular spheroids of an immortalised ovarian surface epithelial (IOSE) cell line. (b) IOSE19*cmyc* (overexpresses c-myc) cells formed loose spheroids, which had a very active morphology. The nuclei were pleomorphic with prominent nucleoli. (c) The epithelial ovarian cancer cell line HEY formed cohesive spheroids. The cells had abundant cytoplasm and pleomorphic nuclei. The mitotic index was high. (d) Spheroid of immortalised normal ovarian fibroblasts (INOFs). Spindle shaped cells grew at the periphery whereas lots of apoptosis was visible at the core of the spheroids. Some hyaline material was present in the middle of the spheroids. (e) Spheroids formed by the mesenchymal stem cell (MSC) 7078 line showed a flattened layer of cells at the periphery whereas a high level of apoptosis could be observed in the middle. Some hyaline material was present.

To establish heterotypic 3D cultures stromal and epithelial cells were mixed at a ratio of 3:1 and plated onto polyHEMA coated tissue culture plastics. After 8 days spheroids were harvested, embedded into paraffin, sectioned and stained with haematoxylin and eosin for morphological characterisation.

Cocultures of INOFs and IOSE cells formed small spheroids with matrix deposits in the centre. The cells seemed to be in a quiescent state as not much activity was seen. This very much resembles the state of a normal ovary where the epithelial cells grow as a single layer of cells on top of the stromal cells and are in a state of quiescence (Figure IV-4 A). Spheroids of IOSE cells with MSCs showed a similar morphology; however there were plenty of apoptotic cells visible at the core of the spheroid (Figure IV-4 D). The c-myc overexpressing cell line IOSE19^{cmyc} formed many spheroids of different sizes when cocultured with INOFs. The spheroids contained a matrix core with a few layers of cells. The morphology was active with some mitoses visible and the cells had pleomorphic nuclei with prominent nucleoli (Figure IV-4 B). When cocultured with MSCs the resulting spheroids appeared larger and less organised. There was still some matrix present at the centre but also many apoptotic cells. The spheroids were covered in layers of cells but many cells were also present within the spheroid (Figure IV-4 E). Spheroids of the HEY cancer cell line with INOFs grew in sheets and showed an active morphology. The cells showed nuclear pleomorphisms with prominent nucleoli. Abundant eosinophilic cytoplasm was visible with some intracytoplasmic vacuoles (Figure IV-4 C). When cultured with MSCs spheroids appeared larger and there were approximately 10 layers of cells until some apoptosis was visible. Pleomorphic nuclei with a variation in size and prominent nucleoli were seen. At the centre of the spheroids there was some matrix and some apoptosis. The mitotic index in these spheroids was high and the sections resembled tumour sections (Figure IV-4 F).

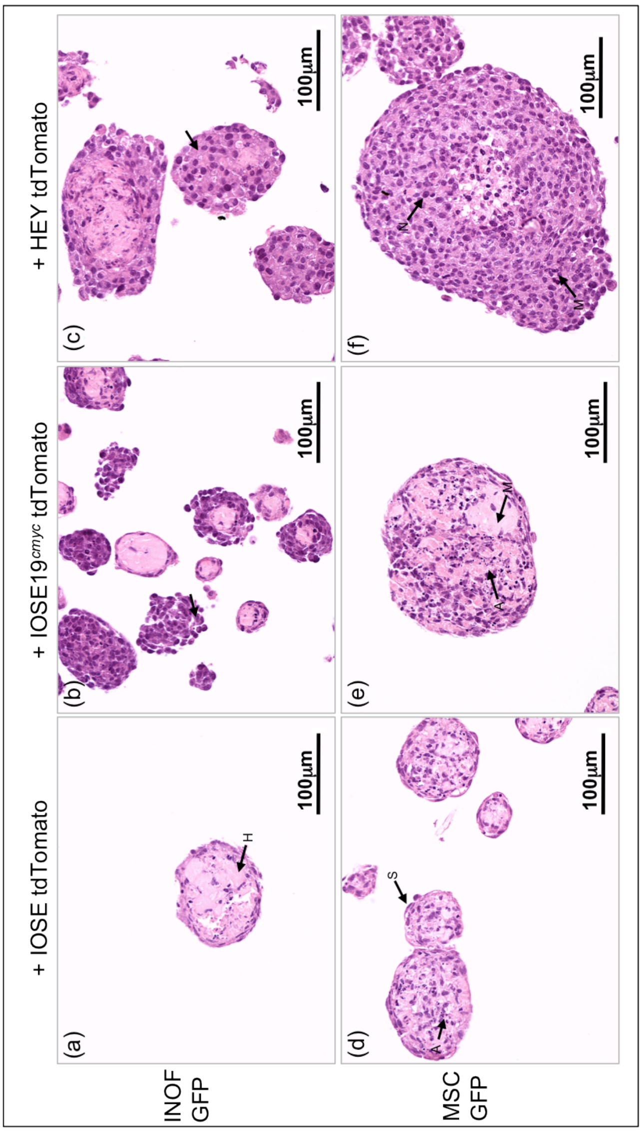

Figure IV-4: Haematoxylin and Eosin (H&E) staining of heterotypic three-dimensional cultures. (a) Spheroids of INOFs and IOSE cells showed not much activity. Cells contained small amounts of cytoplasm and some hyaline material (arrow H) was present. (b) Spheroids of INOFs and IOSE19*cmyc* cells showed variation in size and shape. Several spheroids cut at different levels were visible, which showed that spheroids contain a matrix core, which was surrounded by 2-3 layers of cells. Some mitosis could be detected and the cells had pleomorphic nuclei with prominent nucleoli (arrow). (c) Spheroids of INOFs and HEY cells were arranged in sheets and showed nuclear pleomorphisms. They appeared active and cells had abundant eosinophilic cytoplasm and prominent nucleoli. Some intracytoplasmic vacuoles (arrow) were present. (d) Spheroids of MSCs and IOSE cells. The cells in the core of the spheroid were big, there was a large level of apoptosis (arrow A), whereas the cells at the cap were spindle shaped (arrow S). (e) Spheroids of MSCs and IOSE19*cmyc* cells showed an active morphology. Some large nuclei with prominent nucleoli were present. Several cells in the middle were apoptotic (arrow A) and matrix deposits (arrow M) were observed. (f) Spheroids of MSCs and HEY cells formed very big spheroids and there were approximately 10 cell layers before any apoptosis was seen. Pleomorphic nuclei with a variation in size and prominent nucleoli (arrow N) were present. The mitotic index (arrow M: mitotic figure) was very high and the section resembled an ovarian tumour section. Some ground substance in the centre was visible.

IV.2.3 FACS analysis of heterotypic multicellular spheroids

Stromal and epithelial cells were labelled with GFP and tdTomato as described earlier (IV.2.2) and cultured at a ratio of 3:1. To analyse the behaviour of both cell types within a spheroid culture I chose to use flow cytometry to analyse how the ratio of both cell types changes in culture over time and to see if one cell type 'outcompetes' the other. INOFs and MSCs were used as the stromal component together with the epithelial cell lines IOSE and HEY. 3:1 ratios of stromal and epithelial cells were mixed and seeded in duplicates onto polyHEMA coated tissue culture flasks. The spheroids were harvested after 1, 4 and 7 days in culture, dissociated with accutase to obtain a single cell suspension and analysed using flow cytometry. After 1 day of 3D co-culture spheroids with the INOF cell line as the stromal component still showed a close to 3:1 ratio. Spheroids with MSCs as the stromal cells however, showed a ratio closer to 1:1 of stromal to epithelial cells (Figure IV-5a). After 4 days of culture the normal ovarian epithelial cell line IOSE was outgrown by the stromal cell line suggesting different rates of proliferation. There was no difference in the percentage of epithelium when INOFs or MSCs where co-cultured and more than 90% of cells analysed were stromal cells. The cultures with the ovarian cancer cell line HEY however, showed the opposite effect. The cancer cells outgrew the stromal component regardless whether cultured with INOFs or MSCs (Figure IV-5b). This was similar to the situation after 7 days of co-culture where IOSE cells were outgrown by the stromal component (96% and 99.9% stromal cells) and HEY cells (91.4% and 92% epithelial cells) outgrew the stromal cells (Figure IV-5c).

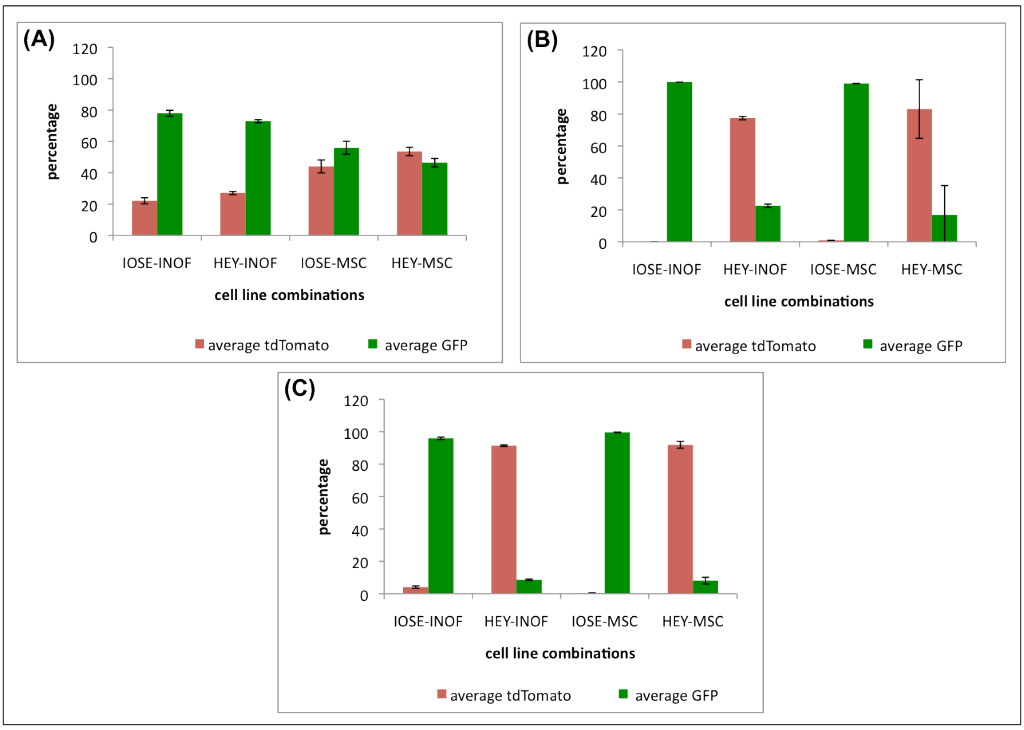

Figure IV-5: Results of FACS analysis of heterotypic three-dimensional cultures. Immortalised ovarian surface epithelial (IOSE) cells and the epithelial ovarian cancer (EOC) cell line HEY were co-cultured with either an immortalised ovarian fibroblast (INOF) cell line or a mesenchymal stem cell (MSC) line. The stromal cells were labelled with GFP whereas the epithelial cells expressed the red fluorescent protein tdTomato. The effect of the coculture on the growth rates of both cell types was observed using FACS analysis. The starting ratio was 3:1 (stromal: epithelial), i.e. 75% stromal (green) and 25% epithelial (red) cells. The cell suspension was plated onto polyHEMA coated tissue culture plastics and incubated for 1, 4 or 7 days. **(A)** Day 1. After 24 hours of co-culture the cells were harvested and prepared for FACS analysis. The heterotypic cultures containing the INOF cells still showed a ratio of around 3:1 (IOSE-INOF 22% : 78%; HEY-INOF 27% : 73%), whereas the ratio of the epithelial cells cocultured with MSCs decreased to closer to 1:1 (IOSE-MSC 44% : 56%; HEY-MSC 54% : 46%) **(B)** Day 4. Analysis on day 4 showed that the IOSE cells were outgrown by the INOFs as well as the MSCs (IOSE-INOF 0.01% : 99.9%; IOSE-MSC 1% : 99%) whereas the EOC cell line HEY continued to grow on a faster rate than the cocultured stromal cells (HEY-INOF 77.4% : 22.6%; HEY-MSC 83% : 17%). **(C)** Day 7. After 7 days of direct co-culture FACS analysis showed that stromal cells had taken over the cultures with IOSE cells (IOSE-INOF 4% : 96%; IOSE:MSC 0.4% : 99.6%) whereas the EOC cell line outgrew the INOFs as well as the MSCs (HEY-INOF 91.4% : 8.5%; HEY-MSC 92%: 8%).

IV.2.4 Confocal analysis of heterotypic multicellular spheroids

IV.2.4.1 Confocal analysis of polyHEMA cultured heterotypic spheroids

Confocal analysis of labelled heterotypic multicellular spheroids was performed to analyse the structure of the spheroids with regards to the location of both cell types relative to each other. Stromal and epithelial cells were mixed and plated at a 3:1 ratio and samples were taken and visualised alongside the flow cytometry experiment to verify the results. After 1 day in culture normal fibroblasts (INOFs) and normal epithelial cells (IOSE) formed dense spheroids with no clear separation of stromal and epithelial cells. Epithelial cells were found to be distributed within the stromal cells and more stromal cells than epithelial cells were visible. Spheroids consisting of the cancer cell line HEY and INOFs however showed some organisation with a stromal core and epithelial cells growing at the periphery. The stromal cells were more abundant than the epithelial cells. After 4 and 7 days of coculture hardly any IOSE cells were visible in the cultures with INOFs, which is supported by previous observations (Lawrenson, Grun et al. 2010). HEY cells however grew rapidly when cultured with INOFs and layer the whole surface of the stromal core after 4 days of culture. HEY cells kept expanding and after 7 days of culture several layers of epithelial cells covered the stromal core (Figure IV-6).

The mesenchymal stem cell (MSC) line was labelled with a different lentiviral vector than the fibroblast cell line (INOF), which led to weaker but clearly visible GFP expression in the MSC line. Similar to the cultures with INOFs normal epithelial cells were found within the MSCs after 1 day of co-culture. After 4 and 7 days of culture stromal cells were the predominant cell type visible. The epithelial ovarian cancer cells (HEY) also grew in a similar way when cultured with MSCs as to when cultured with INOFs. After 1 day in culture a few epithelial cells were visible growing around a stromal core whereas after 4 and 7 days in culture predominately epithelial cells were seen covering the MSCs core (Figure IV-7).

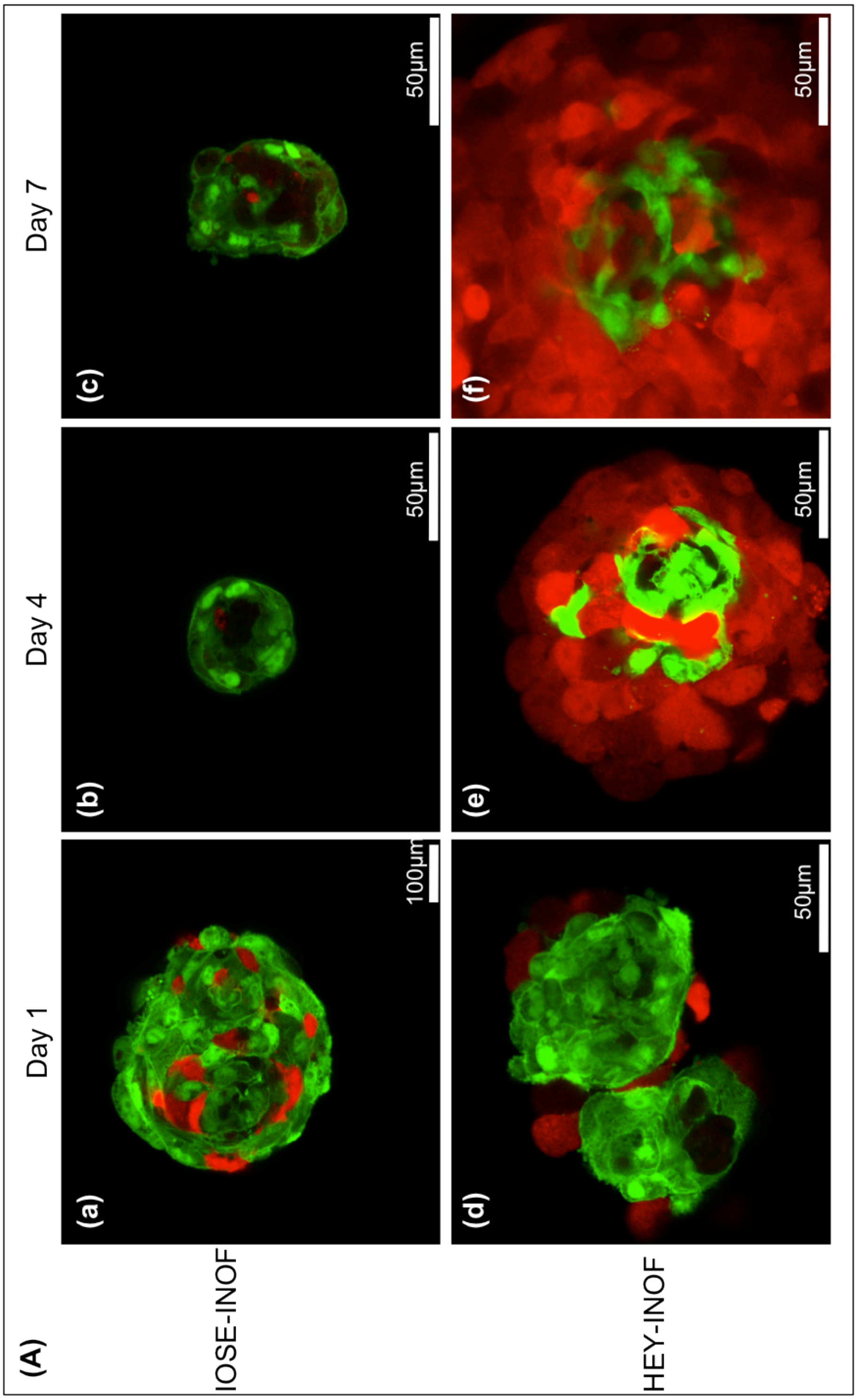

Figure IV-6: Confocal images of heterotypic three-dimensional cultures taken at different time points. Representative pictures of multicellular spheroids (MCSs) taken alongside FACS analysis. The pictures visualise the co-culture of GFP labelled stromal cells and tdTomato labelled epithelial cells. Pictures were taken after 1,4 and 7 days in culture. **(A)** Green labelled immortalised normal ovarian fibroblasts (INOFs) formed the core of the multicellular spheroid when cultured with the epithelial ovarian cancer (EOC) cell line HEY (d-f). If cultured with the immortalised ovarian surface epithelial (IOSE) cells there was no clear separation and some epithelial cells could be found within the stromal core (a-c).

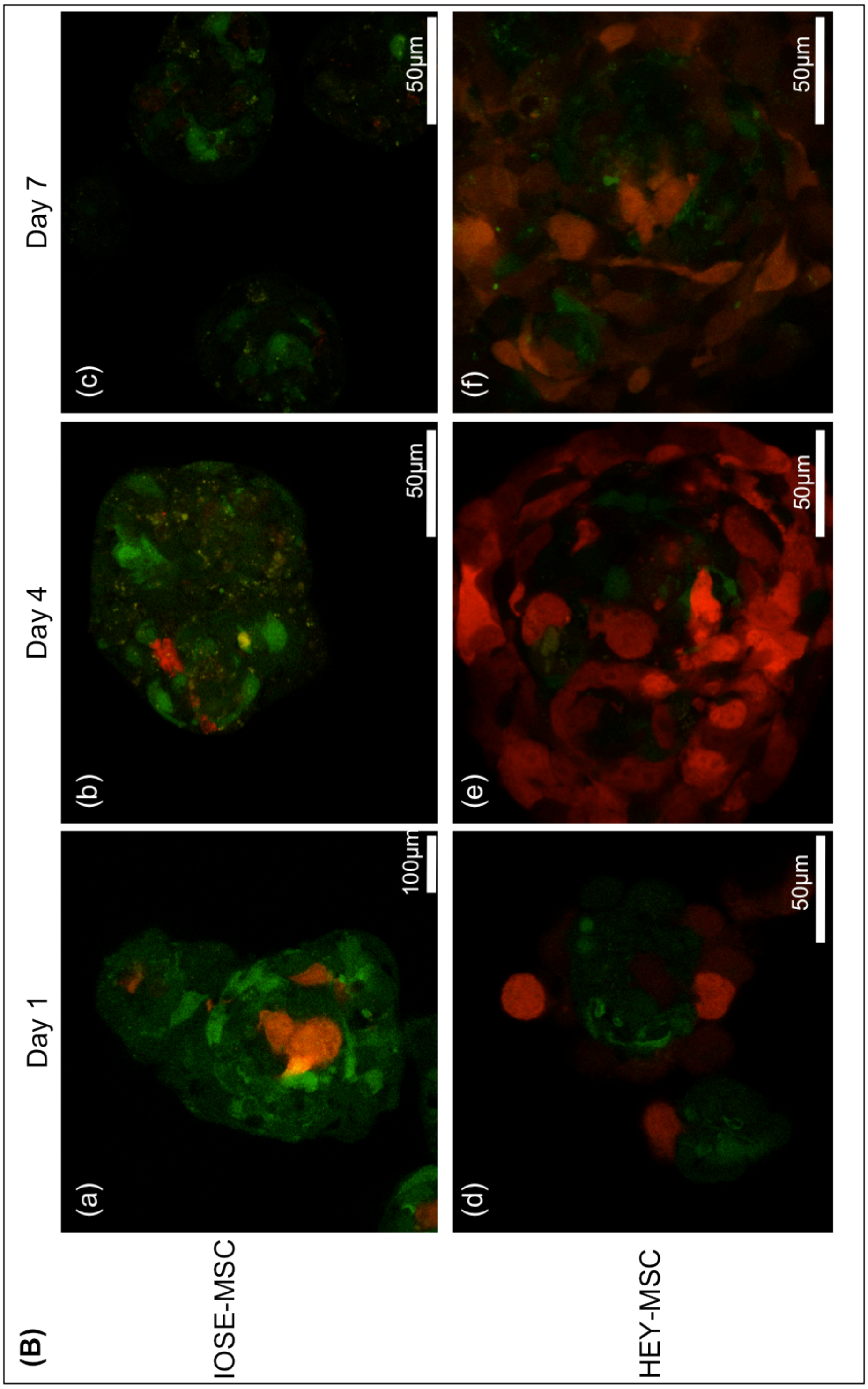

Figure IV-7: Confocal images of heterotypic three-dimensional cultures taken at different time points. Representative pictures of multicellular spheroids (MCSs) taken alongside FACS analysis. The pictures visualise the co-culture of GFP labelled stromal cells and tdTomato labelled epithelial cells. Pictures were taken after 1,4 and 7 days in culture. **(B)** The same applies to the heterotypic cultures using mesenchymal stem cells (MSCs) as the stromal component. From day 4 of co-culture IOSE cells appeared to stop proliferating and only the stromal cells were visible (a-c). The EOC cell line HEY continued to proliferate and overgrew the stromal component (d-f). The pictures confirm the results seen after FACS analysis.

IV.2.4.2 Confocal analysis of heterotypic hanging droplet spheroids

The hanging droplet approach to grow 3D spheroids can be used to grow same size spheroids. This can be particular useful for testing and evaluating the response of cells to drugs or the downregulation/overexpression of genes (Dafou, Grun et al. 2010). I chose this approach to analyse the behaviour of epithelial cells if added to stromal spheroids. The main question was if epithelial cells tend to invade into the stromal core and to address this, uniformly sized stromal spheroids are required. I therefore plated INOFs and MSCs in inverted multiwell plates and left them to incubate for 1 week to allow spheroid formation. Epithelial cells (IOSE, IOSE19^{cmyc} and HEY) were then added at a ratio of 3:1 stromal:epithelial cells (starting cell number) and left to incubate for 1 day and 7 days. Confocal images were taken 1 and 7 days after the addition of epithelial cells and representative pictures of the middle section of the spheroids were taken.

After one day of co-culture, one layer of IOSE cells could be seen covering the stromal core, with slightly more cells visible around the MSC core than the INOF core. There were hardly any IOSE19^{cmyc} cells visible with both stromal cell cores. The epithelial ovarian cancer cell line HEY was clearly visible at the periphery of the stromal core. Several layers of epithelial cells covered the MSC spheroids with slightly less epithelial cells appeared to be growing around the INOF core (Figure IV-8).

After a further week of co-culture hardly any epithelial cells were visible in the cultures with the INOF cells. Only the HEY epithelial cells were still covering the INOF core. In the cultures with the MSC core however, plenty of IOSE cells and HEY cells were visible. IOSE19^{cmyc} cells could still be detected in culture with MSCs but only a few epithelial cells were visible at the edges of the spheroid. IOSE and HEY cells seemed to have invaded the MSC core and were also found within the spheroid in addition to the periphery. HEY cells were found at the centre of the spheroids whereas IOSE cells invaded the edges of the spheroid (Figure IV-9).

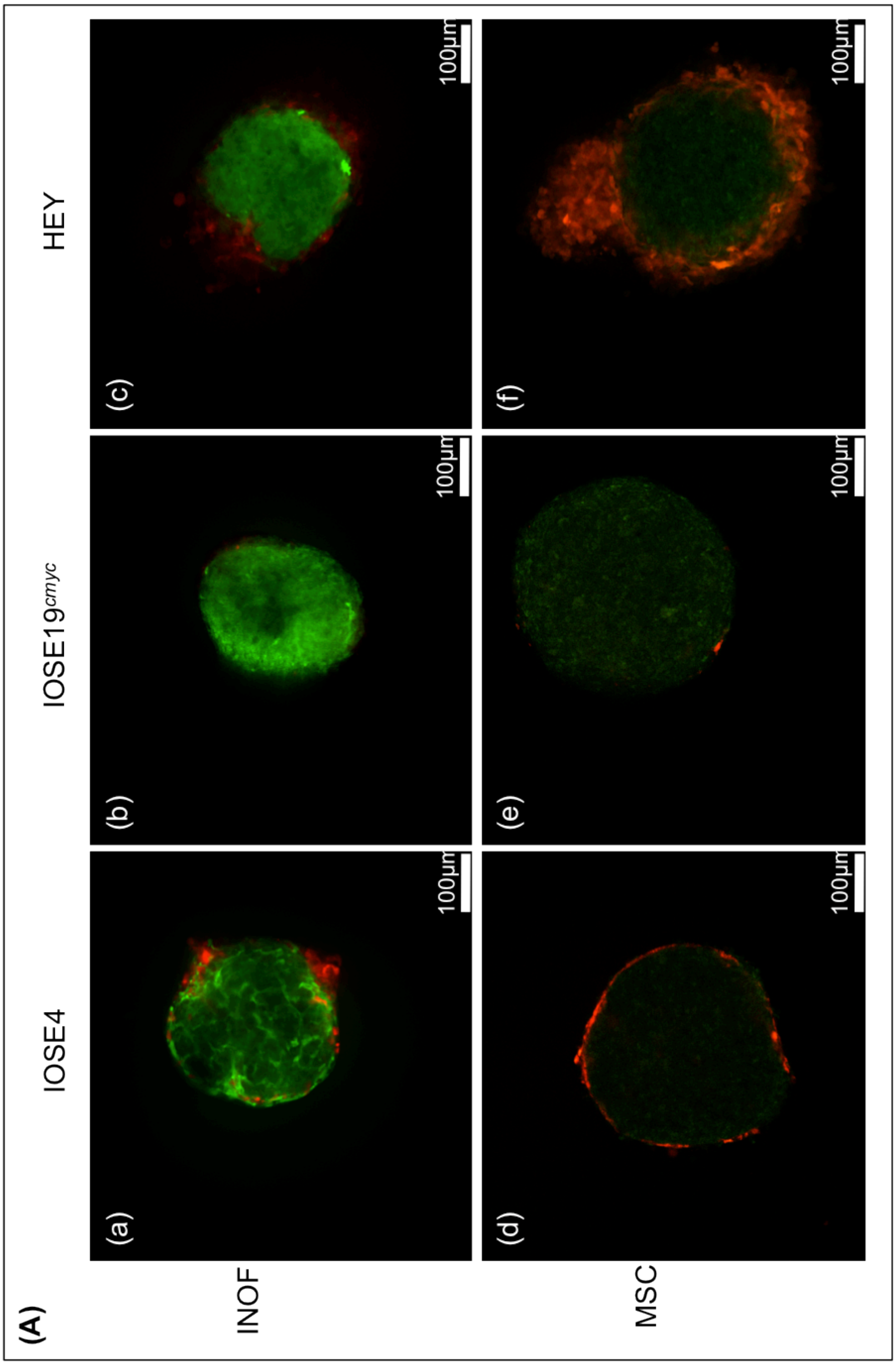

Figure IV-8: Confocal images of hanging droplet co-cultures (A) 1 day after addition of epithelial cells to the stromal spheroids, the epithelial cells could be seen lining the stromal core. IOSE cells and IOSE19^{cmyc} cells appeared to grow at the same rate when co-cultured with INOFs or MSCs and were seen lining the stromal core (a, b ,d ,e). The EOC cell line HEY appeared to grow faster when co-cultured with MSC as compared to INOFs. 1 day after addition the HEY cells could be found growing at the periphery of the stromal core (c) and there appeared to be more epithelial cells in the sample containing MSC (f) as the stromal component.

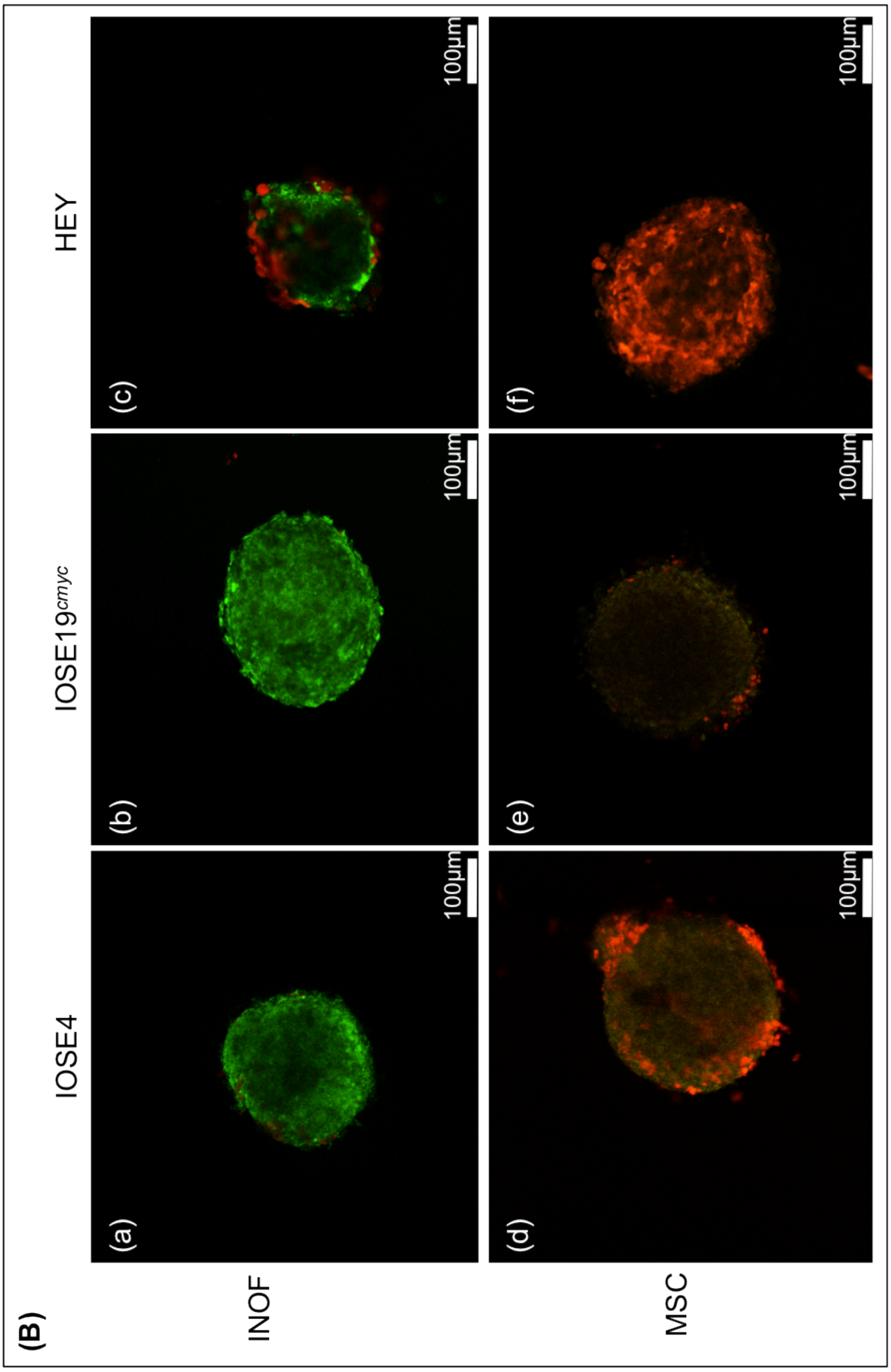

Figure IV-9: Confocal images of hanging droplet co-cultures. (B) Pictures taken 7 days after addition of epithelial cells. No IOSE or IOSE19^{cmyc} cells were visible in the cultures with the INOF core (a, b). Few HEY cells were seen lining the INOF core after 7 days of co-culturing (c). In the cocultures with the MSCs however plenty of epithelial cells were seen lining the stromal core (d, e, f). Several epithelial cells also seemed to have invaded into the MSC containing core of the spheroid (d, f). This was most obvious in the coculture with the HEY cancer cell line (f).

IV.3 Discussion

In the previous chapter I have shown that three-dimensional models of cancer are very good representations of the *in vivo* tumour. These models however, only contained the malignant cell itself, and the interactions of the tumour cells with the microenvironment were disregarded. In the late 19th century Paget formulated the seed and soil hypothesis when he observed that malignant cancer cells form tumours in some organs but not in others (Paget 1989). He postulated that the microenvironment plays an important role where a cancer cell can settle and form a tumour deposit. This observation lay unnoticed until the second half of the 20th century when his theory was revived by a group showing the preference of melanoma cells to metastasise to certain organs (Hart and Fidler 1980). Since then several reports have shown the influence of the microenvironment on tumour cell behaviour (Mintz and Illmensee 1975; Dolberg and Bissell 1984) and it was argued that tissue phenotype is dominant over cellular genotype (Weaver, Petersen et al. 1997). It is now widely accepted that the tumour microenvironment plays an important role in tumour initiation, maintenance, progression and metastasis (Bhowmick, Neilson et al. 2004; Hwang, Moore et al. 2008; Grugan, Miller et al. 2010; Allen and Louise Jones 2011). It is therefore imperative to include the tumour microenvironment when modelling cancer growth *in vitro*.

Previously, a heterotypic three-dimensional model of normal pre-senescent/senescent ovarian fibroblasts with IOSE/IOSE^{cmyc} cells as a model of early transformation of ovarian surface epithelial cells was established in the laboratory (Lawrenson, Grun et al. 2010). The effect of the pre-senescent and senescent fibroblast population on IOSE/IOSE^{cmyc} cell morphology and proliferation was evaluated using immunohistological staining. The actively proliferating epithelial cell population was identified by dual stain for the epithelial marker ck18 and the proliferation marker Mib1. Direct coculture in 3D spheroids of senescent fibroblasts and IOSE^{cmyc} cells led to significantly increased proliferation rates in the epithelial cells compared to cocultures with pre-senescent fibroblasts. No significant differences in epithelial cell proliferation were observed when IOSE cells were cocultured with senescent or pre-senescent fibroblasts.

In this chapter, I have taken this heterotypic 3D model of early transformation a step further by including an epithelial ovarian cancer cell line and cancer associated fibroblasts (CAFs) to generate a heterotypic 3D model of ovarian cancer. I chose to use MSCs to represent CAFs, which are the predominant cell type found within the tumour microenvironment. The relationship between MSCs and CAFs is explored further in the following chapter. Spheroids generated from coculturing normal immortalised ovarian fibroblasts (INOFs) with normal ovarian surface epithelial (IOSE) cells exhibited a quiescent morphology and resembled the state of a normal ovary *in vivo*. The normal ovary consists of the ovarian cortex containing the follicles embedded within the stroma and is covered by a layer of dormant epithelial cells. Only after ovulation changes the state of quiescence to a proliferative one to repair the site of rupture. The addition of MSCs showed no effect on IOSE cells and spheroids still demonstrated a quiescent morphology. Cocultures of the transformed cell line IOSE19^{cmyc} and the cancer cell line HEY with INOF cells demonstrated an active morphology and represented neoplastic growth. When cocultured with MSCs however the resulting spheroids appeared larger in size and less organised. In particular the morphology with stromal and epithelial cell compartments plus the histological features of spheroids coculturing the HEY cancer cell line with MSCs resembled a tumour section. These results show that it is possible to create a heterogeneous three-dimensional model that represents the *in vivo* state of a normal ovary and of ovarian cancer.

The morphological observations also suggest that the choice of stromal cells can affect the growth of the epithelial cell type. The addition of MSCs led to the formation of larger and more disorganised spheroids compared to the addition of INOFs. However, this was only true for the coculture with the transformed epithelial cells and no effect was seen in the cultures with IOSE cells. Lawrenson et al have also shown that differences in the phenotype of fibroblasts affect the behaviour of transformed ovarian epithelial cells (IOSE^{cmyc}) whereas normal ovarian epithelial cells (IOSE) are unaffected (Lawrenson, Grun et al. 2010). Senescent fibroblasts derived from normal ovarian fibroblasts have been shown to lead to increased migration rates in transformed ovarian epithelial cells while not affecting the migration rates of IOSE cells in a 2D migration assay.

In other studies the interactions between stromal and epithelial cells within a heterotypic 3D model have been investigated. In 2008, Krause and coworkers have established a three dimensional model using human mammary fibroblasts and a human mammary epithelial cell line (Krause, Maffini et al. 2008). Coculture of these cell types within a collagen matrix concluded in the formation of ductal and alveolar structures. Another example of a heterotypic three dimensional model incorporates normal/cancer associated lung fibroblasts and normal human bronchial epithelial cells using a collagen matrix (Pageau, Sazonova et al. 2011). Pageau et al observed that the addition of normal fibroblasts led to the generation of a normal respiratory surface epithelium whereas the addition of cancer associated fibroblasts resulted in invasion of the epithelial cells into the surrounding collagen gel.

These results show that the interaction between the different cell types has a significant impact on epithelial cell behaviour. Heterotypic three-dimensional models are therefore essential to further study those interactions *in vitro*. To advance the use of the heterotypic 3D model established here I chose to label both cell types using fluorescent proteins and evaluated potential subsequent assays to analyse the effect of INOFs and MSCs on the epithelial cell population.

Using fluorescent activated cell sorting (FACS) I was able to analyse the composition of each spheroid culture and detect differences in population sizes between the epithelial and stromal components. Differences in the size of the epithelial population cultured together with the different stromal components might indicate a promoting/inhibiting effect of the fibroblasts on epithelial cell proliferation rates and vice versa. Initially it seemed as if MSCs had a promoting effect on epithelial cell proliferation, which was lost after 4 days of direct coculture. From this point onwards no difference between INOFs and MSCs on epithelial cell population size could be detected. Alongside FACS analysis I used confocal microscopy to further analyse the composition of each spheroid and the location of the two cell populations relative to each other. This showed that over time the normal ovarian epithelial cells were outgrown by the stromal components whereas the EOC cell line was the predominant cell type within the spheroids after 4 days of co-culture. No difference was seen in response to normal ovarian fibroblasts or MSCs cocultures. This confirmed the results seen by FACS analysis.

This result seems somewhat surprising after the evidence seen in the literature where it has been shown that CAFs have a promoting effect on epithelial tumour growth compared to normal fibroblasts (Olumi, Grossfeld et al. 1999; Orimo, Gupta et al. 2005). However, the chosen experimental setup poses several points that could be improved. Firstly, two different virus vectors have been used to label INOFs and MSCs, which resulted in different fluorescent intensities between both cell lines. Furthermore, even within the labelled stromal cells it was possible to detect subpopulations exhibiting different fluorescent intensities. In addition, some crossover in fluorescence emission for GFP and tdTomato was discovered. These factors compromised FACS analysis since very rigorous cut off points had to be chosen, which only regarded labelled cells that exhibited the strongest fluorescence, thus disregarding parts of the cell populations. To overcome these limitations it will be necessary to use the same vectors to produce virus and infect INOFs and MSCs. It is also advisable to carefully determine the virus titer to limit infection with multiple copies of the fluorescent protein, which can lead to subpopulations exhibiting stronger fluorescence than the rest of the population (Striepen, He et al. 1998). FACS sorting to isolate the subpopulation of cells that show strong fluorescence will also aid to achieve a cell population that reveals homogenous expression of the fluorescent protein. Equal fluorescent intensities of all cell lines tested will also facilitate confocal microscopy. It would then be possible to quantify fluorescent intensities of the different proteins used and conclude population size of the different cell types.

Another factor that could be improved is the dissociation of the spheroids for FACS analysis. A large number of dead cells were detected in every sample and this together with the rigorous gating of only strongly fluorescent cells led to the analysis of only a small proportion of cells from each spheroid. Here I used accutase coupled with repeated pipetting of the spheroids to obtain a single cell suspension. An alternative enzyme could be trypsin, which has been successfully used to dissociate spheroids (Lawrenson, Benjamin et al. 2009; Bartosh, Ylostalo et al. 2010). Furthermore due to the size of the spheroids it might be more effective to test differential dissociation to minimize the exposure time of the single cells to the enzyme. In this method the spheroids are incubated with a dissociation enzyme until the outer layers of the spheroid detach and the reaction is stopped. This will be repeated with the remaining spheroid until a single cell suspension is obtained (Kunz-Schughart and Freyer 1997).

It might also be useful to include an early transformed epithelial cell line (IOSE19^{cmyc}) in this experiment. Since an initial effect of the MSCs on epithelial cell growth was detected, but was lost after a couple of days in culture, it might be necessary to study the effect on an early transformed cell line. The cancer cell line HEY shows very aggressive growth characteristics and may no longer be responsive to microenvironmental signalling to modulate growth properties. Therefore the use of an early neoplastic cell line, which will be more susceptible to environmental stimuli, may enable more sensitive detection of growth promoting and/or growth inhibiting signalling from the microenvironment.

To further understand what occurs within each cell population at the different time points it would be useful to combine the FACS analysis with cell cycle analysis using DAPI staining. This would allow examination of each cell population and confirm any change of cell cycle distribution upon coculture with the different cell types. Therefore it would give a good indication if proliferation rates of the epithelial cell lines after 1 day of coculture with MSCs are increased compared to the culture with INOFs. Furthermore, it would be interesting to determine if there was any change in cell cycle distribution within the epithelial cells upon coculture with the different stromal cells at the later timepoints. This could be coupled with staining of the spheroids with the proliferation marker Mib1 and subsequent confocal microscopy to analyse rates of actively proliferating cells within each cell population.

In conclusion, improvement of the experimental set up may generate a good method to analyse the proliferation rates of different cell types within a spheroid and allows the analysis of stromal epithelial interactions using immunofluorescent staining followed by confocal microscopy.

To assess the tumourigenic behaviour of a cell line, standard invasion assays are usually performed. However, commercially available assays use the 2D culture system to evaluate the invasive ability of a cell line. These assays use a chemoattractant to measure the ability of a cell line to invade through a basement membrane. Here I chose to establish a three-dimensional invasion assay using the hanging droplet method. Spheroids of INOFs were not invaded by any epithelial cell line whereas IOSE and HEY cells can be found within MSC spheroids after 7 days of culture. However, the same limitations regarding the fluorescent proteins apply as they have been described before. It is therefore difficult to determine if the invasion of epithelial cells into the MSC core is a true result or an experimental artefact due to bleed through of the red fluorochrome. However, improvement of the beforementioned steps would lead to an interesting alternative to traditional 2D invasion assays. It would be possible to quantify the invaded cells and cell invasion could be monitored using time-lapse microscopy.

IV.4 Conclusion

In the future the here established heterotypic 3D assays could be used to model changes in candidate gene expression in the stroma and observe how this influences epithelial cell behaviour. Furthermore, these models might also be useful to understand how cocultured stromal cells affect the molecular profiles of epithelial cells and to look at changes in the stromal phenotype and genotype upon coculture with different types of epithelia. Ultimately it is hoped that these models could be used to investigate origins of CAFs (which is explored in the next chapter); identify much needed biomarkers for early ovarian cancer detection; and finally to develop novel therapeutics that target the stromal tumour microenvironment.

V Mesenchymal stem cells or normal resident fibroblasts as the source of cancer associated fibroblasts

V.1 Introduction

It is now widely accepted that the tumour microenvironment plays an important role in the maintenance, development and metastasis of epithelial cancers. The tumour microenvironment consists of extracellular matrix and a heterogeneous population of cells in addition to the tumour epithelia, including immune cells, endothelial cells, pericytes and others. The predominant cell type within the microenvironment is the cancer associated fibroblast (CAF). Marker expression profiles and *in vitro* phenotypes of CAFs differ significantly from those normally found in the tissue stroma; CAFs more closely resemble myofibroblasts that are usually found at sites of wound healing (Sappino, Schurch et al. 1990). These fibroblasts are characterised by their expression of α-smooth muscle actin (αSMA), fibroblast specific protein (FSP) and vimentin. Many studies have reported that the microenvironment influences cancer growth (Mintz and Illmensee 1975; Dolberg and Bissell 1984) and other groups have shown that CAFs promote epithelial cancer growth *in vitro* and *in vivo* (Olumi, Grossfeld et al. 1999; Orimo, Gupta et al. 2005). The interactions between CAFs and epithelial cancer cells seem to be essential for tumour development and growth and therefore represent a potential source of novel targets for anti-tumour therapy. However, these interactions and the characteristics of CAFs remain poorly understood in EOC. The source of CAFs is still unclear and the most popular theories propose normal resident fibroblasts to be the precursor cell of CAFs (Kalluri and Zeisberg 2006; Orimo and Weinberg 2006; Mueller, Goumas et al. 2007) and/or bone marrow derived mesenchymal stem cells (MSCs) (Karnoub, Dash et al. 2007; Mishra, Mishra et al. 2008; Spaeth, Dembinski et al. 2009). To understand the interactions between tumour cells and the microenvironment it is essential to identify the precursor cell type/types of CAFs.

Here I address the question 'can normal ovarian fibroblasts and/or mesenchymal stem cells serve as a source of cancer associated fibroblasts in epithelial ovarian cancer?' I hypothesise that the precursor cell type of CAFs will be able to transdifferentiate into CAF-like cells upon treatment with conditioned medium obtained from epithelial ovarian cancer cells. I further examine the effect of those differentiated cells on transformed epithelial ovarian cells.

V.2 Results

V.2.1 Characterisation and cultivation of mesenchymal stem cells

Two fully characterised mesenchymal stem cell lines were obtained from the Texas A&M Health and Science Centre. Cell line 7076 was isolated and established from a 37-year-old female donor while cell line 7078 was obtained from a 24-year-old male donor. Both cell lines show homogenous expression of mesenchymal stem cell markers.

Mesenchymal stem cells are characterised by their multipotency and can differentiate into chondrocytes, myocytes, adipocytes and osteocytes. Upon prolonged culture however, the cells loose their ability to form colonies from single cells and the ability to differentiate. Maintenance of pluripotency is essential for the subsequent differentiation experiments and it was therefore important to perform quality control assays regularly. Between passage 2 and 4 cell line 7076 forms 56 (+/- 7.1) colonies and cell line 7078 form 47 (+/- 4.2) colonies out of 100 plated single cells. Differentiation assays at passage 2 and 4 showed differentiation of both cell lines into osteocytes with differentiation rates up to 80%. Adipocyte differentiation of cell line 7076 was weaker than cell line 7078 but still approximately 60%. The ability to differentiate is essential for all subsequent assays and therefore the earliest passages are most favourable. Hence, the starting passage number for all following experiments was not higher than 4 and all experiments were concluded by passage 8.

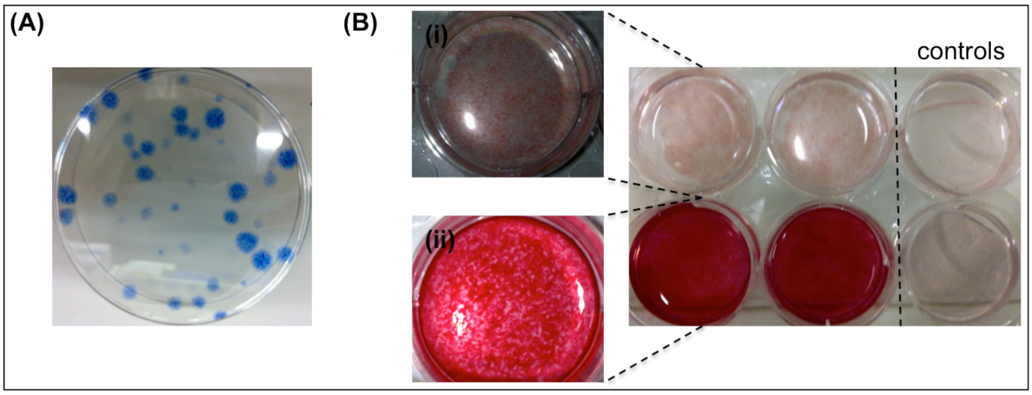

Figure V-1: Quality control assays of mesenchymal stem cells (MSCs). (A) Colony forming units. 100 cells were plated and incubated for 20 days. The MSC line 7076p4 forms 51 colonies and cell line 7078p4 forms 50 colonies. **(B)** Differentiation assays performed at passage 4. 50.000 cells were plated per well and assays were performed in duplicates. As a control, cells were cultured in their normal growth medium. **(i)** Adipocyte differentiation assay. After 21 days of incubation in adipocyte differentiation medium cells were stained with Oil-Red-O to visualise fat deposits. Both cell lines differentiated into adipocytes, 7076 showed 60% positive Oil-Red-O staining whereas 7078 showed 80% positive staining. **(ii)** Osteocyte differentiation assay. After 21 days of incubation with osteocyte differentiation medium, the presence of calcium was confirmed using alizarin red. Both cell lines differentiated well into osteocytes and showed 80% positive staining.

V.2.2 Differentiation of MSCs and normal ovarian fibroblasts into CAF like cells using standard 2D culture methods

V.2.2.1 Pilot experiments – differentiation of MSCs into CAFs

Pilot experiments were performed to analyse the potential of the two MSC lines 7076 and 7078 to differentiate into CAF-like cells by culturing them using conditioned medium obtained from two EOC cell lines (OAW42 and HEY). OAW42 was derived from ascitic fluid tumour cell aggregates from a patient with an ovarian cystadenocarcinoma (Wilson 1984); the HEY ovarian cancer cell line was derived from a human EOC xenograft of a peritoneal lesion removed from a patient with moderately differentiated papillary cystadenocarcinoma (Buick, Pullano et al. 1985). Conditioned medium (CM) was prepared by plating $3x10^6$ cells in a 145mm dish for 24 hours, before washing thoroughly with PBS and then refeeding cells with 15ml serum free medium for 48 hours. The resulting CM was collected, filtered to remove any cells and debris and used for the stromal cell differentiation assays (Figure V-2 for a schematic overview).

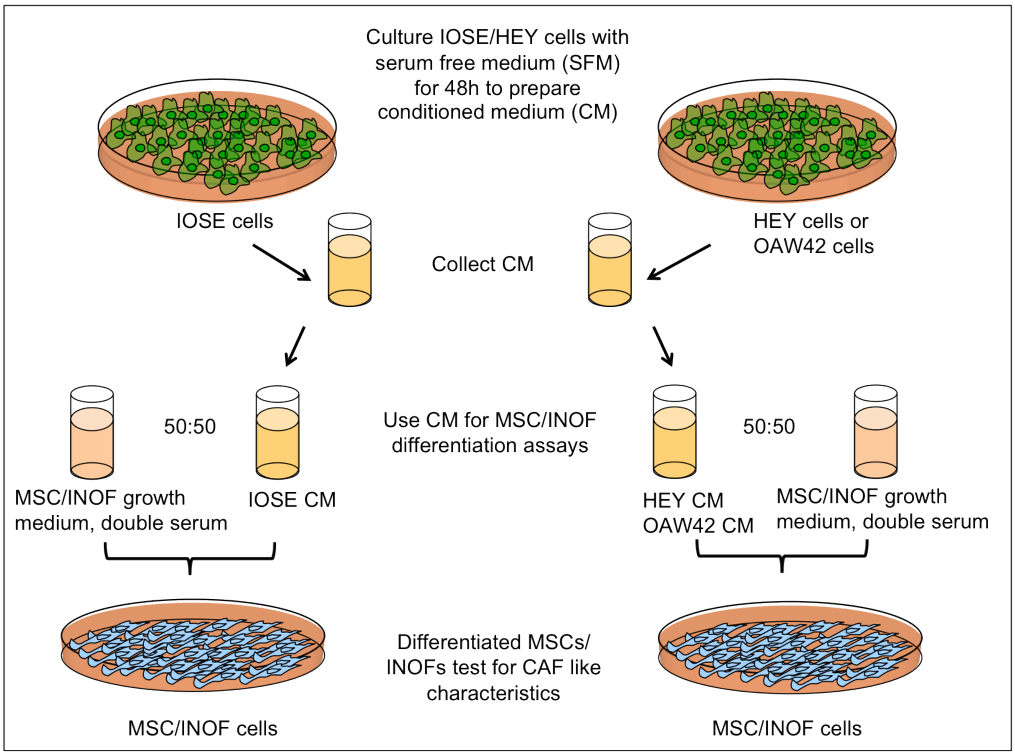

Figure V-2: Schematic view of differentiation assays using conditioned medium. Immortalised ovarian surface epithelial (IOSE) cells and an epithelial ovarian cancer (EOC) cell line HEY (and OAW42 for pilot experiments) were cultured for 48h with serum free medium. The resulting conditioned medium (CM) was harvested after 48h, filtered and either snapfrozen or used immediately for differentiation assays. Mesenchymal stem cells (MSCs) and immortalised normal ovarian fibroblasts (INOFs) were cultured with CM and their normal growth medium at a 50:50 ratio to achieve differentiation towards a CAF like phenotype. At the end of the differentiation experiment MSCs/INOFs were harvested and tested for CAF like characteristics.

Serum free medium (SFM) and conditioned medium from a normal immortalised ovarian surface epithelial (IOSE) cell line were used as controls. Conditioned media were used to culture MSCs and to assay for a CAF phenotype; immunofluorescent cytochemistry and western blotting were performed to measure expression of CAF and differentiated stromal cell markers, namely VIM, FSP and αSMA.

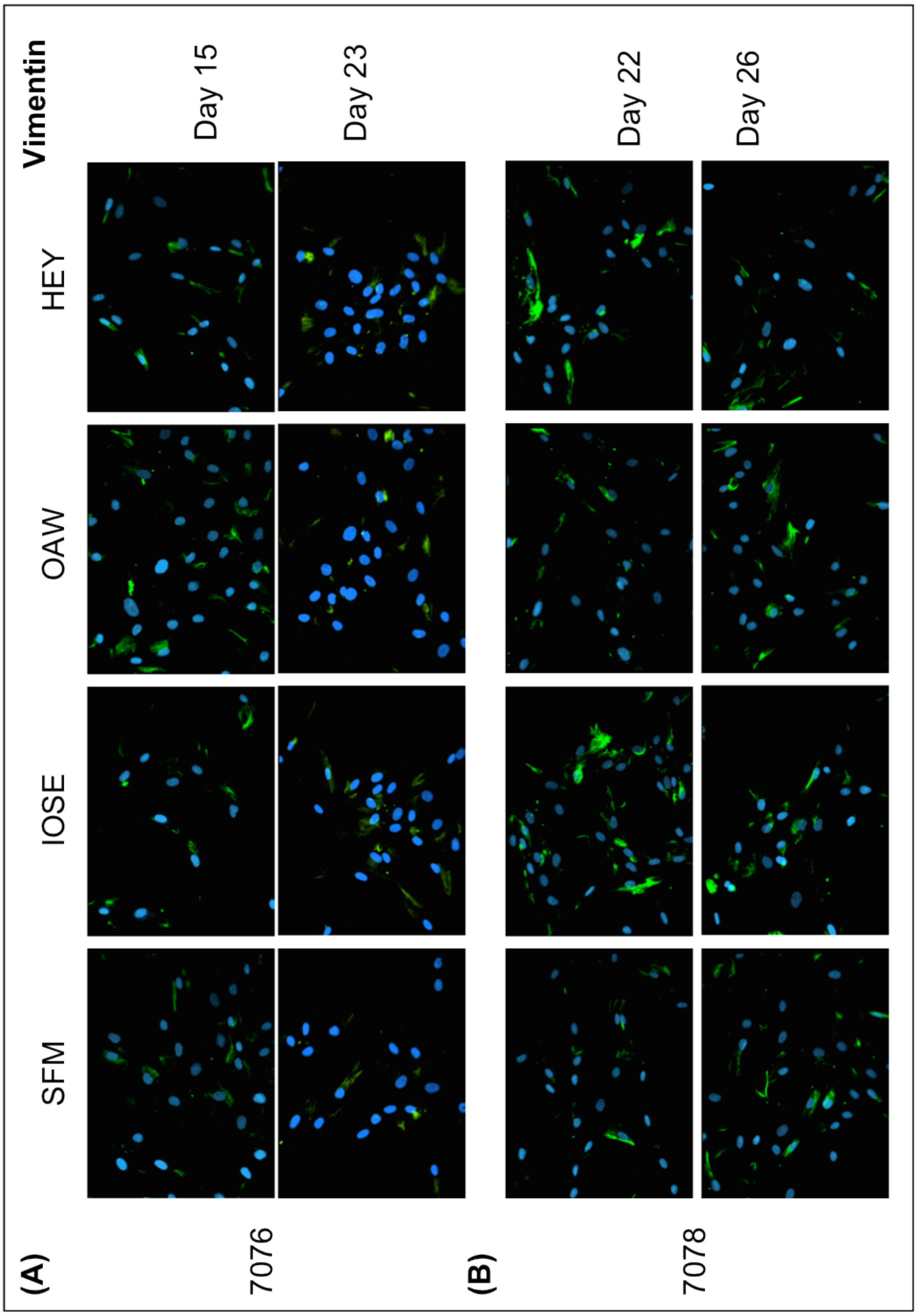

Figure V-3: Immunofluorescence staining for the marker Vimentin. (A) Vimentin expression was found to be increased after treatment with IOSE and HEY CM compared to the SFM control. A slight increase was also seen for OAW42 treated cells. **(B)** MSC line 7078 showed generally higher Vimentin expression rates than cell line 7076. Highest expression rates were found after treatment with IOSE and HEY conditioned medium compared to the SFM control. OAW42 also led to an increase of Vimentin expression compared to the SFM control. All images are 200x magnification.

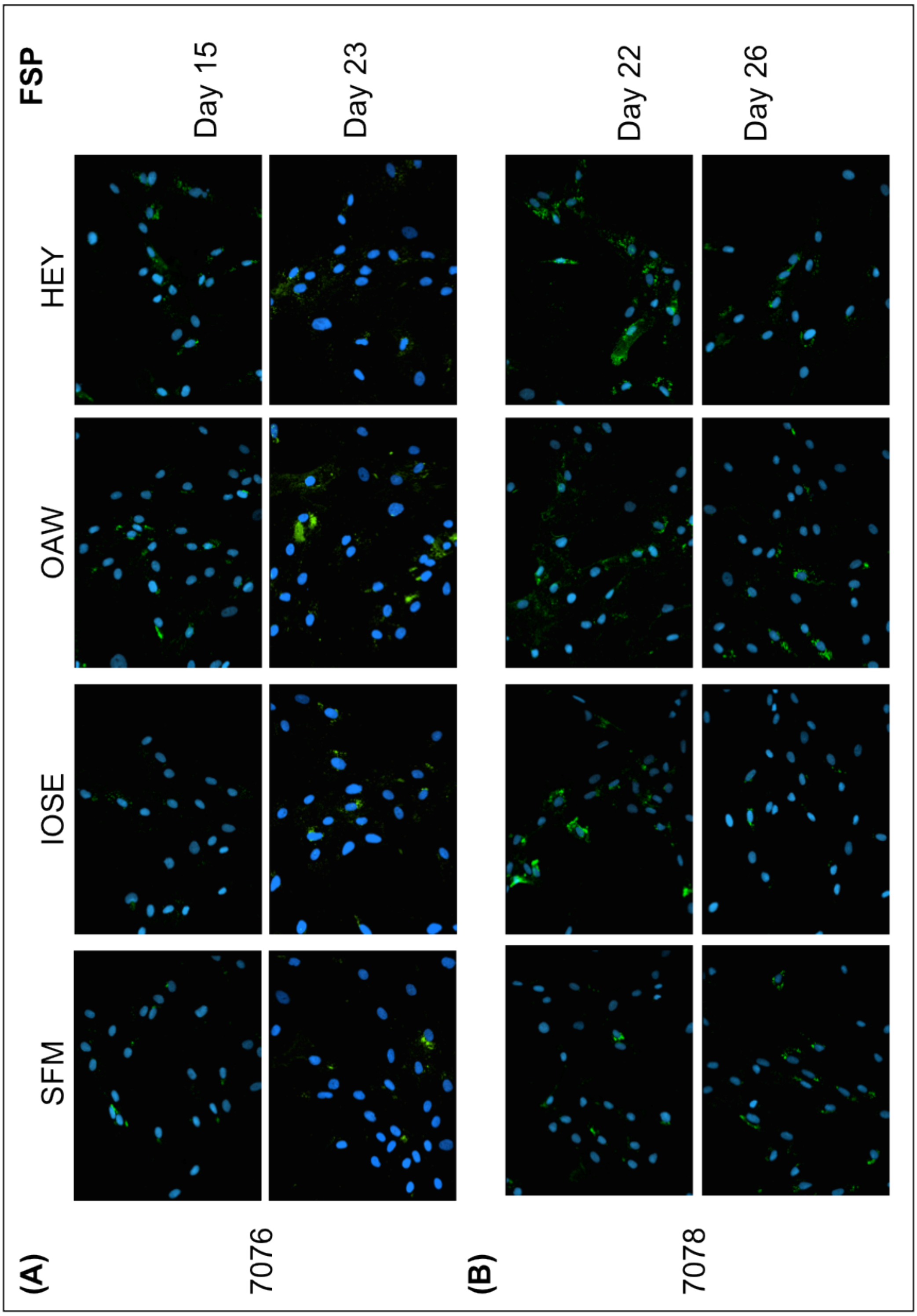

Figure V-4: Immunofluorescence staining for the marker FSP. Increased FSP expression was observed for the 7076 cell line upon treatment with IOSE, OAW42 and HEY CM. Highest expression rates were observed after culture with OAW42 and HEY CM medium. Expression was generally enhanced after 23 days of culture with CM compared to 15 days of CM treatment. The cell line 7078 also showed increased expression of FSP upon treatment with CM compared to the use of SFM. Strongest expression was observed after treatment with HEY CM. Expression rates were similar after 22 and 26 days of culture with CM. All images are 200x magnification.

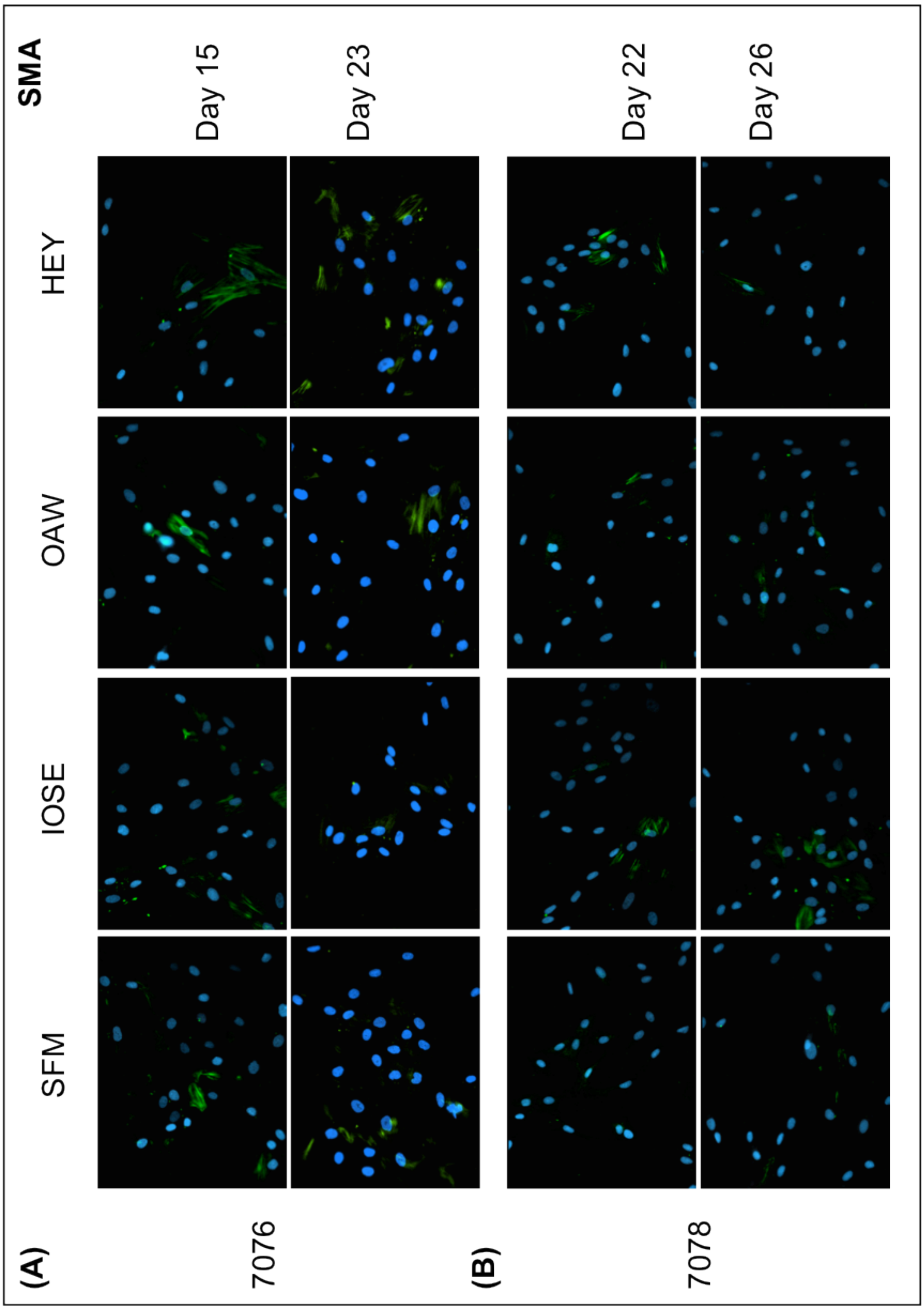

Figure V-5: Immunofluorescence staining for the marker SMA. SMA expression was generally weak compared to the other markers used. The MSC cell line 7076 showed increased SMA expression rates compared to the SFM control only upon treatment with HEY CM. No difference was detected between 15 and 23 days of culture with CM. The MSC line 7078 showed increased SMA expression upon treatment with IOSE and HEY CM compared to the SFM control. The expression rates were slightly increased after 26 days of culture compared to 22 days. All images are 200x magnification.

The MSC line 7076 showed some differentiation towards a CAF like phenotype after treatment with HEY CM. Increased Vimentin, FSP and SMA expression was detected after 23 days in culture. Treatment with OAW42 CM led to increased Vimentin staining after 15 days of culture, but this returned to baseline expression after 23 culture days. SMA expression remained unchanged. The control medium collected from IOSE cells led to increased Vimentin expression after 23 days in culture and a slight increase in FSP expression, but no effect was detected on SMA expression. Culture of 7076 cells in SFM did not induce any observable changes in marker expression over 23 days. (Figure V-3 (A), Figure V-4 (A), Figure V-5 (A), for a summary of immunofluorescence results: Table V-1).

The MSC line 7078 also showed differentiation towards a CAF phenotype upon treatment with HEY conditioned medium. After 22 days in culture strong staining was detected for Vimentin and FSP. Increased SMA expression was also detected. There was no difference in staining for all three markers between 22 and 26 days of culture. Similar results were discovered after treatment with CM obtained from the normal ovarian surface epithelial cell line IOSE, although FSP expression appeared to decrease after 26 days in culture. The EOC cell line OAW42 also led to some expression of Vimentin and FSP after 22 and 26 culture days. However, SMA expression was not detected. Treatment with SFM also resulted in some increased expression of Vimentin and FSP after 26 days in culture, but at 22 days all markers are unchanged and SMA expression was not affected at all. (Figure V-3 (B), Figure V-4 (B), Figure V-5 (B), for a summary of immunofluorescence results: Table V-1)

Table V-1: Summary of immunofluorescence staining results of MSCs cultured with conditioned medium (CM). CM from two epithelial ovarian cell lines led to the expression of cancer associated fibroblast (CAF) associated markers in the mesenchymal stem cell (MSC) lines. Differentiation of the MSCs was examined by staining for the CAF markers vimentin, fibroblast specific protein (FSP) and smooth muscle actin (SMA) at several times during culture with conditioned medium. The conditioned medium (CM) was derived from the immortalised ovarian surface epithelial (IOSE) cell line and from the epithelial ovarian cancer cell lines HEY and OAW42. As a further control unconditioned (serum free medium; SFM) was used. HEY CM led to the highest expression of the CAF associated marker SMA. This was observed in both MSC lines and highest expression rates were discovered from 15 days of culture onwards.

	Antibody	Vimentin		FSP		SMA	
cell line		D 15	D 23	D 15	D 23	D 15	D 23
7076	SFM	+	+	+/-	+/-	+	+
	IOSE	+	+++	+/-	++	+	+/-
	OAW42	+++	+	++	+++	+	+
	HEY	+	++	++	++	+++	+++
	Antibody	Vimentin		FSP		SMA	
cell line		D 22	D 26	D 22	D 26	D 22	D 26
7078	SFM	+	++	+	++	+/-	+/-
	IOSE	+++	+++	++	+	+	++
	OAW42	++	++	+++	+++	+	+
	HEY	++	++	++++	++++	++	++

In summary, these data suggest that changes in vimentin expression in CM-cultured MSCs are not specific to culture in EOC CM, and may be a general change observed in response to culture of MSCs in media conditioned by any epithelial cell line. However, in both cell lines FSP and SMA expression was enhanced upon treatment with CM from the EOC cell line HEY. Especially increased SMA expression was found to be specific to HEY CM treatment.

However, to judge an increase or decrease of marker expression objectively it is necessary to use an appropriate software tool to analyse the fluorescent images. It will then be possible to quantify the fluorescent staining of each sample, compare the different conditions and make a judgement on how vimentin, FSP and SMA expression changes after culture with the different CM. Alternatively, western blotting can be used to compare expression of the analysed markers and protein bands can be quantified. This approach will be explored later in this chapter.

In summary, both MSC lines showed increased expression of the CAF markers FSP and SMA after culture with HEY CM. Cell line 7078 also showed increased Vimentin expression. Conditioned medium of the cell line OAW42 led to some increase of Vimentin and FSP expression in both cell lines but SMA expression was not enhanced. IOSE CM also induced Vimentin and FSP expression in the MSC line 7078 but SMA expression was only marginally increased. Thus, HEY CM showed the strongest ability to induce differentiation towards a CAF phenotype within both MSC cell lines. The data also suggests that cell line 7078 has a greater potential to transdifferentiate into CAF-like cells than MSC line 7076.

CAFs are thought to promote neoplastic development of tumour epithelia. To test whether *in vitro* derived CAFs could promote neoplastic transformation of a partially transformed cell line, MSCs that had been cultured in IOSE, OAW42 or HEY conditioned media were plated as a chemoattractant in a transwell invasion assay. The ability of a partially transformed IOSE cell line (overexpressing *CMYC*, IOSE19^{cmyc}) to invade in the presence of the *in vitro* derived CAFs was then assayed.

In the previous chapter I have observed that the addition of MSCs or INOFs to cultures of the epithelial ovarian cancer (EOC) cell line HEY had no detectable growth promoting effect. This may be due to the fact that this is a highly aggressive EOC cell line that is adapted to grow in cell culture and is likely to have lost dependence on stromal cells. Therefore, here I chose to use a partially transformed cell line for these assays in the hope that this cell line will be responsive to microenvironmental stimuli and respond with altered growth characteristics. IOSE19^{cmyc} cells contain only one oncogenic hit but have acquired the ability to grow in anchorage independent growth assays and are more invasive than parental IOSE cells; thus these cells represent a partially transformed ovarian epithelial cell model (Lawrenson, Sproul et al. 2011).

To investigate the effect of differentiated MSCs and INOFs on transformed ovarian surface epithelial cells I performed transwell invasion assays. Standard transwell invasion assays use foetal bovine serum (FBS) or bovine serum albumin (BSA) as chemoattractant to induce invasion of cells through a basement membrane towards the attractant. These assays were modified to test the ability of the differentiated cells to attract invasion of IOSE19^{cmyc} cells. Instead of a chemoattractant I plated differentiated MSCs and INOFs into the lower chamber of a transwell assay. In this pilotexperiment, the potential of MSCs and INOFs to attract invasion compared to the standard chemoattractant (FBS) was then assayed in using three replicates.

The MSC cell line 7076 treated with IOSE and HEY CM resulted in increased invasion rates of the cell line IOSE19^{cmyc} compared to SFM and OAW42 CM treated cells (data not shown). The MSC line 7078 also affected invasion rates of IOSE19^{cmyc} cells. Increased invasion was detected when SFM/OAW42/HEY treated MSCs were used to attract IOSE19^{cmyc} cells compared to the control (foetal bovine serum (FBS) as chemoattractant). IOSE treated MSCs had no enhancing effect on invasion rates. OAW42 and HEY CM treated MSCs led to increased invasion rates compared to MSCs treated with the CM of the normal control cell line IOSE (data not shown).

Taking into account the differentiation results and the results from the invasion assays I chose to use IOSE CM as a control and HEY CM to achieve transdifferentiation of potential CAF precursor cells for all subsequent assays.

V.2.3 Differentiation of putative precursor cells into CAFs using traditional 2D cell culture methods

Two mesenchymal stem cell (MSC) lines and one immortalised normal ovarian fibroblast cell line (INOF) were investigated as potential precursor cells of ovarian cancer associated fibroblasts (CAFs).

Fibroblast specific protein (FSP), Vimentin and smooth muscle actin (SMA) are markers associated with CAFs and so I evaluated expression of these markers after treatment with conditioned medium (CM) of HEY or IOSE cell lines using immunofluorescence as above. Expression rates were analysed by evaluating three fields of view using a fluorescent microscope for each sample. I measured both the intensity of the staining and the percentage of positively stained cells. All cell lines showed increased expression of FSP (Figure V-6). Both MSC lines exhibited increased expression rates from day 18 of culture with CM onwards. The strongest FSP expression was detected after 27 days of culture with IOSE/HEY CM. No difference was detected between the use of the control CM from IOSE cells and the medium obtained from the EOC cell line HEY. INOFs only displayed increased FSP expression after 27 days of culture with IOSE/HEY CM, but at this timepoint the detected expression was higher than in the MSCs at the same timepoint. Again, I found no difference between IOSE and HEY CM on FSP expression (Summary: Table V-2).

Vimentin is usually expressed by fibroblasts and hence the baseline expression of this marker in INOF cells was quite high (Figure V-7). After treatment with CM expression remained the same. MSCs responded to treatment with CM with increased expression of Vimentin. Consistently higher rates of Vimentin expression were detected following treatment with HEY CM compared to IOSE CM. Highest expression rates were detected in HEY CM treated cells after 27 days of culture (Figure V-7, Summary: Table V-2).

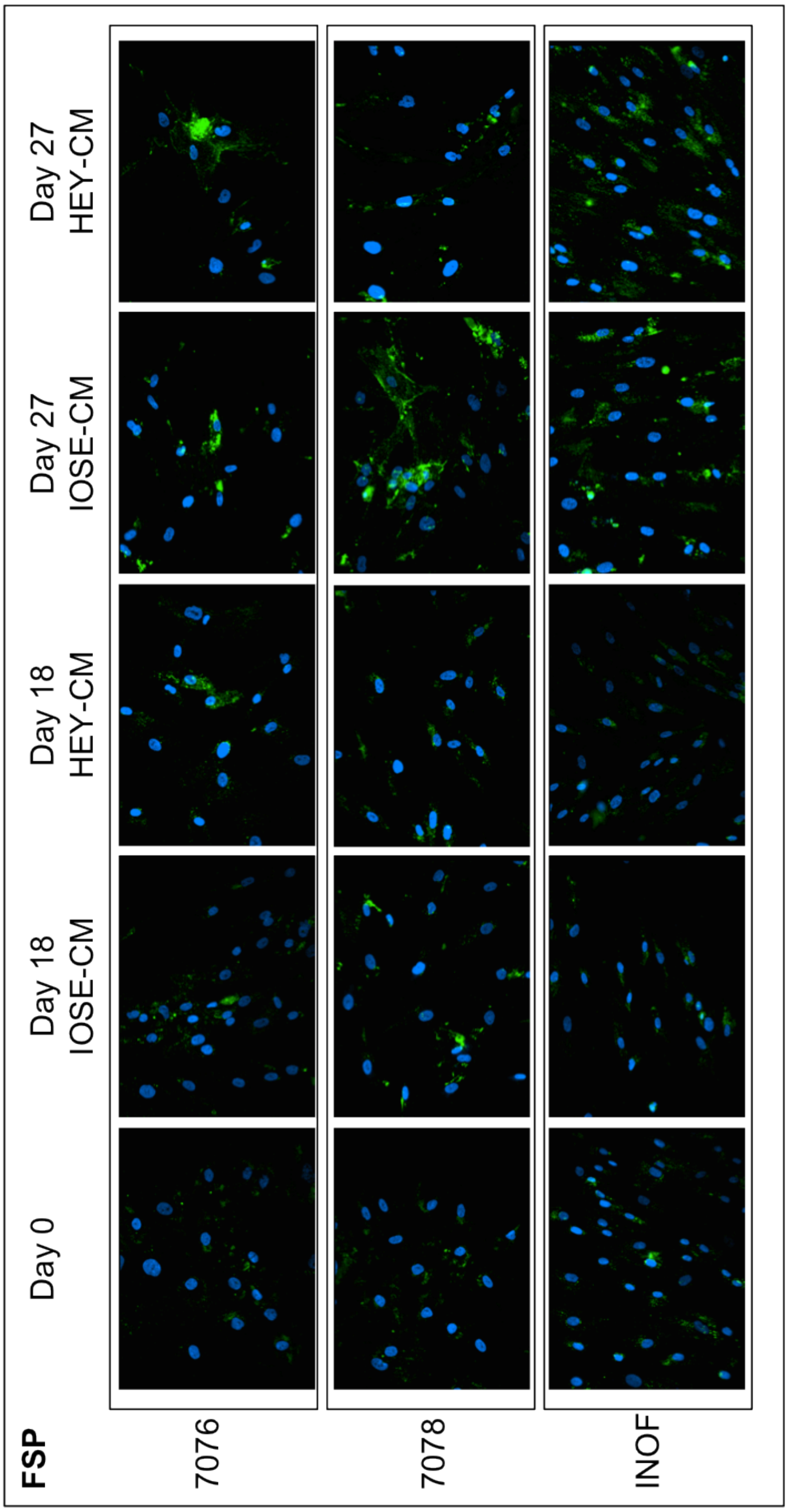

Figure V-6: Immunofluorescence staining for fibroblast specific protein (FSP). Day 0 cells were cultured with their normal culture medium and used as a reference. Both mesenchymal stem cell (MSC) lines and the immortalised normal ovarian fibroblast (INOF) cell line stained faintly positive for FSP. Positive staining increased after culture with conditioned medium (CM) and was strongest after 27 days of incubation, suggesting differentiation of the cell lines towards a cancer associated fibroblast (CAF)-like phenotype. There was no notable difference in FSP expression between using the two different CM. All images are 200x magnification.

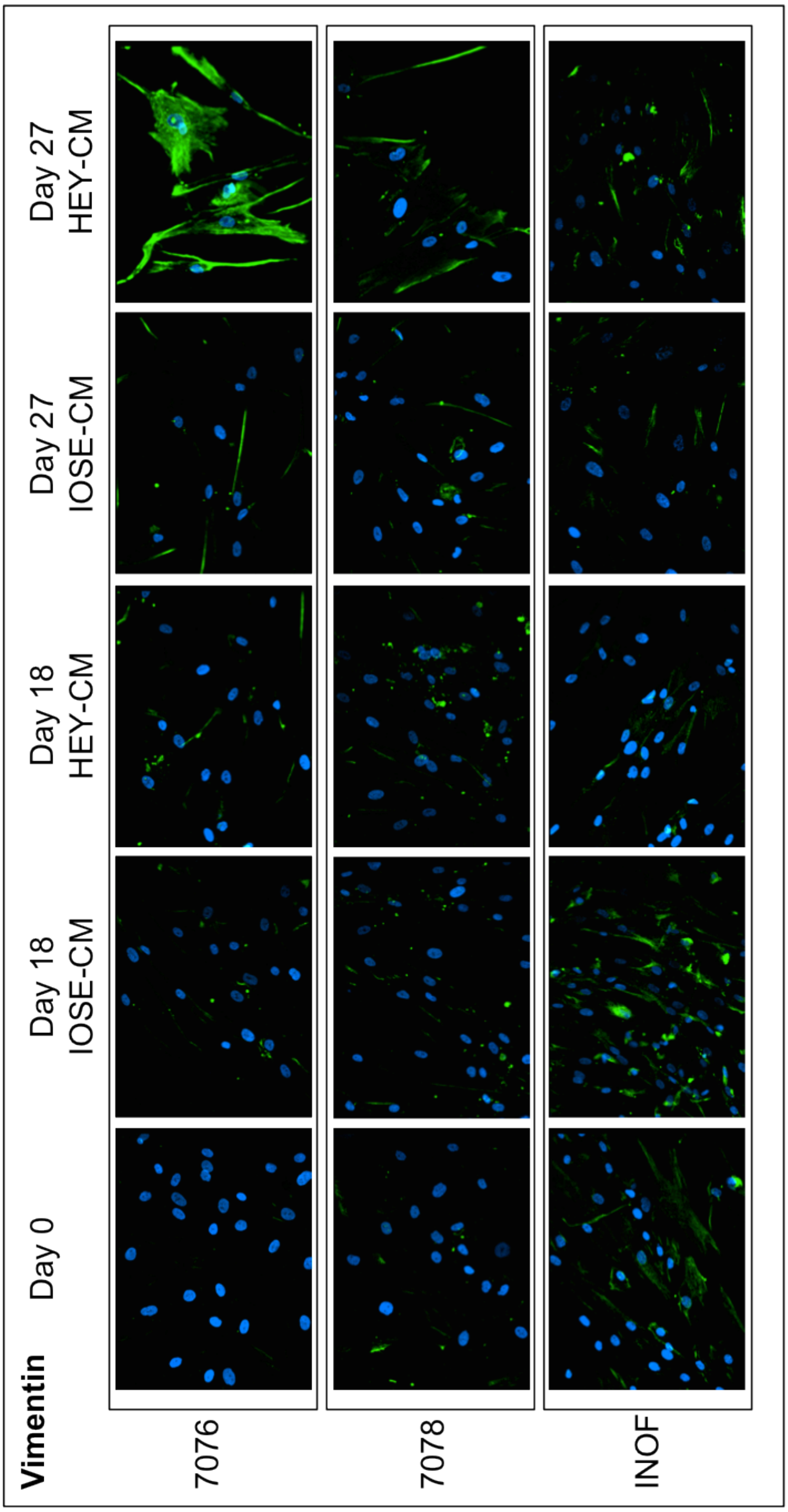

Figure V-7: Immunofluorescence staining for Vimentin. D0 cells were cultured with their normal culture medium and used as a reference. The use of conditioned medium (CM) led to an increased expression of Vimentin in both MSC cell lines. Use of CM from the epithelial ovarian cancer (EOC) cell line HEY resulted in higher Vimentin expression than using CM from an immortalised ovarian surface epithelial (IOSE) cell line. The normal fibroblast cell line (INOF) showed strong Vimentin expression on day 0, which remained on the same level after treatment with CM. All images are 200x magnification.

As mentioned before, it is necessary to quantify staining for Vimentin, FSP and SMA to detect a change in marker expression objectively. I therefore used western blotting to analyse expression of the markers Vimentin, FSP and SMA and compared the results to the immunofluorescent staining of live cells. Whole cell protein lysates were prepared after treatment with CM and samples electrophoresed on a SDS-poly-acrylamide gel. Western blot analysis using the antibodies against Vimentin and FSP resulted in highly unspecific staining and the blots were impossible to analyse. Western blot analysis for SMA however showed highly specific detection of the protein SMA and was used for quantification of SMA expression levels. Quantification was achieved using the software ImageJ. ImageJ is an image processing software developed by the National Institute of Health and is freely available for the research community (Schneider, Rasband et al. 2012). Briefly, the SMA protein bands were normalised using the loading control. The relative densities of each SMA band compared to a D0 control sample (MCSs/INOF cells before treatment with CM) were then determined. A summary of all relative densities can be found in Table V-2. Both MSC cell lines showed visible baseline expression of SMA. After treatment with IOSE and HEY CM this expression was enhanced up to 1.4 fold for both MSC cell lines compared to the D0 control. Comparison of the IOSE CM and HEY CM treated 7076 MSC cell line revealed similar densities of SMA after 18 days of culture whereas after 27 culture days an 1.2 fold increase of SMA expression could be detected in the HEY CM treated cells compared to the IOSE CM treated cells. The MSC cell line 7078 also showed similar expression levels of SMA after 18 days in culture when treated with HEY CM and IOSE CM. After 27 days of culture with CM an 1.3 fold increase of SMA protein band densities could be observed for cells treated with HEY CM compared to IOSE CM. INOFs showed very subtle expression levels of SMA at the D0 control. However, expression levels increased greatly upon treatment with CM (up to 25.7 fold increase). After 18 days of CM treatment a 6-fold increase of SMA expression in HEY CM treated INOFs was detected compared to IOSE CM treated cells. At day 27 a 2.4 fold increase of SMA band densities was observed in HEY CM treated cells compared to IOSE CM treated cells.

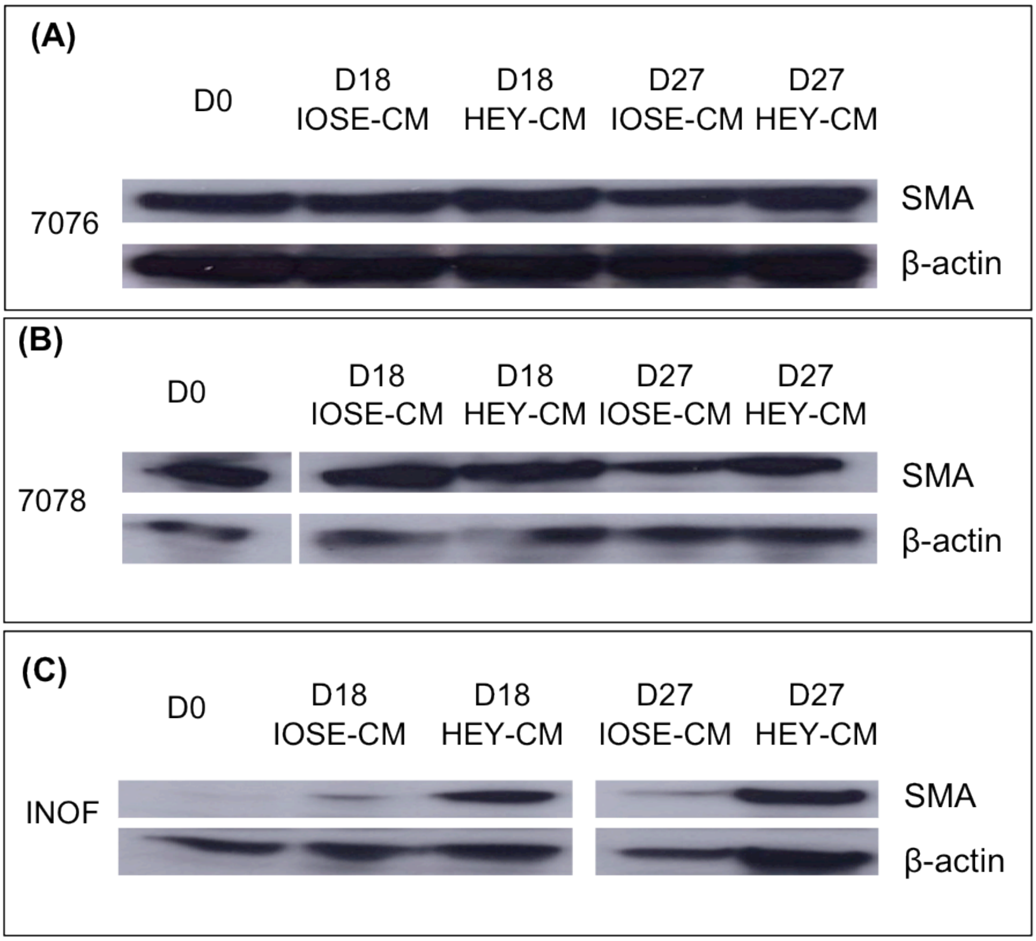

Figure V-8: Western Blot analysis for the expression of smooth muscle actin. Both mesenchymal stem cell (MSC) lines and the immortalised normal ovarian fibroblast (INOF) cell line were cultured with conditioned medium (CM) to facilitate differentiation into a ‚cancer associated fibroblast (CAF) -like' phenotype. The CM was derived from an immortalised ovarian surface epithelial (IOSE) cell line and from the epithelial ovarian cancer (EOC) cell line HEY. Whole cell lysates were prepared after different culture times and the proteins were separated by size before detection of the CAF marker smooth muscle actin (SMA). β-actin was used as a loading control. **(A)** The MSC line 7076 showed slightly increased expression of SMA after 18 days with HEY CM compared to IOSE CM and the D0 control. The same effect was seen after 27 days of culture, were IOSE CM cultured cells showed no difference compared to the D0 control but HEY CM culture led to increased SMA expression. **(B)** The MSC line 7078 showed no differences in SMA expression at day 18. On day 27 increased SMA expression could be detected after culturing with HEY CM. **(C)** INOF cells expressed very low rates of SMA when cultured with their normal growth medium. This expression increased when cultured with CM. HEY CM led to higher expression levels of SMA compared to IOSE CM. This effect was visible on days 18 and 27.

Table V-2: Summary of CAF marker expression. +/- less than 10% positive staining; + 10-20% positive staining; ++ 20-40% positive staining; +++ 40-60% positive staining, ++++ 60-80% positive staining; +++++ more than 80% positive staining. **Western blot quantification:** Samples were normalised using the relative densities of the β-acting loading control. The densities of each band were then quantified relative to the D0 control for each sample. Both MSC cell lines showed increased densities of SMA expression upon treatment with CM. HEY CM led to a 1.2 and 1.3 fold increase compared to IOSE CM after 27 days in culture in the 7076 and 7078 MSC cell line. SMA expression of treated INOFs was increased more that 4 fold. HEY CM led to a 6-fold increase of SMA expression of the HEY CM treated cells compared to IOSE CM treated cells at day 18. Further culture with CM led to a 2.4 fold increase of SMA in HEY CM treated cells compared to IOSE CM.

FSP	Day 0	Day 18		Day 27	
		IOSE-CM	HEY-CM	IOSE-CM	HEY-CM
7076	+	++	++	+++	+++
7078	+	++	++	++++	+++
INOF	+	+	+	+++++	+++++
Vimentin	Day 0	Day 18		Day 27	
		IOSE-CM	HEY-CM	IOSE-CM	HEY-CM
7076	+/-	+	++	++	++++
7078	+	+	++	++	+++
INOF	++	+++	++	++	+++
Western blot quantification					
SMA	Day0	Day 18		Day 27	
		IOSE-CM	HEY-CM	IOSE-CM	HEY-CM
7076	1	1.381	1.433	1.182	1.375
7078	1	1.2	1.249	1.028	1.362
INOF	1	4.285	25.73	8.236	19.379

V.2.4 Functional analysis of CAF-like cells differentiated using 2D culture methods

To analyse if the differentiated MSCs and INOFs exhibit tumour promoting properties, which has been reported for CAFs, I tested the influence of differentiated MSCs and INOFs on the transformed phenotype of the ovarian surface epithelial cell line IOSE19^{cmyc}.

V.2.4.1 Effect of CAF like cells on proliferation rates of transformed ovarian surface epithelial cells

MSCs and INOFs were differentiated for 27 days in a 2D culture system using conditioned medium harvested from the EOC cell line HEY. Medium derived from a normal ovarian surface epithelial (IOSE) cell line was used as a control. The resulting MSC and INOF cell lines were cocultured with the transformed epithelial ovarian cell line (IOSE19^{cmyc}), using porous, non-cell permeable cell culture inserts. After one week of co-culture the proliferation rate of the IOSE19^{cmyc} cells was assayed using MTT, a colourimetric cell viability assay. Each experiment was replicated twice using 3 replicates. As an experimental control IOSE19^{cmyc} cells alone were added to the assay. However, because the effect of HEY differentiated MSCs compared to IOSE differentiated MSCs should be assayed, IOSE19^{cmyc} cells only serve as a reference and not as the control in this experiment. IOSE19^{cmyc} cells co-cultured with undifferentiated MSCs could have been added as an alternative control.

The addition of the differentiated MSCs led to significantly increased proliferation rates in the transformed epithelial ovarian cell line compared to culture of IOSE19^{cmyc} cells alone. However, no difference could be detected between the use of HEY CM and the use of the control medium obtained from IOSE cells (Figure V-9 A). The addition of INOFs also led to increased proliferation rates of IOSE19^{cmyc} cells after indirect co-culture but only HEY CM treated INOFs led to a significant difference in proliferation rates compared to non-cocultured IOSE19^{cmyc} cells. Again, no significant difference between the use of HEY CM and the control CM obtained from IOSE cells (Figure V-9 B) was observed.

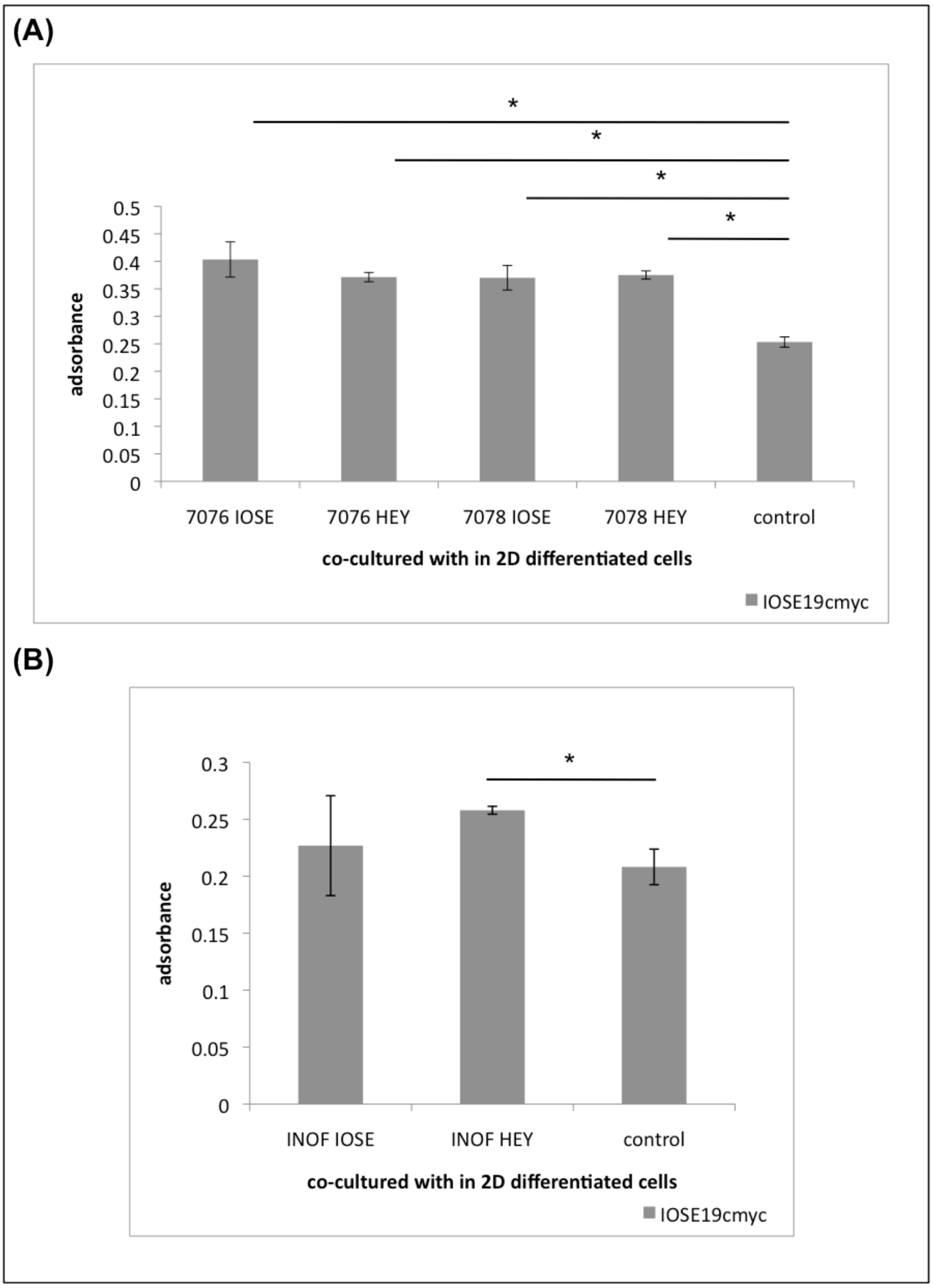

Figure V-9: MTT Proliferation assay of IOSE19^{cmyc} cells after co-culture with differentiated MSCs/INOFs. MSCs and INOFs were differentiated using conditioned medium from an immortalised ovarian surface epithelial (IOSE) cell line and the epithelial ovarian cancer (EOC) cell line HEY using standard tissue culture plastics. IOSE19^{cmyc} cells were co-cultured for 1 week with the differentiated cells and their effect on cell proliferation was assayed. **(A)** Co-culture of IOSE19^{cmyc} cells with MSCs led to significantly increased proliferation rates compared to not co-cultured IOSE19^{cmyc} cells. No significant difference between the two CM was observed. **(B)** INOFs differentiated with HEY-CM led to increased proliferation rates in the IOSE19^{cmyc} cells compared to IOSE19^{cmyc} cells alone. IOSE-CM did not lead to a significant increase, while HEY-CM treated INOFs led to significantly enhanced proliferation rate in the IOSE19^{cmyc} cells. There was also no significant difference between the use of HEY and IOSE-CM.

V.2.4.2 Effect of CAF like cells on the invasive abilities of transformed ovarian surface epithelial cells

To further investigate the effect of differentiated MSCs and INOFs on transformed ovarian surface epithelial cells I performed modified transwell invasion assays (V.2.2.1). The potential of the MSCs and INOFs to attract invasion compared to the standard chemoattractant (FBS) was then assayed in two independent experiments (II.2.5). Each experiment included three replicates.

MSCs and INOFs differentiated in standard 2D culture assays did not attract IOSE19^{cmyc} cells significantly more than the control of 10% FBS (Figure V-10). No difference in the use of HEY or IOSE conditioned medium was observed.

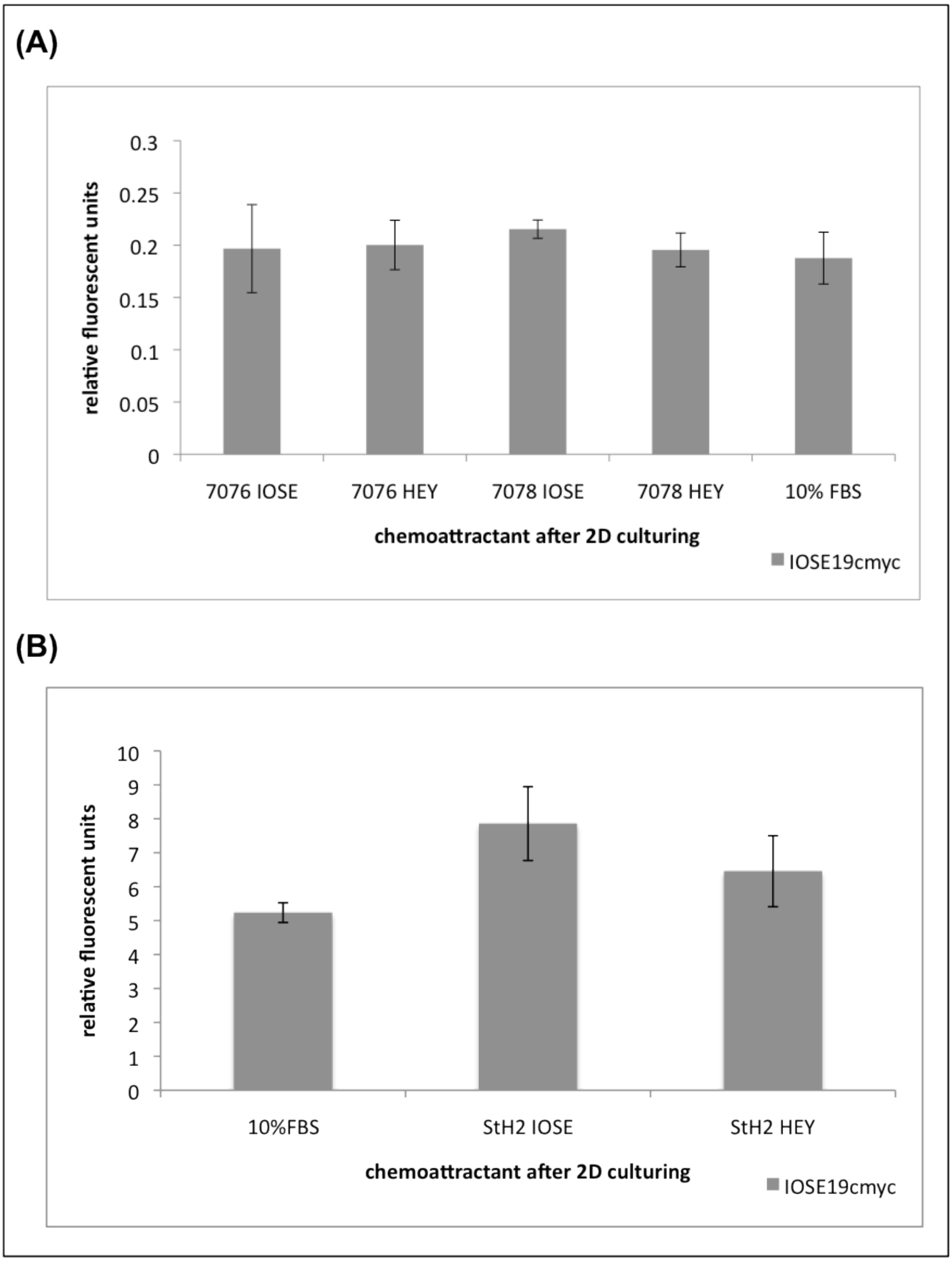

Figure V-10: (A) Invasion assays using in 2D differentiated mesenchymal stem cells (MSCs) and (B) immortalised normal ovarian fibroblasts (INOFs) as chemoattractants. MSCs and INOFs were differentiated using conditioned medium from an immortalised ovarian surface epithelial (IOSE) cell line and the epithelial ovarian cancer (EOC) cell line HEY using standard tissue culture plastics. The differentiated cells were used to attract IOSE19*cmyc* cells to invade through an ECM membrane. No significant difference in the use of the different CM on the invasive activity of the IOSE19*cmyc* cells was observed.

V.2.5 Differentiation of MSCs and normal ovarian fibroblasts in 3D *in vitro* cell culture models

In the previous chapters I have shown that three dimensional culture methods are better at mimicking *in vivo* conditions than traditional 2D cultures. Therefore differentiation assays of MSCs and INOFs were performed in a 3D cell culture system, to investigate whether transdifferentiation into CAFs is differently regulated in a 3D environment.

V.2.5.1 Morphological examination of MSCs and INOFs after 3D differentiation assays

To examine the effect of culturing MSCs and INOFs with CM derived from normal and malignant epithelial ovarian cells in a three-dimensional culture system I analysed the resulting spheroids morphologically and by immunohistochemistry. Cells were cultured using polyHEMA coated tissue culture plastics and spheroids were harvested after 26 days in culture with CM. Spheroids were embedded into paraffin and sections were stained with haematoxylin and eosin for morphological analysis.

The MSC line 7076 formed spheroids exhibiting a flattened layer of cells at the periphery. Many apoptotic cells at all stages of apoptosis were observed within the spheroids. Extensive areas of karyorrhexis were visible and rare mitoses could be seen (Figure V-11 A, a). After culture with IOSE CM the appearance of the spheroids was similar to the control spheroid (Figure V-11 A, b). Culture of the MSCs with HEY CM led to spheroids that contained less nuclear dust and less karyorrhectic debris, but many necrotic cells were still visible (Figure V-11 A, c).

Control spheroids of the MSC line 7078 exhibited areas of extensive apoptosis and many degenerate cells. Degenerate changes were even present from the surface of the spheroid, suggesting apoptosis was not due to reduced access to oxygen or other nutrients, which might be an explanation for the presence of necrotic cells within the core of large spheroids (Figure V-11 B, a). Upon treatment with IOSE CM, spheroids had a vacuolated appearance. Degenerate changes and nuclear dust were also present (Figure V-11 B, b). HEY CM led to the formation of spheroids containing degenerate cells and areas of apoptosis. The cells at the periphery showed nuclear pleomorphism (Figure V-11 B, c).

Spheroids of the INOF cell line contained a central core of matrix protein. The cells layering the core showed a flattened and elongated morphology as previously described (Lawrenson, Grun et al. 2010). Some areas of apoptosis were present (Figure V-11 C, a). The addition of IOSE CM to the culture medium led to the formation of spheroids showing characteristics of an active stroma. Spheroids were bigger and cells could be found within the stromal core as well as at the periphery; areas of extensive apoptosis were visible. There were also some circular bodies present which are likely to be calcifications called psammoma bodies (Figure V-11 C, b). These formations are often found in serous ovarian tumours and are thought to be associated with cellular degeneration (Ferenczy, Talens et al. 1977). They are also found in benign and borderline tumours and the existence of psammoma bodies within serous tumours is thought to be associated with a better prognosis than serous ovarian carcinomas lacking these features (Gilks, Bell et al. 1990).

After culture with HEY CM, spheroids had a similar appearance. Spheroids were large and contained areas of matrix deposits. Apoptotic areas were also visible and numerous psammoma bodies could be seen (Figure V-11 C, c).

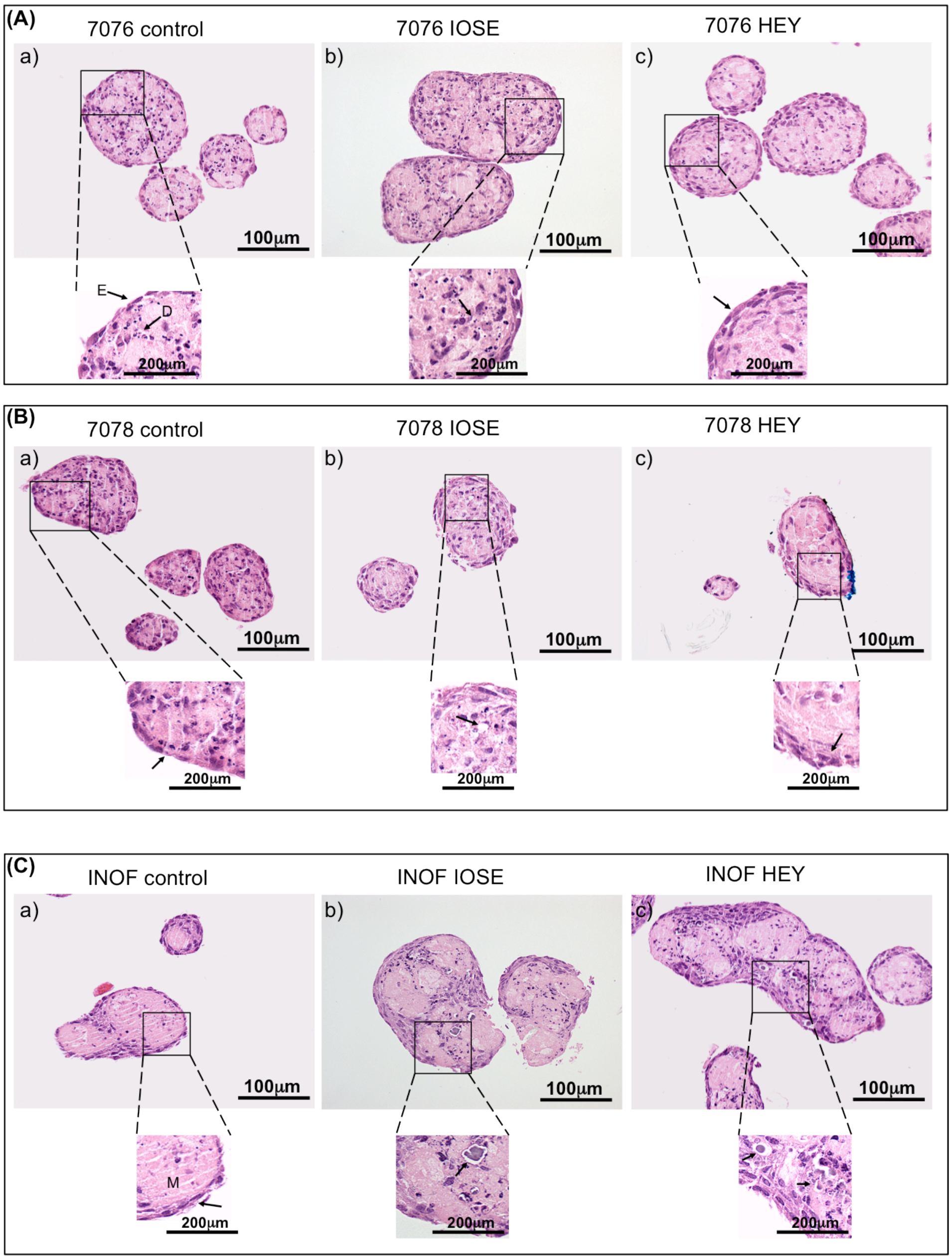

Figure V-11: Haematoxylin and Eosin (H&E) staining of multicellular spheroids grown in 3D with conditioned medium and controls. (A) All samples of the MSC line 7076 showed high levels of apoptosis and a flattened layer of cells (arrow E) at the periphery. The control sample (a) and the sample cultured with IOSE-CM (b) exhibited high amounts of karyorrhexis, seen as nuclear dust (arrows D), whereas the MSCs cultured with HEY-CM (c) showed less karyorrhectic debris. Elongated and flattened cells at the periphery were visible (arrow) **(B)** The MSC line 7078 (a) formed spheroids that consisted of numerous degenerate cells which could even be found at the periphery of the spheroid (arrow). High levels of apoptosis were also visible. The numbers and size of the spheroids obtained after culturing with CM were smaller. IOSE-CM (b) led to formation of spheroids with degenerate changes and vacuolated appearances (arrow). Some nuclear dust was also visible. Cells on the periphery of spheroids after culture with HEY-CM (c) showed nuclear pleomorphisms (arrow). **(C)** Spheroids formed by the INOF cell line (a) showed spindle cells (arrow) layering a core consisting of matrix protein (M). The culture of INOFs with CM (b.c) led to the appearance of an active stroma with circular bodies, called psammoma bodies (arrows).

To evaluate the ability of MSCs to differentiate in a 3D cell culture system I went on to perform immunohistochemistry for MSC and CAF markers. To analyse if MSCs undergo differentiation towards a CAF-like phenotype while loosing the expression of standard MSC markers I investigated the expression of CD44 in control spheroids of the MSC line 7076 as well as in IOSE and HEY CM treated spheroids. CD44 is a cell surface glycoprotein located in the plasma membrane and is expressed by mesenchymal stem cells. Positive staining is indicative of an undifferentiated MSC phenotype. There was strong and dense positive staining in the control spheroid. IOSE CM treated spheroids showed equally strong positive staining. Staining in HEY CM treated MSC spheroids showed less dense positive staining (Figure V-12 a-c) indicating a conversion towards a more differentiated phenotype. I also investigated the expression of the CAF markers vimentin and SMA in the 3D spheroids. Staining for vimentin was strongly positive in all three samples (Figure V-12 e-g), whereas SMA only showed unspecific staining (Figure V-12 i-k). Furthermore, to establish if the addition of CM led to higher rates of actively proliferating cells in the 3D MSC spheroids I stained for the proliferation marker Mib1. The control spheroid showed no positive staining whereas some positively stained cells could be found at the periphery of IOSE and HEY CM treated spheroids (Figure V-12 m-o). However, staining was generally weak and no difference could be found between IOSE and HEY CM cultured spheroids.

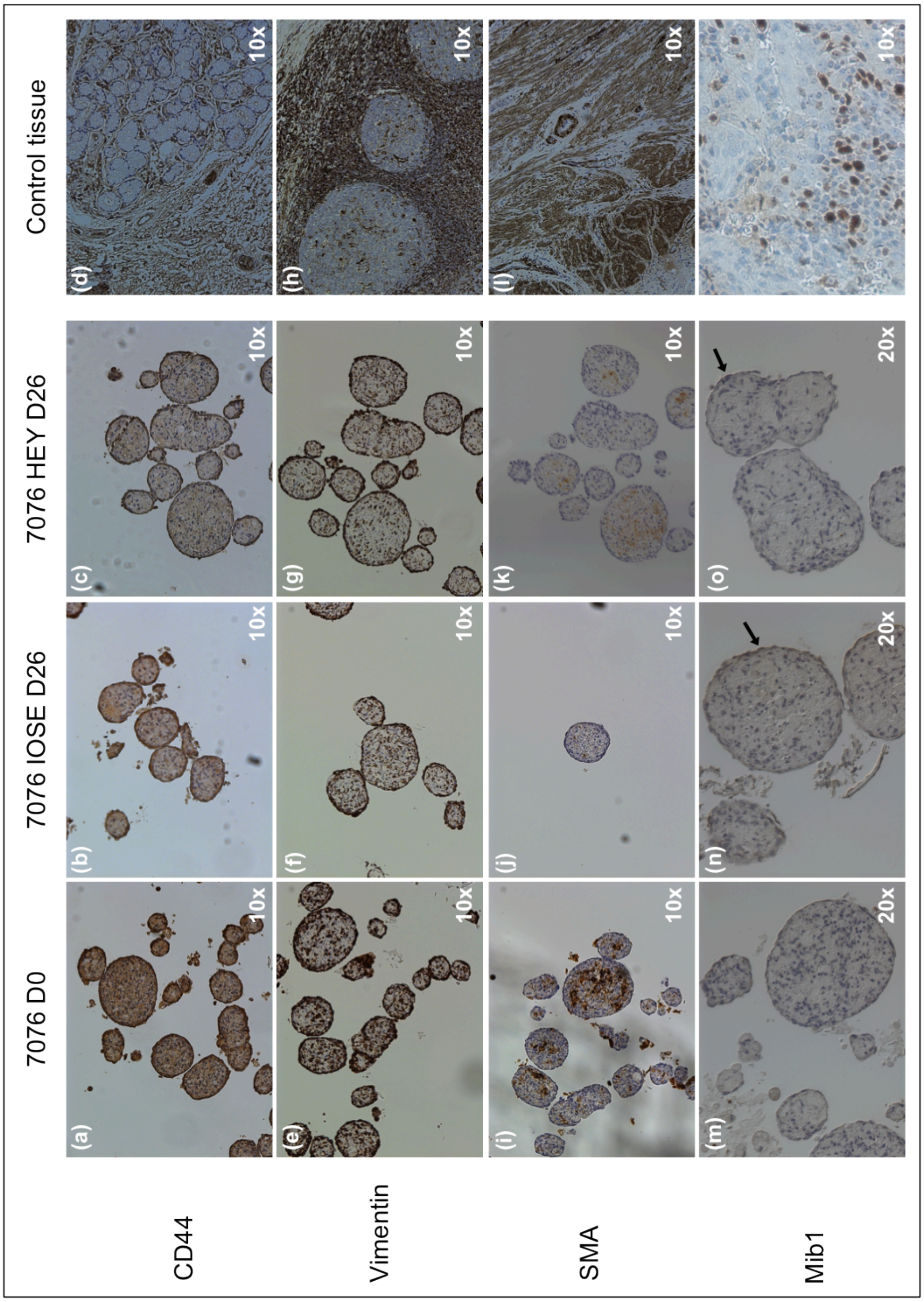

Figure V-12: Immunohistochemical staining of 7076 MSC 3D spheroids after differentiation using conditioned medium. Staining for the MSC marker CD44 was strongly positive in the control (D0) sample (a) and in the IOSE CM treated sample (b). HEY CM treated MSCs also stained positive for CD44, but the staining was less strong and dense (c). Staining for the CAF marker Vimentin showed strongly positive staining in all three samples (e-g). Immunohistochemistry for SMA resulted only in unspecific staining (i-k). Staining for the proliferation marker Mib1 is weak with some positive stained cells (arrows) in the IOSE and HEY differentiated MSC spheroids (m-0). Appropriate control tissues were used for each marker (d, h, l, p).

V.2.5.2 Effect of conditioned medium on the proliferation rates of putative CAF precursor cells

During the 3D differentiation assays I observed what seemed like increased spheroid production in the samples cultured with HEY CM compared to the control media (IOSE CM). More spheroids could be observed in the cultures with the HEY CM medium. This observation was underlined by the finding that RNA concentrations in the HEY CM treated MSC samples were significantly higher than IOSE CM treated MSCs (Table V-3).

Table V-3: RNA concentrations of MSCs/INOFs after culturing in 3D with HEY and IOSE CM. Equal numbers of cells were plated and cultured with the different CM for 26 days before spheroids were harvested and RNA extracted. Concentrations of RNA were significantly higher in MSC samples cultured in 3D with HEY CM compared to IOSE CM (t-test). No difference was seen in the INOF samples cultured in 3D with the different CM.

7076 IOSE CM	19.3ng/µl	*p*=0.009	7078 IOSE CM	19.5ng/µl	*P*=0.005	INOF IOSE CM	35.7ng/µl	*p*=0.441
	19.2ng/µl			17.9ng/µl			32.9ng/µl	
	22.2ng/µl			16.9ng/µl			34.4ng/µl	
7076 HEY CM	64.1ng/µl		7078 HEY CM	54.9ng/µl		INOF HEY CM	31.6ng/µl	
	54.1ng/µl			61.9ng/µl			34 ng/µl	
	70.3ng/µl			53.2ng/µl			33.1ng/µl	

To assess if the addition of the different CM led to differences in proliferation rates of MSCs and normal fibroblasts I decided to perform proliferation assays. I first examined this using traditional 2D culture methods. Here, replicates of each cell type were plated into 24-well plates and cultured for 4 days and alamarBlue® was used to monitor proliferation. In the 2D setup no difference in proliferation could be observed following the culture with IOSE or HEY CM.

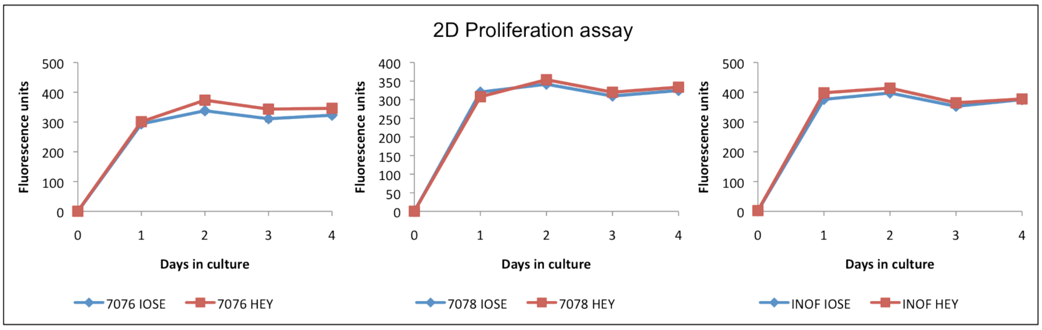

Figure V-13: Proliferation assay of mesenchymal stem cells (MSCs) and immortalised normal ovarian fibroblasts (INOFs) during culture with conditioned medium (CM) in 2D tissue culture. The different CM led to no significant difference in proliferation in a standard 2D tissue culture setup.

I then went on to perform the proliferation assays in a 3D microenvironment. Proliferation was determined over a period of 6 days utilising alamarBlue®. No differences in proliferation rates were seen for the MSC cell line 7078 and the stromal cell line INOF after culture with IOSE or HEY CM. The MSC cell line 7076 however showed a trend towards increased proliferation during culture with HEY CM compared to IOSE CM.

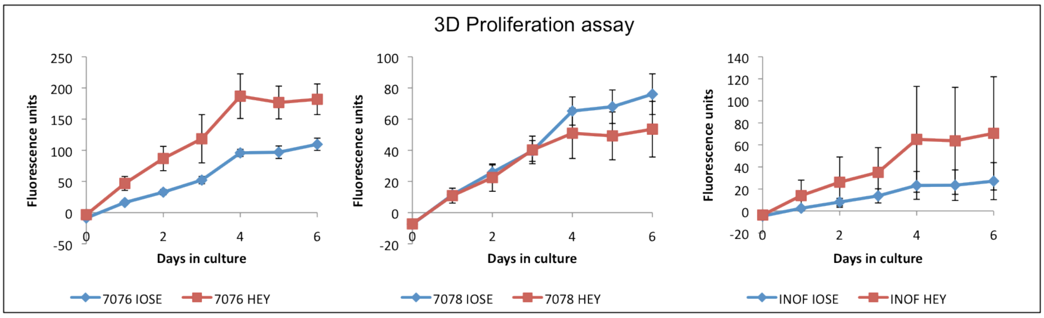

Figure V-14: Proliferation assay of mesenchymal stem cells and immortalised normal ovarian fibroblasts during culture with conditioned medium in 3D tissue culture. No differences in 3D proliferation rates were seen for the MSC line 7078 and INOF upon treatment with HEY or IOSE CM. The MSC cell line 7076 however, responded with increased proliferation when cultured with HEY CM compared to IOSE CM.

V.2.6 Functional analysis of CAF-like cells differentiated using 3D culture methods

I performed functional assays to analyse if in a 3D environment differentiated MSCs and INOFs have an effect on the behaviour of a transformed ovarian cell line (IOSE19^{cmyc}).

V.2.6.1 Effect of CAF like cells on proliferation rates of transformed ovarian surface epithelial cells

To investigate the effect of differentiated MSCs and INOFs on IOSE19^{cmyc} cell growth I performed a proliferation assay. MSCs and INOFs were differentiated in a 3D environment using conditioned medium from an EOC cell line (HEY). As a control, conditioned medium from an immortalised ovarian surface epithelial (IOSE) cell line was used. The resulting differentiated 3D spheroids of MSCs and INOFs were harvested and dissociated using trypsin treatment to obtain a single cell suspension. An appropriate number of cells were plated into porous, non-cell permeable cell culture inserts. The differentiated cells were then cocultured with the transformed ovarian cells (IOSE19^{cmyc}) for one week. At the end of the incubation period the proliferation rate of IOSE19^{cmyc} cells was determined using a colourimetric cell viability assay (MTT).

MSCs and INOFs differentiated in a 3D cell culture system led to significantly increased proliferation rates in IOSE19^{cmyc} cells compared to IOSE19^{cmyc} cells cultured alone. There was no difference in the use of HEY CM or IOSE CM.

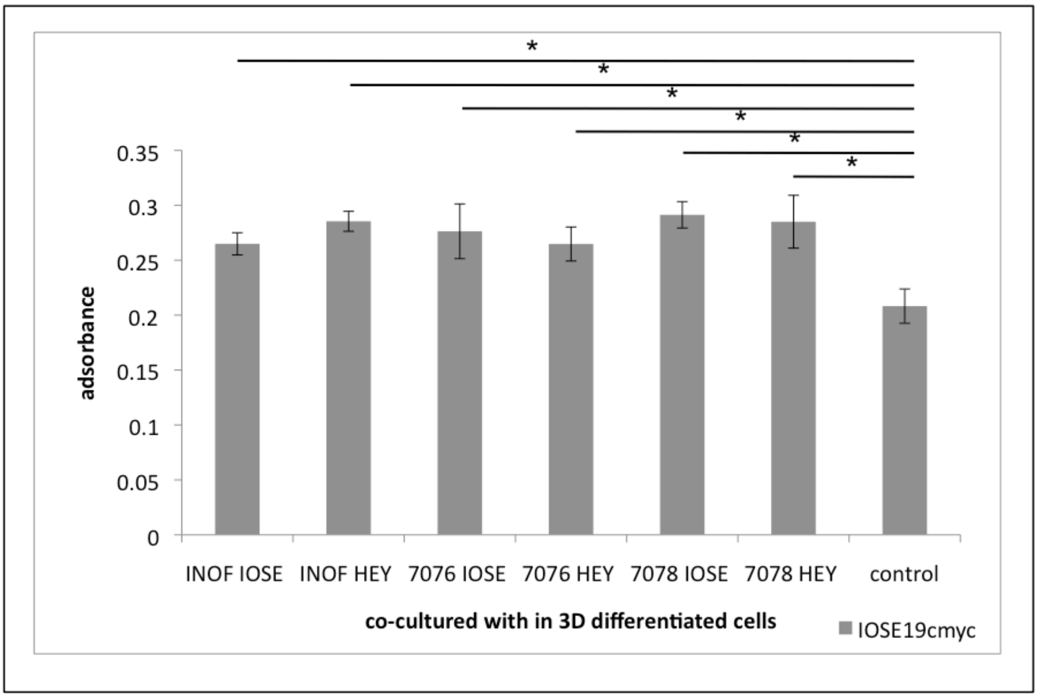

Figure V-15: MTT Proliferation assay of IOSE19*cmyc* after co-culturing with in 3D differentiated mesenchymal stem cells (MSCs) and immortalised normal ovarian fibroblasts (INOFs). MSCs and INOFs were differentiated using IOSE and HEY-CM in a three-dimensional tissue culture setup. IOSE19*cmyc* cells were co-cultured for 1 week with the differentiated cells and their effect on cell proliferation was assayed. Proliferation rates of IOSE19*cmyc* cells were significantly increased after co-culture with MSCs and INOFs compared to the cells cultured alone. There was no significant difference between the use of the different CM.

V.2.6.2 Effect of CAF like cells on the invasive abilities of transformed ovarian surface epithelial cells

I then went on to test the ability of MSCs and INOFs differentiated in a 3D cell culture system to attract invasion of IOSE19*cmyc* cells. Spheroids of the differentiated MSCs and INOFs were dissociated as described above (V.2.6.1) and an appropriate number of cells was plated into each well of a 24-well plate to serve as a chemoattractant. The ability of the differentiated cells to attract invasion of IOSE19*cmyc* cells was compared to a control sample containing 10% FBS.

MSCs treated with HEY CM were able to attract the transformed epithelial cells significantly more than the control. MSCs treated with IOSE CM also led to increased invasion rates compared to the control but no significance was discovered. Both IOSE and HEY treated INOFs were able to attract invasion of IOSE19*cmyc* cells significantly more than 10% FBS. No significant difference between the use of IOSE and HEY CM was detected.

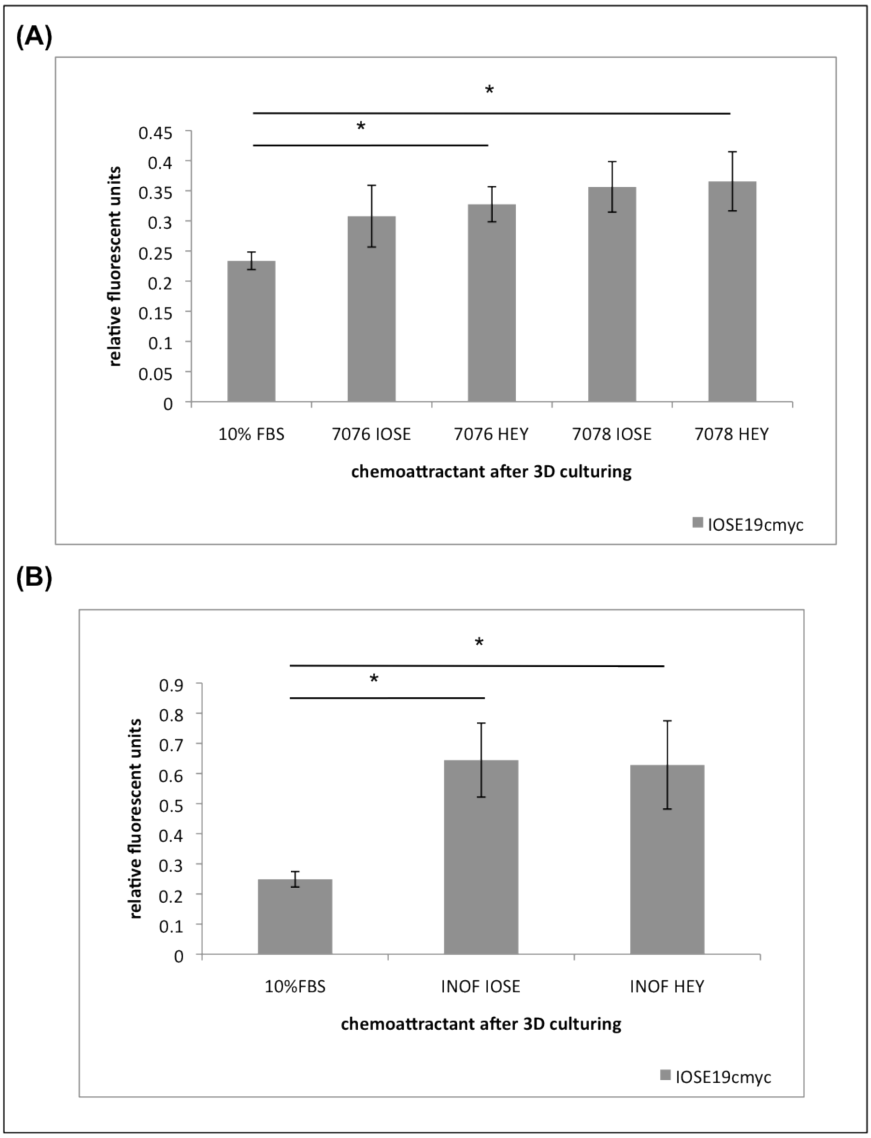

Figure V-16: Invasion assays using differentiated mesenchymal stem cells (MSCs) and immortalised normal ovarian fibroblasts (INOFs) as chemoattractants. MSCs and INOFs were differentiated using conditioned medium in a three-dimensional tissue culture setup. The differentiated cells were used to attract IOSE19^{cmyc} cells to invade through an ECM membrane. No significant difference between the different CM was observed. Compared to the FBS control the use of MSCs and INOFs as chemoattractants led to increased invasion rates of the IOSE19^{cmyc} cells. A significant increase in IOSE19^{cmyc} invasion rates was observed for the MSC lines treated with HEY-CM and for the INOF cell line treated with IOSE and HEY-CM.

V.3 Discussion

In 1999 Olumi and coworker showed that in a model of prostate cancer, CAFs were able to promote tumour growth of initiated prostate epithelial cells *in vivo* and *in vitro* (Olumi, Grossfeld et al. 1999). Normal prostate fibroblast cells did not affect tumour growth. Furthermore, it was shown that CAFs had no effect on normal prostate epithelial cell growth indicating that normal epithelial cells are not responsive to growth stimuli secreted by CAFs. Similar results were obtained using a model of breast cancer. Orimo et al isolated CAFs from human breast carcinomas, mixed them with human breast cancer cells and injected them into mice. They found that CAFs significantly increased the growth of the cancer cells compared to normal fibroblasts (Orimo, Gupta et al. 2005). However, the source of CAFs is still unclear and several different origins have been proposed. Petersen and coworkers discovered epithelial to mesenchymal transition in human breast cancer as a source of the tumour associated stroma (Petersen, Nielsen et al. 2003) whereas Zeisberg et al postulated endothelial to mesenchymal transition as a source of CAFs (Zeisberg, Potenta et al. 2007). The most popular theories however suggest mesenchymal stem cells and normal resident fibroblasts as the precursor cell types of CAFs. This is based on observations that it is possible to induce a myofibroblast phenotype, characterised by SMA expression, in both cell types. In 1993 it was shown that TGF-β treatment of human breast stromal cells leads to the expression of SMA. This effect could be repeated by treating the stromal cells with tumour cell conditioned medium (Ronnov-Jessen and Petersen 1993). Similarly, it has been shown that MSCs can exhibit a myofibroblast phenotype upon treatment with conditioned medium obtained from colon carcinoma cell lines or upon treatment with TGF-β (Emura, Ochiai et al. 2000). MSCs can be recruited to sites of wounding and tumours (Kidd, Spaeth et al. 2009) and MSCs preferentially implant into the tumour microenvironment (Studeny, Marini et al. 2002). These observations make MSCs a potential vehicle for the delivery of anti-cancer drugs and also a candidate for a precursor cell type of CAFs.

Furthermore, while it has been shown that the tumour stroma exhibits numerous gene expression changes no genetic alterations could be detected (Allinen, Beroukhim et al. 2004). This indicates that the stromal cells are genetically stable. It is therefore concluded that stromal cells are less likely to evolve resistance towards therapeutic drugs compared to the malignant epithelial cells, making it a promising target for effective anti-cancer therapy. An example for targeting the tumour microenvironment therapeutically is the use of a monoclonal antibody (Bevacizumab), which inhibits vascular endothelial growth factor (VEGF). Neovascularisation to provide oxygen and nutrients for the progressing tumour is essential. Without vasculature tumour growth is mostly restricted to 2-3mm (Folkman 1995). By inhibiting VEGF bevacizumab prevents tumour angiogenesis and has, in combination with chemotherapeutic drugs, been shown to significantly improve survival in patients with metastatic colorectal cancer (Hurwitz, Fehrenbacher et al. 2004). It is also used to treat metastatic breast cancer (not in the US), lung and ovarian cancer (Han and Monk 2007; Di Costanzo, Mazzoni et al. 2008; Stevenson, Nagahashi et al. 2012).

Taken together, the importance of the microenvironment for tumour growth and development is undeniable and the potential for targeting the tumour microenvironment with anti-cancer therapy a very compelling proposal. However, it is imperative to understand the recruitment of cells into the tumour supporting microenvironment to successfully interfere with the recruitment process and avert the formation of the tumour stroma. Here I chose to investigate immortalised normal ovarian fibroblasts (INOFs) and human mesenchymal stem cells (MSCs) as a potential source of CAFs in ovarian cancers. In a pilot experiment I showed that MSCs can exhibit a myofibroblast-like phenotype upon treatment with conditioned medium from epithelial ovarian cancer cell lines. Some differentiation towards a myofibroblast phenotype was also observed using conditioned medium from a normal immortalised ovarian surface epithelial (IOSE) cell line (Figure V-3, Figure V-4, Figure V-5). I therefore went on to compare the differentiation ability of MSCs with INOFs upon treatment with different CM.

Previous studies have compared the transdifferentiation ability of MSCs after culture with tumour cell conditioned medium to MSCs treated with serum free medium (Mishra, Mishra et al. 2008; Spaeth, Dembinski et al. 2009) or compared MSCs co-cultured with tumour cells to non-cocultured MSCs (Emura, Ochiai et al. 2000). The data presented in this thesis shows that secreted molecules of normal ovarian surface epithelial cells can also induce phenotypic changes within MSCs and INOFs. This is an observation that should not be overlooked and aids the identification of changes that are specifically induced by EOC cell conditioned medium when compared to IOSE conditioned medium. Hence I concluded that CM obtained from IOSE cells would be the most appropriate control for the following differentiation assays.

Differentiation assays confirmed that both INOFs and MSCs were able to differentiate towards a myofibroblast phenotype after culture with conditioned medium from an EOC cancer cell line (HEY). The use of the control conditioned medium (IOSE) also led to increased staining for the markers FSP, Vimentin and to some extent SMA. However, Vimentin expression was higher after HEY CM culture compared to IOSE CM culture, and a considerable increase in SMA expression was detected upon HEY CM treatment compared to IOSE CM treatment (Figure V-6, Figure V-7, Figure V-8). Functional analysis of the differentiated MSCs and INOFs showed an enhancing effect of these cell lines on proliferation rates of a transformed ovarian epithelial cell line (IOSE19^{cmyc}). Interestingly, IOSE (control CM) and HEY CM treated MSCs and INOFs had the same effect on IOSE19^{cmyc} proliferation rates (Figure V-9). These differentiated MSCs and INOFs were not able to attract significantly increased rates of invasion of IOSE19^{cmyc} cells (Figure V-10).

These results are reflected in previous studies where MSC differentiation was achieved using conditioned medium from an ovarian, breast, glioma and pancreatic cancer cell line (Mishra, Mishra et al. 2008; Spaeth, Dembinski et al. 2009). In 2008 Mishra and coworkers used conditioned medium from a breast cancer cell line to induce *in vitro* differentiation of a human MSC line towards a myofibroblast phenotype. In functional analyses of the differentiated MSCs and controls they found that tumour cell exposed MSCs led to an increased growth of a breast cancer cell line in a 2D co-culture system. A control MSC cell line treated with 5-azacytidine to induce differentiation towards a myogenic phenotype however, also promoted growth of the breast cancer cell line and showed expression of the CAF markers FSP, Vimentin and SMA. Growth factor (e.g. SDF1) production and secretion is another characteristic of CAFs and the growth factor SDF1 was only observed in the MSCs treated with tumour cell conditioned medium but not in the MSCs differentiated towards the myogenic phenotype (Mishra, Mishra et al. 2008). This shows that a myofibroblastic phenotype characterised by FSP, vimentin and SMA expression is not enough to define CAFs, but further functional and molecular analysis of the proposed CAFs is essential.

Spaeth et al also observed differentiation of MSCs towards CAFs after coinjection into SCID mice with an ovarian cancer cell line (Skov3), and after treatment with conditioned medium from this cell line. They further detected increased tumour volumes after coinjection of MSCs and Skov3 cells into mice compared to Skov3 cells alone. Functional analysis revealed increased levels of secreted growth factors IL-6, TGF-β and VEGF by MSCs treated with Skov-3 conditioned medium compared to naive MSCs (Spaeth, Dembinski et al. 2009). This group only compared the differentiated MSCs with naive MSCs and did not compare with a reference medium.

Differentiation of a normal mammary fibroblast cell line into tumour associated myofibroblasts was observed by Kojima et al in a coimplantation xenograft model (Kojima, Acar et al. 2010). The CAF phenotype was determined by SMA expression and the ability to promote tumour growth. In this model autocrine signalling of TGF-β and SDF1 was essential for inducing and maintaining a myofibroblasts phenotype among normal resident mammary fibroblasts.

In the previous chapters I have established 3D models of ovarian cancer and have shown that these models reflect *in vivo* conditions better than traditional 2D culture methods. Furthermore, it has been shown that osteogenic differentiation of MSCs is enhanced in a 3D model compared to a standard 2D approach (Kabiri, Kul et al. 2012). I therefore chose to perform *in vitro* differentiation experiments in a 3D environment and compare the conversion towards a myofibroblast phenotype and the functional analysis with the results obtained using traditional 2D culture methods.

Morphological comparison of the differentiated MSC spheroids revealed extensive areas of apoptosis and necrosis within the spheroids. Only very subtle morphological differences could be observed between the IOSE (control CM) and HEY CM treated MSCs samples. The spheroids of MSC line 7076 treated with HEY CM showed less signs of apoptosis compared to the IOSE CM (control CM) treated spheroids, whereas spheroids of the MSC line 7078 treated with HEY CM exhibited cells at the outer layer which showed nuclear pleomorphisms. This was not seen in 7078 MSC spheroids treated with IOSE CM (Figure V-11). Although few differences could be detected by H&E, immunohistochemical staining of 7076 MSC spheroid sections revealed decreased staining for the MSC marker CD44 after treatment with HEY CM compared to IOSE CM and naive MSCs. Further staining for the proliferation marker Mib1 showed some actively proliferating cells in the IOSE and HEY CM treated spheroids compared to naive MSC spheroids (Figure V-12). Taken together these results indicate that treatment with HEY CM leads to increased proliferation rates and reduced levels of apoptosis in a 3D culture model. Furthermore the appearance of nuclear pleomorphism in spheroids of a

HEY CM treated MSC line might indicate neoplastic changes within the MSC population. It is of note that current data suggest that ovarian and breast cancer associated fibroblasts do not appear to require any somatic genetic mutations in order to fulfil their role as tumour supporting cells. Whilst it has been shown that gene expression profiles of CAFs differ greatly from those of normal resident fibroblasts mutations in the ovarian cancer stroma are scarce (Qiu, Hu et al. 2008). The changes seen here might therefore represent experimental artefacts.

3D differentiation assays of the normal ovarian fibroblast (INOF) cell line revealed the formation of calcifications (psammoma bodies) in the HEY CM and IOSE CM treated spheroids. Psammoma bodies are often found within low-grade serous ovarian tumours, though the source and development of psammoma bodies is not well understood. Some suggest a connection between apoptosis and the formation of psammoma bodies (Kim 1995), whereas another study indicates an involvement of an osteoinductive bone morphogenic protein in inducing tumour cells to form psammoma bodies (Kiyozuka, Nakagawa et al. 2001). A further theory implies the involvement of macrophages in the production of psammoma bodies (Maki, Hirota et al. 2000). Here we observed psammoma body formation within 3D spheroids of normal ovarian fibroblasts after treatment with conditioned medium of normal ovarian epithelial cells (IOSE) and epithelial ovarian cancer cells (HEY). To my knowledge this is the first time where it has been shown that calcifications arise within the stroma of the ovary as opposed to within the epithelial portion of an ovarian neoplasm. Further investigation would be needed to fully understand the formation of psammoma bodies within the spheroids and to identify pathways involved. However, in this experiment the appearance of psammoma bodies indicates differentiation of the normal stromal cells towards a phenotype frequently seen in serous ovarian tumours.

To verify the transdifferentiation of MSCs and INOFs into CAFs using the 3D approach, functional assays were performed. All differentiated cell lines were able to induce significantly increased proliferation rates in a transformed epithelial ovarian cell line (IOSE19^{cmyc}) and no differences could be observed between the use of IOSE CM (control CM) or HEY CM (Figure V-13). Invasion assays however, showed that only the HEY CM treated, and not IOSE CM treated, MSCs were able to significantly increase invasion rates in IOSE19^{cmyc} cells. INOFs treated with IOSE and HEY CM both led to significantly increased rates of invasion (IOSE19^{cmyc} cells) compared to a control (Figure V-14).

In both 2D and 3D differentiation assays I found that normal immortalised ovarian surface epithelial (IOSE) cells could induce some degree of transdifferentiation of MSCs and INOFs towards a CAF like phenotype characterised by FSP, Vimentin and SMA expression. Furthermore, IOSE CM treated MSCs and INOFs were able to significantly enhance proliferation and to some degree invasion of transformed epithelial cells. This may indicate typical changes induced in stromal cells cocultured with normal epithelia. An alternative explanation is that the IOSE cells are not completely phenotypically normal and represent a pre-malignant/ benign epithelial cell due to the methods used for establishing and maintaining the IOSE cell line in culture. Primary normal ovarian surface epithelial (NOSE) cells exhibit a limited life span *in vitro* of around 20 days. This can be increased by using a growth factor rich medium, and immortalisation can then be achieved by introducing the catalytic subunit of the human telomerase enzyme (hTERT). The IOSE cell line used in this thesis has been established using a highly mitogenic medium which does not provide the microenvironment of a quiescent surface epithelial cell but might resemble the environment during wound repair and hence induce an epithelial phenotype seen during wound repair. It is well known that wounding leads to changes within the stromal compartment specifically the appearance of SMA expressing myofibroblasts (Darby, Skalli et al. 1990). Thus, the changes seen within MSCs and INOFs after treatment with IOSE CM might resemble the stromal response to wounding as opposed to differentiation towards a CAF phenotype. However, whilst IOSE CM did induce phenotypic changes in the stromal cells, the changes were much smaller than when the same cells were cultured in HEY CM. In 2D differentiation assays, SMA expression was increased upon HEY CM treatment compared to IOSE CM treatment. SMA is a marker of myofibroblasts and the presence of myofibroblasts in the tumour stroma has originally been characterised by the simultaneous expression of Vimentin and SMA (Ronnov-Jessen, Petersen et al. 1995; De Wever and Mareel 2002). In this model the increase of SMA expression upon treatment with conditioned medium from an epithelial ovarian cancer cell line indicates that SMA is a robust marker for transdifferentiation towards a CAF phenotype.

Many different sources of CAFs have been implicated in the literature (Petersen, Nielsen et al. 2003; Zeisberg, Potenta et al. 2007; Mishra, Mishra et al. 2008; Spaeth, Dembinski et al. 2009). All the evidence so far points to a heterogeneous origin of the myofibroblasts found within the tumour stroma. A possible explanation would be that precursor cells are being recruited from different origins depending on the stage of tumour development. One could hypothesise that the first line of recruitment are resident fibroblasts due to their proximity to the initial tumour (Figure V-17). Tumour initiation is most probably a synergistic event that requires a permissive microenvironment and genetic alterations within the epithelial cells. This was formulated as the seed and soil theory in the late 19th century by Paget (Paget 1989). He observed that breast cancer cells would form metastasis in some organs but not in others. The role of the microenvironment for tumour development was studied intensely by Bissell and coworkers. In 1984 they published their findings that the rous sarcoma virus (RSV) did not lead to tumour formation when injected into 4 day old chicken embryos (Dolberg and Bissell 1984) indicating a role for the microenvironment in suppressing neoplastic changes. In further experiments they discovered that wounding is associated with the spreading of tumours induced by the RSV within chickens (Dolberg, Hollingsworth et al. 1985). All these studies show that the environment plays an important role in determining the phenotype of cells, and specifically the development of tumours.

More recent studies investigating the tumour microenvironment have shown an important role for fibroblasts in tumour development. It has been demonstrated that changes within the stromal compartment can have a pro-neoplastic effect on otherwise non tumourigenic epithelial cell lines (Olumi, Grossfeld et al. 1999). Tumour associated fibroblasts were able to induce growth of a non-tumourigenic epithelial prostate cell line when co-injected into immunocompromised nude mice. On the other hand, normal prostate fibroblasts admixed with the same epithelial cell line did not result in tumour growth. In 2000 another study investigated the effect of an altered host stroma on epithelial tumour formation. Mouse mammary fat pats were cleared of epithelial cells leaving only the stromal compartment and subjected to irradiation. A non-tumourigenic mammary epithelial cell line harbouring mutations in the p53 gene was then transplanted into the irradiated fat pats. Significantly more and larger tumours were observed in the irradiated animals compared to control non-irradiated animals (Barcellos-Hoff and Ravani 2000).

Furthermore, *in vitro* experiments using senescent ovarian fibroblasts and transformed surface epithelial cells showed an enhancing effect of the senescent fibroblast on epithelial cell proliferation and invasion compared to normal non-senescent fibroblasts (Lawrenson, Grun et al. 2010). These examples show the important role of the tumour microenvironment and indicate that changes in both stromal and epithelial compartment precede tumour development.

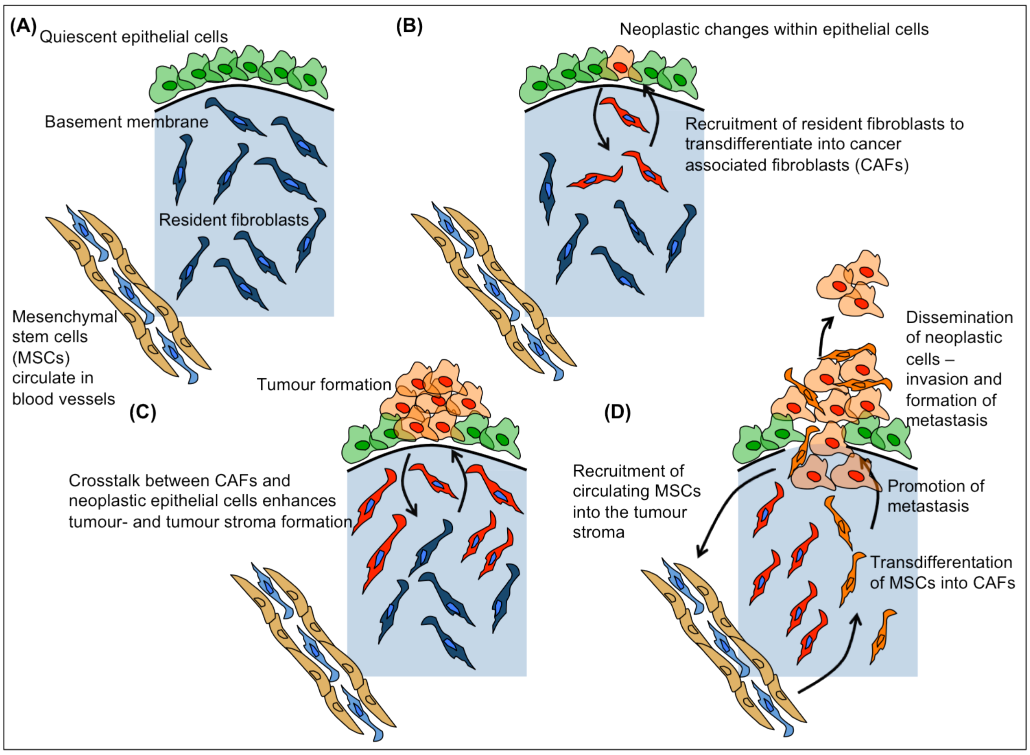

Figure V-17: Hypothetical recruitment of cancer associated fibroblasts at different stages during tumour development. (A) Normal quiescent ovary. A single layer of epithelial cells is covering the stromal core of the ovary. The two cell types are separated by the basement membrane. **(B)** Neoplastic changes within the epithelial cells lead to altered signalling and the recruitment of resident fibroblasts to transdifferentiate into cancer associated fibroblasts. **(C)** Signalling between neoplastic cells and cancer associated fibroblasts leads to tumour formation and the establishment of the tumour stroma. **(D)** Recruitment of circulating mesenchymal stem cells (MSCs) into the tumour stroma leads to promotion of invasion and metastasis formation. CAFs are found at the invasive front.

The stromal distribution within an epithelial tumour differs according to the stage of tumour development. For example, in mammary carcinomas *in situ*, most of the myofibroblasts can be found in proximity to the tumour mass separated by the basement membrane. As malignancy progresses, the stromal composition of the tumour changes and a considerable amount of myofibroblasts is found at the invasive front (Schurch, Seemayer et al. 1998). It is therefore likely that in more advanced stages of tumour development CAFs are recruited from a different source for example from MSCs circulating in the bloodstream (Figure V-17). Metastasis is an important step for tumour development and it has been shown that MSCs promote metastasis of breast cancer cells in a tumour xenograft model (Karnoub, Dash et al. 2007). Furthermore, the fact that psammoma bodies have only been found in low-grade serous tumours that are not metastasing might strengthen this hypothesis. I have observed that psammoma bodies are formed within spheroids of INOFs upon treatment with conditioned medium and not within MSCs spheroids. This might indicate a prevalence of resident fibroblasts within the tumour stroma of low-grade serous tumours, which frequently contain psammoma bodies, and might explain the relative good prognosis for patients due to the absence of metastasis.

In advanced ovarian tumours it was found that the abundance of the stromal tumour microenvironment was correlated with decreased overall survival. No significant association with the ratio of the stroma within an ovarian tumour and the histological subtype could be detected (Labiche, Heutte et al. 2010).

V.4 Conclusion and Future Direction

Here I describe the differentiation of normal resident ovarian fibroblasts towards a myofibroblast phenotype and compare this to the differentiation ability of MSCs. To my knowledge this is the first time ovarian fibroblasts have been investigated as the source of ovarian CAFs alongside another potential CAF precursor cell type. Taken together the results of the 2D and 3D differentiation assays with subsequent morphological assessment, immunohistochemistry and western blotting, it can be concluded that MSCs and INOFs both show differentiation potential towards a CAF like phenotype. Functional assays of the differentiated cells revealed an enhancing effect on the proliferation rate of a transformed epithelial cell line. Invasion assays showed that cells that differentiated in a 3D environment were able to induce increased invasion of the transformed epithelial cell line as opposed to MSCs and INOFs differentiated using 2D culture methods.

These results form the basis for ongoing investigations of the interaction between the stromal microenvironment and the malignant epithelial cells. Gene expression analysis is being used to identify changes at the molecular level within the differentiated cells and will be able to discover the pathways by which the stromal cells are recruited into the tumour microenvironment as well as the altered expression rates of genes potentially involved in stromal and epithelial interactions. These results will give a unique opportunity to better understand the pathways by which fibroblasts and/or mesenchymal stem cells are recruited into the tumour stroma. This might offer a way of blocking or altering the communication between stromal and epithelial cells to hinder formation of a tumour supporting microenvironment. It might also be possible to identify substances that can potentially serve as biomarkers of disease. Ovarian cancer is usually diagnosed at an advanced stage when the tumour has already spread due to largely asymptomatic early stages of disease. Approximately 75% of all tumours are discovered at an advanced stage, which is associated with a 25% 5-year survival rate. However, for tumours detected at an early stage when they are still confined to the ovary the 5-year survival rates are 80-90% (Colombo, Van Gorp et al. 2006; Quaye, Gayther et al. 2008). This clearly shows the need for the discovery of novel biomarkers associated with the early stages of tumour development. The present study has the potential to deliver important information about the recruitment of fibroblasts and/or mesenchymal stem cells into the tumour stroma. This is an important step during tumour initiation and is very likely to go in hand with altered signalling between stromal and epithelial cells, which is characteristic for the formation of the tumour microenvironment, and the development of epithelial tumours. A secreted molecule could serve as a specific biomarker for the early detection of epithelial ovarian cancer.

By understanding the formation of the tumour microenvironment and the communication between the stromal and epithelial cells it is ultimately hoped to identify novel targets for therapy and to discover new biomarkers for early detection of disease.

VI Final conclusion

In this thesis I have established three dimensional cell culture models of gynaecological epithelial cancers to create models of disease that recapitulate the three dimensional architecture of *in vivo* tumours *in vitro*.

I have used three different methods to create 3D models of disease; the rotary cell culture system (RCCS), the polyHEMA method and the hanging droplet approach. The RCCS used in chapter 3 of this thesis facilitates spheroid formation by keeping the cell suspension in constant rotation. This leads to the generation of 1 - 2 large spheroids in each vessel. Using this approach I was able to create multicellular spheroids of primary epithelial ovarian and endometrial cancer cell lines that represent *in vivo* tumour growth (Grun, Benjamin et al. 2009) (III.2.4). It has also been shown that using the RCCS to culture primary mammary carcinoma cell lines resulted in tissue-like constructs exhibiting highly proliferative cells. Transfer of these cells into static culture methods however resulted in growth arrest (Becker and Blanchard 2007). On the other hand, the RCCS only produces 1-2 spheroids per culture vessel and is therefore not suitable for large-scale projects.

Due to the high costs of the rotary vessels together with the limited number of replicates possible at any one time I went on to explore alternative methods. By using polyHEMA it is possible to achieve spheroid formation by inhibiting attachment of cells to tissue culture plastic. Several groups have applied this technique to establish 3D spheroids of cell lines that closely resemble the *in vivo* tissue (Ghosh, Spagnoli et al. 2005; Lawrenson, Benjamin et al. 2009). This approach results in the formation of numerous differently sized spheroids and is particularly suitable for large-scale spheroid production with subsequent assays including FACS analysis, growth assays and characterisation of marker expression by immunohistochemistry. This method is a cost effective way to generate a large amount of spheroids. In the present thesis I used this method to generate heterotypic spheroids comprising stromal and epithelial cells to models the interactions of different cell types and by this creating an even more realistic model of disease. Using this approach I was able to create heterotypic models of ovarian cancer and the normal ovary. Morphological examination revealed striking similarities to primary tumour sections whereas models using normal cells showed a quiescent morphology; thus replicating the state of the normal ovary *in vitro* (IV.2.2). To further characterise the interactions of the different cell types I used fluorescent proteins to distinguish between the two cell populations. Subsequent assays including FACS analysis and confocal microscopy have shown promising results in analysing heterotypic spheroids. However, several experimental steps need to be optimised as described in IV.3. In particular, it is necessary to create two homogenously labelled cell populations using fluorescent proteins that are easily separable using FACS and confocal microscopy. Optimisation of the experimental setup will generate an ideal model to study interactions of stromal and epithelial cells in a 3D environment. It will be possible to study the effect of the co-culture on growth characteristics of both cell types using FACS analysis. Furthermore there is a potential to monitor marker expression in both cell types and to detect co-culture induced changes. A compatible secondary antibody (eg. DAPI labelled) could detect a specific antigen and the distribution of this marker could be examined using confocal microscopy. Another interesting utilisation of 3D models would be to analyse invasion of one cell type into a 3D spheroid comprising another cell type. This approach has been explored in chapter 4 of this thesis (IV.2.4.2) and requires small and uniformly sized spheroids. To achieve this I used the hanging droplet method. Using this method, cells are suspended in a small amount of growth medium in a multi-well plate. The plate is then inverted to allow spheroid formation in a hanging droplet. These spheroids are particularly suited for confocal microscopy as they are small enough to scan through the individual layers of the whole spheroid (IV.2.4.2). Using homogenously labelled cell populations it will be possible to monitor the invasion of cells into the spheroid core using time-lapse confocal microscopy.

Taken together all three culturing methods have advantages and limitations that depend on the anticipated subsequent assays and the growth characteristics of the examined cell line. To analyse the interactions of stromal and epithelial cells as investigated in this thesis I propose the polyHEMA approach as the ideal model. If uniformly sizes spheroids are needed this method could be complemented with the hanging droplet method.

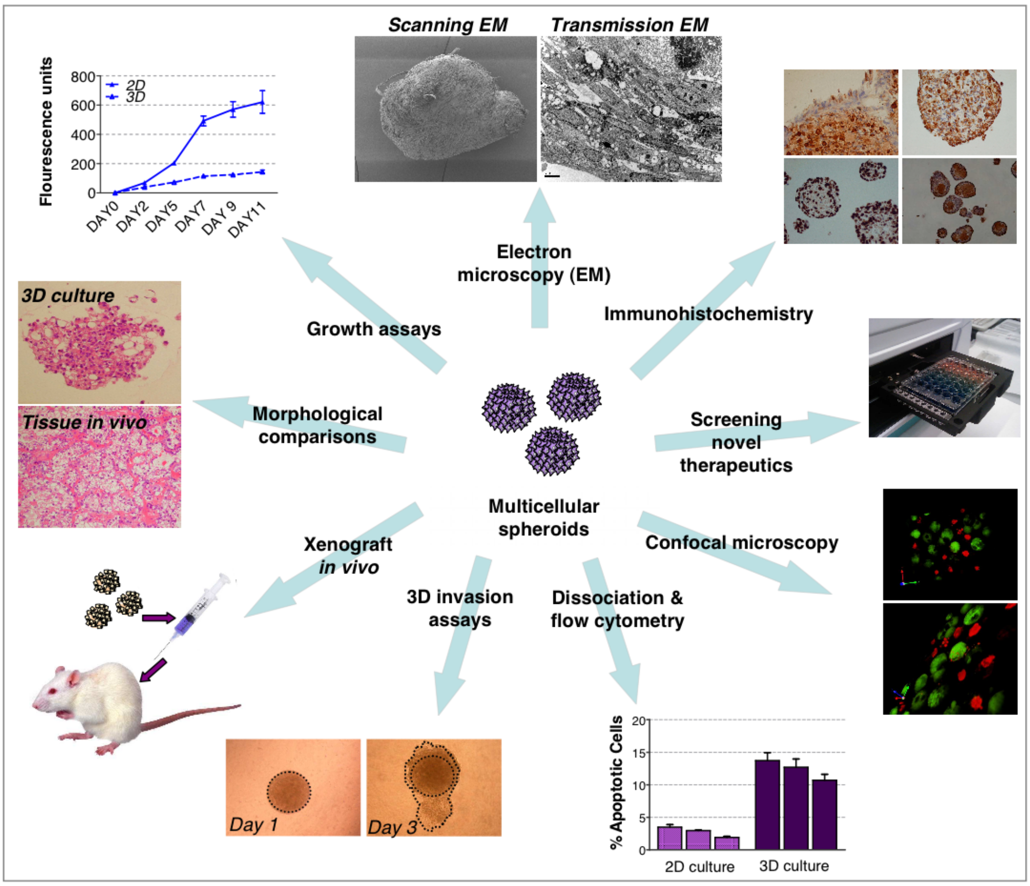

Figure VI-1: Summary of potential secondary assays for spheroids generated using the RCCS, polyHEMA coated tissue culture plastics or the hanging droplet method. Phenotypic characterisation of spheroids can be achieved by immunohistochemistry and growth assays; Structural analysis of spheroids can be performed using electron microscopy or confocal microscopy; Morphological features can be studied by haematoxylin and eosin staining of paraffin embedded spheroids; Dissociation of spheroids enables the analysis of cells using flow cytometry; Spheroids can be transferred into extracellular matrix (ECM) gel to perform 3D invasion assays; Spheroid cultures can be used for the screening of potential novel therapeutics; Xenografting of spheroids can examine the behaviour of a cell line *in vivo*. (Figure from method paper (Lawrenson, Grun et al. 2012) published on the protocol exchange website http://www.nature.com/protocolexchange/)

In general, 3D models can be used to perform numerous secondary assays. Some examples of possible assays are summarised in Figure VI-1. The morphology of 3D spheroids can be analysed by H&E staining and compared to primary tumours/normal tissue. The structure of spheroids can be examined further by electron microscopy. Immunohistochemistry can also be performed on spheroid sections to analyse marker expression and to compare to the primary tumour/normal tissue. Another approach to examine spheroid structure or marker expression is the use of confocal microscopy. 3D spheroids can also be used for functional assays including growth/apoptosis assays, invasion assays and *in vivo* experiments. 3D spheroid models are also promising tools for the screening of novel therapeutics. The variety of possible secondary assays including the different research questions one might want to answer determines the ideal 3D culturing method.

VII Bibliography

Abdollahi, A., A. K. Godwin, et al. (1997). "Identification of a gene containing zinc-finger motifs based on lost expression in malignantly transformed rat ovarian surface epithelial cells." Cancer Res **57**(10): 2029-2034.

Abu-Hamad, S., N. Arbel, et al. (2009). "The VDAC1 N-terminus is essential both for apoptosis and the protective effect of anti-apoptotic proteins." J Cell Sci **122**(Pt 11): 1906-1916.

Adams, A. T. and N. Auersperg (1981). "Transformation of cultured rat ovarian surface epithelial cells by Kirsten murine sarcoma virus." Cancer Res **41**(6): 2063-2072.

Akimov, S. S., A. Ramezani, et al. (2005). "Bypass of senescence, immortalization, and transformation of human hematopoietic progenitor cells." Stem Cells **23**(9): 1423-1433.

Allen, M. and J. Louise Jones (2011). "Jekyll and Hyde: the role of the microenvironment on the progression of cancer." J Pathol **223**(2): 162-176.

Allinen, M., R. Beroukhim, et al. (2004). "Molecular characterization of the tumor microenvironment in breast cancer." Cancer Cell **6**(1): 17-32.

Auersperg, N., M. I. Edelson, et al. (1998). "The biology of ovarian cancer." Semin Oncol **25**(3): 281-304.

Auersperg, N., C. H. Siemens, et al. (1984). "Human ovarian surface epithelium in primary culture." In Vitro **20**(10): 743-755.

Barcellos-Hoff, M. H. and S. A. Ravani (2000). "Irradiated mammary gland stroma promotes the expression of tumorigenic potential by unirradiated epithelial cells." Cancer Res **60**(5): 1254-1260.

Bartosh, T. J., J. H. Ylostalo, et al. (2010). "Aggregation of human mesenchymal stromal cells (MSCs) into 3D spheroids enhances their antiinflammatory properties." Proc Natl Acad Sci U S A **107**(31): 13724-13729.

Bast, R. C., Jr., D. Badgwell, et al. (2005). "New tumor markers: CA125 and beyond." Int J Gynecol Cancer **15 Suppl 3**: 274-281.

Bast, R. C., Jr., M. Feeney, et al. (1981). "Reactivity of a monoclonal antibody with human ovarian carcinoma." J Clin Invest **68**(5): 1331-1337.

Bast, R. C., Jr., T. L. Klug, et al. (1983). "A radioimmunoassay using a monoclonal antibody to monitor the course of epithelial ovarian cancer." N Engl J Med **309**(15): 883-887.

Becker, J. L. and D. K. Blanchard (2007). "Characterization of primary breast carcinomas grown in three-dimensional cultures." J Surg Res **142**(2): 256-262.

Bell, E., H. P. Ehrlich, et al. (1981). "Living tissue formed in vitro and accepted as skin-equivalent tissue of full thickness." Science **211**(4486): 1052-1054.

Bhowmick, N. A., E. G. Neilson, et al. (2004). "Stromal fibroblasts in cancer initiation and progression." Nature **432**(7015): 332-337.

Bissell, M. J. and W. C. Hines (2011). "Why don't we get more cancer? A proposed role of the microenvironment in restraining cancer progression." Nat Med **17**(3): 320-329.

Buick, R. N., R. Pullano, et al. (1985). "Comparative properties of five human ovarian adenocarcinoma cell lines." Cancer Res **45**(8): 3668-3676.

Burger, J. A. and A. Peled (2009). "CXCR4 antagonists: targeting the microenvironment in leukemia and other cancers." Leukemia **23**(1): 43-52.

Camps, J. L., S. M. Chang, et al. (1990). "Fibroblast-mediated acceleration of human epithelial tumor growth in vivo." Proc Natl Acad Sci U S A **87**(1): 75-79.

Castello-Cros, R. and E. Cukierman (2009). "Stromagenesis during tumorigenesis: characterization of tumor-associated fibroblasts and stroma-derived 3D matrices." Methods Mol Biol **522**: 275-305.

Chen, G., T. G. Gharib, et al. (2002). "Discordant protein and mRNA expression in lung adenocarcinomas." Mol Cell Proteomics **1**(4): 304-313.

Cherry, R. S. (1993). "Animal cells in turbulent fluids: details of the physical stimulus and the biological response." Biotechnol Adv **11**(2): 279-299.

Colombo, N., T. Van Gorp, et al. (2006). "Ovarian cancer." Crit Rev Oncol Hematol **60**(2): 159-179.

Connolly, D. C., R. Bao, et al. (2003). "Female mice chimeric for expression of the simian virus 40 TAg under control of the MISIIR promoter develop epithelial ovarian cancer." Cancer Res **63**(6): 1389-1397.

Coussens, L. M. and Z. Werb (2002). "Inflammation and cancer." Nature **420**(6917): 860-867.

Cvetkovic, D., D. Pisarcik, et al. (2004). "Altered expression and loss of heterozygosity of the LOT1 gene in ovarian cancer." Gynecol Oncol **95**(3): 449-455.

Dafou, D., B. Grun, et al. (2010). "Microcell-mediated chromosome transfer identifies EPB41L3 as a functional suppressor of epithelial ovarian cancers." Neoplasia **12**(7): 579-589.

Dafou, D., S. J. Ramus, et al. (2009). "Chromosomes 6 and 18 induce neoplastic suppression in epithelial ovarian cancer cells." Int J Cancer **124**(5): 1037-1044.

Darby, I., O. Skalli, et al. (1990). "Alpha-smooth muscle actin is transiently expressed by myofibroblasts during experimental wound healing." Lab Invest **63**(1): 21-29.

De Wever, O. and M. Mareel (2002). "Role of myofibroblasts at the invasion front." Biol Chem **383**(1): 55-67.

De Wever, O. and M. Mareel (2003). "Role of tissue stroma in cancer cell invasion." J Pathol **200**(4): 429-447.

Di Costanzo, F., F. Mazzoni, et al. (2008). "Bevacizumab in non-small cell lung cancer." Drugs **68**(6): 737-746.

Dinulescu, D. M., T. A. Ince, et al. (2005). "Role of K-ras and Pten in the development of mouse models of endometriosis and endometrioid ovarian cancer." Nat Med **11**(1): 63-70.

DiSaia, P. J., M. Morrow, et al. (1975). "Two new tissue culture lines from ovarian cancer." Gynecol Oncol **3**(3): 215-219.

Dolberg, D. S. and M. J. Bissell (1984). "Inability of Rous sarcoma virus to cause sarcomas in the avian embryo." Nature **309**(5968): 552-556.

Dolberg, D. S., R. Hollingsworth, et al. (1985). "Wounding and its role in RSV-mediated tumor formation." Science **230**(4726): 676-678.

Drewinko, B., M. Patchen, et al. (1981). "Differential killing efficacy of twenty antitumor drugs on proliferating and nonproliferating human tumor cells." Cancer Res **41**(6): 2328-2333.

Dubeau, L. (2008). "The cell of origin of ovarian epithelial tumours." Lancet Oncol **9**(12): 1191-1197.

Dunfield, L. D., T. G. Shepherd, et al. (2002). "Primary culture and mRNA analysis of human ovarian cells." Biol Proced Online **4**: 55-61.

Dvorak, H. F. (1986). "Tumors: wounds that do not heal. Similarities between tumor stroma generation and wound healing." N Engl J Med **315**(26): 1650-1659.

Edmondson, R. J. and J. M. Monaghan (2001). "The epidemiology of ovarian cancer." Int J Gynecol Cancer **11**(6): 423-429.

El-Serag, H. B. (2012). "Epidemiology of viral hepatitis and hepatocellular carcinoma." Gastroenterology **142**(6): 1264-1273 e1261.

Emerman, J. T., J. Enami, et al. (1977). "Hormonal effects on intracellular and secreted casein in cultures of mouse mammary epithelial cells on floating collagen membranes." Proc Natl Acad Sci U S A **74**(10): 4466-4470.

Emura, M., A. Ochiai, et al. (2000). "Development of myofibroblasts from human bone marrow mesenchymal stem cells cocultured with human colon carcinoma cells and TGF beta 1." In Vitro Cell Dev Biol Anim **36**(2): 77-80.

Fathalla, M. F. (1971). "Incessant ovulation--a factor in ovarian neoplasia?" Lancet **2**(7716): 163.

Fearon, E. R. and B. Vogelstein (1990). "A genetic model for colorectal tumorigenesis." Cell **61**(5): 759-767.

Ferenczy, A., M. Talens, et al. (1977). "Ultrastructural studies on the morphogenesis of psammoma bodies in ovarian serous neoplasia." Cancer **39**(6): 2451-2459.

Ferrara, N., K. J. Hillan, et al. (2004). "Discovery and development of bevacizumab, an anti-VEGF antibody for treating cancer." Nat Rev Drug Discov **3**(5): 391-400.

Flesken-Nikitin, A., K. C. Choi, et al. (2003). "Induction of carcinogenesis by concurrent inactivation of p53 and Rb1 in the mouse ovarian surface epithelium." Cancer Res **63**(13): 3459-3463.

Folkman, J. (1995). "Seminars in Medicine of the Beth Israel Hospital, Boston. Clinical applications of research on angiogenesis." N Engl J Med **333**(26): 1757-1763.

Freyer, J. P. and R. M. Sutherland (1980). "Selective dissociation and characterization of cells from different regions of multicell tumor spheroids." Cancer Res **40**(11): 3956-3965.

Gharbi, S., P. Gaffney, et al. (2002). "Evaluation of two-dimensional differential gel electrophoresis for proteomic expression analysis of a model breast cancer cell system." Mol Cell Proteomics **1**(2): 91-98.

Ghosh, S., G. C. Spagnoli, et al. (2005). "Three-dimensional culture of melanoma cells profoundly affects gene expression profile: a high density oligonucleotide array study." J Cell Physiol **204**(2): 522-531.

Gilks, C. B., D. A. Bell, et al. (1990). "Serous psammocarcinoma of the ovary and peritoneum." Int J Gynecol Pathol **9**(2): 110-121.

Goncalves, A. and F. Bertucci (2011). "Clinical application of proteomics in breast cancer: state of the art and perspectives." Med Princ Pract **20**(1): 4-18.

Goodwin, T. J., T. L. Prewett, et al. (1993). "Reduced shear stress: a major component in the ability of mammalian tissues to form three-dimensional assemblies in simulated microgravity." J Cell Biochem **51**(3): 301-311.

Grugan, K. D., C. G. Miller, et al. (2010). "Fibroblast-secreted hepatocyte growth factor plays a functional role in esophageal squamous cell carcinoma invasion." Proc Natl Acad Sci U S A **107**(24): 11026-11031.

Grun, B., E. Benjamin, et al. (2009). "Three-dimensional in vitro cell biology models of ovarian and endometrial cancer." Cell Prolif **42**(2): 219-228.

Gudjonsson, T., L. Ronnov-Jessen, et al. (2002). "Normal and tumor-derived myoepithelial cells differ in their ability to interact with luminal breast epithelial cells for polarity and basement membrane deposition." J Cell Sci **115**(Pt 1): 39-50.

Haga, K., S. Ohno, et al. (2007). "Efficient immortalization of primary human cells by p16INK4a-specific short hairpin RNA or Bmi-1, combined with introduction of hTERT." Cancer Sci **98**(2): 147-154.

Hahn, W. C. and R. A. Weinberg (2002). "Rules for making human tumor cells." N Engl J Med **347**(20): 1593-1603.

Hammond, T. G. and J. M. Hammond (2001). "Optimized suspension culture: the rotating-wall vessel." Am J Physiol Renal Physiol **281**(1): F12-25.

Han, E. S. and B. J. Monk (2007). "Bevacizumab in the treatment of ovarian cancer." Expert Rev Anticancer Ther **7**(10): 1339-1345.

Han, X., A. J. Papadopoulos, et al. (1999). "Cholera toxin-induced alteration of the phenotype and behaviour of an ovarian carcinoma cell line, SR8." Immunol Cell Biol **77**(5): 377-384.

Harach, H. R., K. O. Franssila, et al. (1985). "Occult papillary carcinoma of the thyroid. A "normal" finding in Finland. A systematic autopsy study." Cancer **56**(3): 531-538.

Hart, I. R. and I. J. Fidler (1980). "Role of organ selectivity in the determination of metastatic patterns of B16 melanoma." Cancer Res **40**(7): 2281-2287.

Hayflick, L. and P. S. Moorhead (1961). "The serial cultivation of human diploid cell strains." Exp Cell Res **25**: 585-621.

Holliday, D. L., K. T. Brouilette, et al. (2009). "Novel multicellular organotypic models of normal and malignant breast: tools for dissecting the role of the microenvironment in breast cancer progression." Breast Cancer Res **11**(1): R3.

Hurwitz, H., L. Fehrenbacher, et al. (2004). "Bevacizumab plus irinotecan, fluorouracil, and leucovorin for metastatic colorectal cancer." N Engl J Med **350**(23): 2335-2342.

Hwang, R. F., T. Moore, et al. (2008). "Cancer-associated stromal fibroblasts promote pancreatic tumor progression." Cancer Res **68**(3): 918-926.

Iodice, S., M. Barile, et al. (2010). "Oral contraceptive use and breast or ovarian cancer risk in BRCA1/2 carriers: a meta-analysis." Eur J Cancer **46**(12): 2275-2284.

Itahana, K., Y. Zou, et al. (2003). "Control of the replicative life span of human fibroblasts by p16 and the polycomb protein Bmi-1." Mol Cell Biol **23**(1): 389-401.

Ivascu, A. and M. Kubbies (2006). "Rapid generation of single-tumor spheroids for high-throughput cell function and toxicity analysis." J Biomol Screen **11**(8): 922-932.

Janke, C. and J. C. Bulinski (2011). "Post-translational regulation of the microtubule cytoskeleton: mechanisms and functions." Nat Rev Mol Cell Biol **12**(12): 773-786.

Jemal, A., R. Siegel, et al. (2007). "Cancer statistics, 2007." CA Cancer J Clin **57**(1): 43-66.

Jones, S., T. L. Wang, et al. (2010). "Frequent mutations of chromatin remodeling gene ARID1A in ovarian clear cell carcinoma." Science **330**(6001): 228-231.

Kabawat, S. E., R. C. Bast, et al. (1983). "Immunopathologic characterization of a monoclonal antibody that recognizes common surface antigens of human ovarian tumors of serous, endometrioid, and clear cell types." Am J Clin Pathol **79**(1): 98-104.

Kabiri, M., B. Kul, et al. (2012). "3D mesenchymal stem/stromal cell osteogenesis and autocrine signalling." Biochem Biophys Res Commun **419**(2): 142-147.

Kalluri, R. and R. A. Weinberg (2009). "The basics of epithelial-mesenchymal transition." J Clin Invest **119**(6): 1420-1428.

Kalluri, R. and M. Zeisberg (2006). "Fibroblasts in cancer." Nat Rev Cancer **6**(5): 392-401.

Karnoub, A. E., A. B. Dash, et al. (2007). "Mesenchymal stem cells within tumour stroma promote breast cancer metastasis." Nature **449**(7162): 557-563.

Kaur, P. and W. G. Carter (1992). "Integrin expression and differentiation in transformed human epidermal cells is regulated by fibroblasts." J Cell Sci **103 (Pt 3)**: 755-763.

Kenny, H. A., S. Kaur, et al. (2008). "The initial steps of ovarian cancer cell metastasis are mediated by MMP-2 cleavage of vitronectin and fibronectin." J Clin Invest **118**(4): 1367-1379.

Kenny, H. A., T. Krausz, et al. (2007). "Use of a novel 3D culture model to elucidate the role of mesothelial cells, fibroblasts and extra-cellular matrices on adhesion and invasion of ovarian cancer cells to the omentum." Int J Cancer **121**(7): 1463-1472.

Kidd, S., E. Spaeth, et al. (2009). "Direct evidence of mesenchymal stem cell tropism for tumor and wounding microenvironments using in vivo bioluminescent imaging." Stem Cells **27**(10): 2614-2623.

Kido, M. and M. Shibuya (1998). "Isolation and characterization of mouse ovarian surface epithelial cell lines." Pathol Res Pract **194**(10): 725-730.

Kim, J. B. (2005). "Three-dimensional tissue culture models in cancer biology." Semin Cancer Biol **15**(5): 365-377.

Kim, K. M. (1995). "Apoptosis and calcification." Scanning Microsc **9**(4): 1137-1175; discussion 1175-1138.

Kinnula, V. L. and J. D. Crapo (2004). "Superoxide dismutases in malignant cells and human tumors." Free Radic Biol Med **36**(6): 718-744.

Kiyozuka, Y., H. Nakagawa, et al. (2001). "Bone morphogenetic protein-2 and type IV collagen expression in psammoma body forming ovarian cancer." Anticancer Res **21**(3B): 1723-1730.

Kojima, Y., A. Acar, et al. (2010). "Autocrine TGF-beta and stromal cell-derived factor-1 (SDF-1) signaling drives the evolution of tumor-promoting mammary stromal myofibroblasts." Proc Natl Acad Sci U S A **107**(46): 20009-20014.

Krause, S., M. V. Maffini, et al. (2008). "A novel 3D in vitro culture model to study stromal-epithelial interactions in the mammary gland." Tissue Eng Part C Methods **14**(3): 261-271.

Kruitwagen, R. F., L. G. Poels, et al. (1989). "ETN-1: a new human endometrial carcinoma cell line producing ascites and distant metastases in nude mice." Int J Cancer **43**(6): 1098-1103.

Kunz-Schughart, L. A. and J. P. Freyer (1997). "Adaptation of an automated selective dissociation procedure to two novel spheroid types." In Vitro Cell Dev Biol Anim **33**(2): 73-76.

Kunz-Schughart, L. A., P. Heyder, et al. (2001). "A heterologous 3-D coculture model of breast tumor cells and fibroblasts to study tumor-associated fibroblast differentiation." Exp Cell Res **266**(1): 74-86.

Kusakari, T., M. Kariya, et al. (2003). "C-erbB-2 or mutant Ha-ras induced malignant transformation of immortalized human ovarian surface epithelial cells in vitro." Br J Cancer **89**(12): 2293-2298.

Labiche, A., N. Heutte, et al. (2010). "Stromal compartment as a survival prognostic factor in advanced ovarian carcinoma." Int J Gynecol Cancer **20**(1): 28-33.

Lawrenson, K., E. Benjamin, et al. (2009). "In vitro three-dimensional modelling of human ovarian surface epithelial cells." Cell Prolif **42**(3): 385-393.

Lawrenson, K., B. Grun, et al. (2012). "Three-dimensional in vitro cell biology models of normal ovarian surface epithelial cells and epithelial ovarian cancer cells." protocol exchange.

Lawrenson, K., B. Grun, et al. (2010). "Senescent fibroblasts promote neoplastic transformation of partially transformed ovarian epithelial cells in a three-dimensional model of early stage ovarian cancer." Neoplasia **12**(4): 317-325.

Lawrenson, K., D. Sproul, et al. (2011). "Modelling Genetic and Clinical Heterogeneity in Epithelial Ovarian Cancers." Carcinogenesis.

Li, S., J. Lao, et al. (2003). "Genomic analysis of smooth muscle cells in 3-dimensional collagen matrix." FASEB J **17**(1): 97-99.

Liu, J., G. Yang, et al. (2004). "A genetically defined model for human ovarian cancer." Cancer Res **64**(5): 1655-1663.

Maki, M., S. Hirota, et al. (2000). "Expression of osteopontin messenger RNA by macrophages in ovarian serous papillary cystadenocarcinoma: a possible association with calcification of psammoma bodies." Pathol Int **50**(7): 531-535.

Marquez, R. T., K. A. Baggerly, et al. (2005). "Patterns of gene expression in different histotypes of epithelial ovarian cancer correlate with those in normal fallopian tube, endometrium, and colon." Clin Cancer Res **11**(17): 6116-6126.

Masters, J. R. (2000). "Human cancer cell lines: fact and fantasy." Nat Rev Mol Cell Biol **1**(3): 233-236.

Matysiak-Budnik, T. and F. Megraud (2006). "Helicobacter pylori infection and gastric cancer." Eur J Cancer **42**(6): 708-716.

McGuire, W. P., W. J. Hoskins, et al. (1996). "Cyclophosphamide and cisplatin compared with paclitaxel and cisplatin in patients with stage III and stage IV ovarian cancer." N Engl J Med **334**(1): 1-6.

Medeiros, F., M. G. Muto, et al. (2006). "The tubal fimbria is a preferred site for early adenocarcinoma in women with familial ovarian cancer syndrome." Am J Surg Pathol **30**(2): 230-236.

Menon, U., A. Gentry-Maharaj, et al. (2009). "Sensitivity and specificity of multimodal and ultrasound screening for ovarian cancer, and stage distribution of detected cancers: results of the prevalence screen of the UK Collaborative Trial of Ovarian Cancer Screening (UKCTOCS)." Lancet Oncol **10**(4): 327-340.

Mintz, B. and K. Illmensee (1975). "Normal genetically mosaic mice produced from malignant teratocarcinoma cells." Proc Natl Acad Sci U S A **72**(9): 3585-3589.

Mishra, P. J., P. J. Mishra, et al. (2008). "Carcinoma-associated fibroblast-like differentiation of human mesenchymal stem cells." Cancer Res **68**(11): 4331-4339.

Morinaka, A., Y. Funato, et al. (2011). "Oligomeric peroxiredoxin-I is an essential intermediate for p53 to activate MST1 kinase and apoptosis." Oncogene **30**(40): 4208-4218.

Mueller, L., F. A. Goumas, et al. (2007). "Stromal fibroblasts in colorectal liver metastases originate from resident fibroblasts and generate an inflammatory microenvironment." Am J Pathol **171**(5): 1608-1618.

Mueller, M. M. and N. E. Fusenig (2004). "Friends or foes - bipolar effects of the tumour stroma in cancer." Nat Rev Cancer **4**(11): 839-849.

Navran, S. (2008). "The application of low shear modeled microgravity to 3-D cell biology and tissue engineering." Biotechnol Annu Rev **14**: 275-296.

Nederman, T. (1984). "Effects of vinblastine and 5-fluorouracil on human glioma and thyroid cancer cell monolayers and spheroids." Cancer Res **44**(1): 254-258.

Olive, K. P., M. A. Jacobetz, et al. (2009). "Inhibition of Hedgehog signaling enhances delivery of chemotherapy in a mouse model of pancreatic cancer." Science **324**(5933): 1457-1461.

Olumi, A. F., G. D. Grossfeld, et al. (1999). "Carcinoma-associated fibroblasts direct tumor progression of initiated human prostatic epithelium." Cancer Res **59**(19): 5002-5011.

Orimo, A., P. B. Gupta, et al. (2005). "Stromal fibroblasts present in invasive human breast carcinomas promote tumor growth and angiogenesis through elevated SDF-1/CXCL12 secretion." Cell **121**(3): 335-348.

Orimo, A. and R. A. Weinberg (2006). "Stromal fibroblasts in cancer: a novel tumor-promoting cell type." Cell Cycle **5**(15): 1597-1601.

Orsulic, S., Y. Li, et al. (2002). "Induction of ovarian cancer by defined multiple genetic changes in a mouse model system." Cancer Cell **1**(1): 53-62.

Ouellet, V., M. Zietarska, et al. (2008). "Characterization of three new serous epithelial ovarian cancer cell lines." BMC Cancer **8**: 152.

Pageau, S. C., O. V. Sazonova, et al. (2011). "The effect of stromal components on the modulation of the phenotype of human bronchial epithelial cells in 3D culture." Biomaterials **32**(29): 7169-7180.

Paget, S. (1989). "The distribution of secondary growths in cancer of the breast. 1889." Cancer Metastasis Rev **8**(2): 98-101.

Park, D. W., D. S. Choi, et al. (2003). "A well-defined in vitro three-dimensional culture of human endometrium and its applicability to endometrial cancer invasion." Cancer Lett **195**(2): 185-192.

Petersen, O. W., H. L. Nielsen, et al. (2003). "Epithelial to mesenchymal transition in human breast cancer can provide a nonmalignant stroma." Am J Pathol **162**(2): 391-402.

Petersen, O. W., L. Ronnov-Jessen, et al. (1992). "Interaction with basement membrane serves to rapidly distinguish growth and differentiation pattern of normal and malignant human breast epithelial cells." Proc Natl Acad Sci U S A **89**(19): 9064-9068.

Ponnampalam, A. P. and P. A. Rogers (2006). "Cyclic changes and hormonal regulation of annexin IV mRNA and protein in human endometrium." Mol Hum Reprod **12**(11): 661-669.

Prat, J. (2012). "Ovarian carcinomas: five distinct diseases with different origins, genetic alterations, and clinicopathological features." Virchows Arch **460**(3): 237-249.

Provencher, D. M., H. Lounis, et al. (2000). "Characterization of four novel epithelial ovarian cancer cell lines." In Vitro Cell Dev Biol Anim **36**(6): 357-361.

Qiu, W., M. Hu, et al. (2008). "No evidence of clonal somatic genetic alterations in cancer-associated fibroblasts from human breast and ovarian carcinomas." Nat Genet **40**(5): 650-655.

Quaye, L., S. A. Gayther, et al. (2008). "The effects of common genetic variants in oncogenes on ovarian cancer survival." Clin Cancer Res **14**(18): 5833-5839.

Quiros, R. M., M. Valianou, et al. (2008). "Ovarian normal and tumor-associated fibroblasts retain in vivo stromal characteristics in a 3-D matrix-dependent manner." Gynecol Oncol **110**(1): 99-109.

Reis-Filho, J. S. and L. Pusztai (2011). "Gene expression profiling in breast cancer: classification, prognostication, and prediction." Lancet **378**(9805): 1812-1823.

Riman, T., P. W. Dickman, et al. (2002). "Risk factors for invasive epithelial ovarian cancer: results from a Swedish case-control study." Am J Epidemiol **156**(4): 363-373.

Rizwani, W., M. Alexandrow, et al. (2009). "Prohibitin physically interacts with MCM proteins and inhibits mammalian DNA replication." Cell Cycle **8**(10): 1621-1629.

Ronnov-Jessen, L. and O. W. Petersen (1993). "Induction of alpha-smooth muscle actin by transforming growth factor-beta 1 in quiescent human breast gland fibroblasts. Implications for myofibroblast generation in breast neoplasia." Lab Invest **68**(6): 696-707.

Ronnov-Jessen, L., O. W. Petersen, et al. (1995). "The origin of the myofibroblasts in breast cancer. Recapitulation of tumor environment in culture unravels diversity and implicates converted fibroblasts and recruited smooth muscle cells." J Clin Invest **95**(2): 859-873.

Rosano, L., F. Spinella, et al. (2006). "Endothelin-1 is required during epithelial to mesenchymal transition in ovarian cancer progression." Exp Biol Med (Maywood) **231**(6): 1128-1131.

Rosenberg, L., J. R. Palmer, et al. (1994). "A case-control study of oral contraceptive use and invasive epithelial ovarian cancer." Am J Epidemiol **139**(7): 654-661.

Runswick, S. K., M. J. O'Hare, et al. (2001). "Desmosomal adhesion regulates epithelial morphogenesis and cell positioning." Nat Cell Biol **3**(9): 823-830.

Sadlonova, A., Z. Novak, et al. (2005). "Breast fibroblasts modulate epithelial cell proliferation in three-dimensional in vitro co-culture." Breast Cancer Res **7**(1): R46-59.

Sainz de la Cuesta, R., J. H. Eichhorn, et al. (1996). "Histologic transformation of benign endometriosis to early epithelial ovarian cancer." Gynecol Oncol **60**(2): 238-244.

Sakr, W. A., G. P. Haas, et al. (1993). "The frequency of carcinoma and intraepithelial neoplasia of the prostate in young male patients." J Urol **150**(2 Pt 1): 379-385.

Sappino, A. P., W. Schurch, et al. (1990). "Differentiation repertoire of fibroblastic cells: expression of cytoskeletal proteins as marker of phenotypic modulations." Lab Invest **63**(2): 144-161.

Satelli, A. and S. Li (2011). "Vimentin in cancer and its potential as a molecular target for cancer therapy." Cell Mol Life Sci **68**(18): 3033-3046.

Sauer, B. (1993). "Manipulation of transgenes by site-specific recombination: use of Cre recombinase." Methods Enzymol **225**: 890-900.

Schneider, C. A., W. S. Rasband, et al. (2012). "NIH Image to ImageJ: 25 years of image analysis." Nature Methods.

Schoenenberger, C. A., H. G. Mannherz, et al. (2011). "Actin: from structural plasticity to functional diversity." Eur J Cell Biol **90**(10): 797-804.

Schurch, W., T. A. Seemayer, et al. (1998). "The myofibroblast: a quarter century after its discovery." Am J Surg Pathol **22**(2): 141-147.

Serini, G. and G. Gabbiani (1999). "Mechanisms of myofibroblast activity and phenotypic modulation." Exp Cell Res **250**(2): 273-283.

Shaner, N. C., R. E. Campbell, et al. (2004). "Improved monomeric red, orange and yellow fluorescent proteins derived from Discosoma sp. red fluorescent protein." Nat Biotechnol **22**(12): 1567-1572.

Sharma, A., A. Gentry-Maharaj, et al. (2012). "Assessing the malignant potential of ovarian inclusion cysts in postmenopausal women within the UK Collaborative Trial of Ovarian Cancer Screening (UKCTOCS): a prospective cohort study." BJOG **119**(2): 207-219.

Shaw, T. J., M. K. Senterman, et al. (2004). "Characterization of intraperitoneal, orthotopic, and metastatic xenograft models of human ovarian cancer." Mol Ther **10**(6): 1032-1042.

Shih Ie, M. and R. J. Kurman (2004). "Ovarian tumorigenesis: a proposed model based on morphological and molecular genetic analysis." Am J Pathol **164**(5): 1511-1518.

Shoshan-Barmatz, V., A. Israelson, et al. (2006). "The voltage-dependent anion channel (VDAC): function in intracellular signalling, cell life and cell death." Curr Pharm Des **12**(18): 2249-2270.

Shu, X. O., L. A. Brinton, et al. (1989). "Population-based case-control study of ovarian cancer in Shanghai." Cancer Res **49**(13): 3670-3674.

Siu, W. Y., T. Arooz, et al. (1999). "Differential responses of proliferating versus quiescent cells to adriamycin." Exp Cell Res **250**(1): 131-141.

Spaeth, E. L., J. L. Dembinski, et al. (2009). "Mesenchymal stem cell transition to tumor-associated fibroblasts contributes to fibrovascular network expansion and tumor progression." PLoS ONE **4**(4): e4992.

Spellman, P. and e. al. (2011). "Integrated genomic analyses of ovarian carcinoma." Nature **474**(7353): 609-615.

Stevenson, C. E., M. Nagahashi, et al. (2012). "Bevacizumab and breast cancer: what does the future hold?" Future Oncol **8**(4): 403-414.

Striepen, B., C. Y. He, et al. (1998). "Expression, selection, and organellar targeting of the green fluorescent protein in Toxoplasma gondii." Mol Biochem Parasitol **92**(2): 325-338.

Studeny, M., F. C. Marini, et al. (2002). "Bone marrow-derived mesenchymal stem cells as vehicles for interferon-beta delivery into tumors." Cancer Res **62**(13): 3603-3608.

Sugimoto, H., T. M. Mundel, et al. (2006). "Identification of fibroblast heterogeneity in the tumor microenvironment." Cancer Biol Ther **5**(12): 1640-1646.

Sutherland, R. M. and R. E. Durand (1976). "Radiation response of multicell spheroids--an in vitro tumour model." Curr Top Radiat Res Q **11**(1): 87-139.

Sutherland, R. M., W. R. Inch, et al. (1970). "A multi-component radiation survival curve using an in vitro tumour model." Int J Radiat Biol Relat Stud Phys Chem Med **18**(5): 491-495.

Unsworth, B. R. and P. I. Lelkes (1998). "Growing tissues in microgravity." Nat Med **4**(8): 901-907.

Valeriote, F. and L. van Putten (1975). "Proliferation-dependent cytotoxicity of anticancer agents: a review." Cancer Res **35**(10): 2619-2630.

van den Berg-Bakker, C. A., A. Hagemeijer, et al. (1993). "Establishment and characterization of 7 ovarian carcinoma cell lines and one granulosa tumor cell line: growth features and cytogenetics." Int J Cancer **53**(4): 613-620.

Weaver, V. M., O. W. Petersen, et al. (1997). "Reversion of the malignant phenotype of human breast cells in three-dimensional culture and in vivo by integrin blocking antibodies." J Cell Biol **137**(1): 231-245.

Webb, J. D. and M. C. Simon (2010). "Novel insights into the molecular origins and treatment of lung cancer." Cell Cycle **9**(20): 4098-4105.

Weeks, M. E., J. Sinclair, et al. (2006). "A parallel proteomic and metabolomic analysis of the hydrogen peroxide- and Sty1p-dependent stress response in Schizosaccharomyces pombe." Proteomics **6**(9): 2772-2796.

Weigelt, B., A. T. Lo, et al. (2009). "HER2 signaling pathway activation and response of breast cancer cells to HER2-targeting agents is dependent strongly on the 3D microenvironment." Breast Cancer Res Treat.

Wikborn, C., F. Pettersson, et al. (1996). "Delay in diagnosis of epithelial ovarian cancer." Int J Gynaecol Obstet **52**(3): 263-267.

Wilhelm, S. M., C. Carter, et al. (2004). "BAY 43-9006 exhibits broad spectrum oral antitumor activity and targets the RAF/MEK/ERK pathway and receptor tyrosine kinases involved in tumor progression and angiogenesis." Cancer Res **64**(19): 7099-7109.

Wilson, A. P. (1984). "Characterization of a cell line derived from the ascites of a patient with papillary serous cystadenocarcinoma of the ovary." J Natl Cancer Inst **72**(3): 513-521.

Yamashita, M. and M. Emerman (2006). "Retroviral infection of non-dividing cells: old and new perspectives." Virology **344**(1): 88-93.

Yang, G., D. G. Rosen, et al. (2006). "The chemokine growth-regulated oncogene 1 (Gro-1) links RAS signaling to the senescence of stromal fibroblasts and ovarian tumorigenesis." Proc Natl Acad Sci U S A **103**(44): 16472-16477.

Yuan, Y., W. H. Kim, et al. (1997). "Establishment and characterization of human ovarian carcinoma cell lines." Gynecol Oncol **66**(3): 378-387.

Yuhas, J. M., A. P. Li, et al. (1977). "A simplified method for production and growth of multicellular tumor spheroids." Cancer Res **37**(10): 3639-3643.

Zeisberg, E. M., S. Potenta, et al. (2007). "Discovery of endothelial to mesenchymal transition as a source for carcinoma-associated fibroblasts." Cancer Res **67**(21): 10123-10128.

Zhau, H. E., T. J. Goodwin, et al. (1997). "Establishment of a three-dimensional human prostate organoid coculture under microgravity-simulated conditions: evaluation of androgen-induced growth and PSA expression." In Vitro Cell Dev Biol Anim **33**(5): 375-380.

Zietarska, M., C. M. Maugard, et al. (2007). "Molecular description of a 3D in vitro model for the study of epithelial ovarian cancer (EOC)." Mol Carcinog.